PREDICTION OF DROPLET SIZE DISTRIBUTION FROM SUBSURFACE OIL RELEASES WITH AND WITHOUT CHEMICAL DISPERSANTS APPLICATION

by

Linlu Weng

Submitted in partial fulfilment of the requirements
for the degree of Master of Applied Science

at

Dalhousie University
Halifax, Nova Scotia
April 2017

Table of Contents

LIST OF TABLES

LIST OF FIGURES

ABSTRACT

Several deep water oil spill models have been developed to simulate the fate and transport of oil from subsurface releases in marine environments and provide guidance for emergency responses. Prediction of oil droplet size distribution from the subsurface blowout is a critical part of the modeling because it has direct influences on the estimated fate and transport of oil in the marine environment. Currently, our capability to predict droplet size distribution from subsurface release is still limited mainly due to the limited experimental studies, especially the cases with subsurface chemical dispersant application. To have a better understanding of oil droplet size distribution from subsurface oil blowout, a series of subsurface oil release experiments were conducted in an outdoor horizontal wave tank, with different release rates and at different ambient water temperatures. Two crude oils, the Intermediate Fuel Oil 120 (IFO-120, heavy crude oil) and the Alaska North Slope (ANS, medium crude oil) crude oil, were used. To study the effect of dispersant application on droplet size distribution, a chemical dispersant, Corexit 9500, was applied at four dispersant-to-oil-ratios (DORs). The oil droplet size distributions were measured using a LISST-100Xs.

Based on the measured droplet size distribution data, the corresponding median droplet diameters (d_{50}) and relative droplet size (d_{50}/D) were calculated for each experiment. The values of d_{50} revealed that the dispersant had a strong influence on reducing droplet size for both oils. With the same DOR, ANS was more effectively dispersed than IFO-120 with its d_{50} being much smaller than that of IFO-120. A relationship between the relative droplet size (d_{50}/D) and the Reynolds Number (Re) was then established. It was found that the empirical coefficient (A) in the Reynolds Number Scaling was dependent on DORs, as well as oil types. The study also found that the spreading coefficient, based on the Rosin-Rammler approach, was different for droplets smaller than d_{50} ($d/d_{50} \leq 1$) and those of $d/d_{50} > 1$. A two-step Rosin-Rammler approach (using two spreading parameters, α_1 for $d/d_{50} \leq 1$ and α_2 for $d/d_{50} > 1$) was then proposed to improve the accuracy of prediction of statistical droplet size distributions. A case study of a hypothetical oil spill on Scotian Shelf was then conducted using the improved oil droplet size distribution equations. The result showed that these equations worked well on predicting the fate of oil from subsurface oil blowout, and application of dispersant greatly reduced surface oil for IFO-120 (heavy crude oil) case.

LIST OF ABBREVIATIONS AND SYMBOLS USED

A	A parameter that accounts for normalization condition
ANS	Alaskan North Slope
BP	British Petroleum
B	Tuning coefficient
BSD	Bubble size distribution model
BIO	Bedford Institute of Oceanography
CDOG	Clarkson Deepwater Oil and Gas
cm	Centimetre
C	Tuning coefficient
COOGER	Center for Offshore Oil, Gas and Energy Research
DWH	Deepwater Horizon
DSD	Droplet Size Distribution
DOR	Dispersant to oil ratio
d	Droplet size
D	Diameter of release nozzle
d_{50}/D	The relative median droplet size
d_{50}	Median Volume droplet diameter
d_i	Diameter of droplets (i)
d_j	Breakage of droplets diameter (a larger)
d_n	Top diameter value of each bins
d_{n-1}	Top diameter value of previous bins
d_m	The median diameter value
d_p	Peak droplet diameter
d/d_{50}	Relative droplet diameters
Ec	Average excess of surface energy
Ev	Resistance Energy
e	Energy of the turbulent eddy
exp	Exponential function
f	Probability density function
f_N	Number-based probability density function
fv	Volume based probability density function
$g(d_i)$	Breakage rate
g/mL	Gram per milliliter
IFT	Interfacial tension
IFO-120	Intermediate Fuel Oil 120
k	Coefficient
k_b	Droplet breakage
LISST	Laser In-Situ Scattering and Transmissometry
m	Meter
mm	Millimetre
MIT	Massachusetts Institute of Technology
MWN	Modified Weber Number
MPa	Megapascal
MEF	Maximum Entropy Formalism

m^3	Million cubic metres
mL	Milliliter
mPa·s	MilliPascal seconds
mN/m	Millinewton per meter
NS	Nova Scotia
NL	Newfoundland and Labrador
NaCl	Sodium chloride
n	Number concentration of droplets diameter at a given time
n_e	Number concentration of eddies
No.	Number
N	North
SINTEF	The Foundation for Scientific and Industrial Research
sec.	Second
OSCAR	Oil Spill Contingency and Response
PDPA	Phase Doppler Particle Analyzer
PDF	Probability Density Function
PBE	Population balance equation
Psi	Pounds per square inch
ROVs	Remotely Operated Vehicles
RPM	Revolutions per minute
Re	Reynold number
R^2	Regression coefficient
TAMOC	Texas A&M Oil spill Calculator
µm	Micrometre
UH	University of Hawaii
UHP	Ultra-High Purity
u*	Non-dimensional droplet velocity
u_e	Turbulent velocity of an eddy
u_d	Droplet velocity
Vi	Viscosity number
V (d)	Cumulative volume fraction
ΔV	Volume fraction for each size bin
V_n	Volume fraction for size n
V_{n-1}	Volume fraction for size n-1
VMD	Volume median diameter
wt%	Weight percentage
We	Weber number
We^*	Modified Weber number
W	West
X	Values of DORs
Y	Values of empirical coefficient (A)
δ_{max}	Maximum droplet size
δ_{30}	The mass mean volume equivalent
δ_{32}	Sauter mean (Volume surface) diameter
δ^*	Non-dimensional droplet diameter
λ_i	The Lagrangian multiplier

α	Spreading parameter
α_1	Spreading parameter for droplet size smaller than median diameter
α_2	Spreading parameter for droplet size smaller than median diameter
β (d_i,d_j)	The breakage probability density function
Γ (d_k,d_j)	Droplet coalescence rate
θ	Constant value
°C	Temperature degree
*	Data were not considered
/	Data is unavailable
%	Percentage

ACKNOWLEDGEMENTS

I would like to express my sincere gratitude to my supervisor Dr. Haibo Niu, for his guidance and support throughout my graduate life. His patient and perpetual energy has motivated me, and it is always being a pleasure to work for him. I would also like to thank my co-supervisor professor Lei Liu for his support and guidance on my research work as well as graduate life. Meanwhile, thanks also extend to my committee members Dr. Mysore Satish and Dr. Quan Sophia He whose work improve my research. Thanks to all of them for their excellent supervision and guidance throughout my graduate life at Dalhousie University, without their support this thesis would not be possible.

Thank also extend to the faculty and staff in the Graduate Environmental Engineering Program, especially Ms. June Ferguson for her patient helping me out on many of administrative affairs. I also gratefully acknowledge the Centre for Offshore Oil, Gas, and Energy Research (COOGER), Fisheries and Oceans Canada, Bedford Institute of Oceanography, Marine Environmental Observation Prediction and Response (MEOPAR) Network, and Natural Sciences and Engineering Research Council of Canada (NSERC) for financial support. Personal thanks to the staffs from COOGER: Brain Robinson, Tom King, Patrick Toole, Claire Mclntyre, Scott Ryan, for their help during the research. Without their help, this experiment would not be done.

Last but no means least, I would like to express my deepest appreciation to my families for their struggle and hardship, as well as love and encouragement. Moreover, I want to thank my many friends who make my lift enjoyable and meaningful.

CHAPTER 1. INTRODUCTION

Offshore oil and gas exploration and recovery activities in shallow water (around 100 metres below the water surface) have been developed over more than 100 years around the world. These activities were expanded to deep water (water depth in excess of 500 metre) to meet the increasing demand for oil (Chen and Yapa, 2007; Zhang *et al*., 2002). According to the report presented by Cambridge Energy Research Associates, the amount of global deep water oil production is dramatically increasing (ExxonMobil, 2009). For example, in the Gulf of Mexico, the oil production from deep water wells rose by 30% with the growth of deep water exploration from 1996 to 1998 (Lane and LaBelle, 2000). It was further increased to 81% of total oil production from 1998 to 2010 (BSEE, 2015). In Canada, offshore oil exploration activities have also been expanded to deep water to meet the oil demand. For instance, *Shell* has conducted oil exploration activity off Nova Scotia, ranging from 1500 to 3500m of water depth (CNSOPB, 2013). Moreover, *Statoil* has undertaken geophysical activities in waters ranging from 2500 to 3000 metres in offshore Newfoundland, and analogous seismic surveys in the water depth ranging from 100 to 4000 m have also conducted by BP (British Petroleum) in Nova Scotia's offshore for future drilling (LGL Limited, 2011; BP, 2013).

During these exploration and production activities, oil blowout or leakage from wellheads may occur. In the offshore oil exploration history, a most serious deep water oil blowout incident, the Deepwater Horizon (DWH) blowout, occurred in the Gulf of Mexico (water depth over 1000 m) in 2010; around 4.93 million barrels of Macondo crude oil was released over three months. This disaster had strong negative effects on environmental, socio-economic activities and the ecology of this area. Even though subsurface oil blowout incidents do not occur as commonly as surface oil spills caused by transportation, the potential risk of subsurface oil spill is still highly concerning to scientists and the public. Once there is a large oil blowout from subsurface/deep water, oil may move quickly to the water surface and transport to sensitive coastline without valid countermeasures being applied immediately, and consequently, this results in serious damage to marine wildlife and coastal area (TFISG-OBCSET, 2010; OPT, 2015; Ortmann, 2012).

To better understand the behaviour of oil and gas release from deep water, several models, such as, DEEPBLOW (Johansen, 2000), OSCAR (Oil Spill Contingency and Response) model (Reed et al., 2000), CDOG (Clarkson Deepwater Oil and Gas) model (Zheng *et al*., 2002), and OILMAPDEEP (ASA, 2005) have been developed to simulate deepwater blowout and predict the fate and transport of oil, as well as to address the safety and environmental concerns (oil spill risk evaluation and contingency planning). More recently, TAMOC (Texas A&M Oil Spill Calculator) model has also been developed for more comprehensive simulations of oil spill (Socolofsky *et al*., 2015). These oil spill models answered the questions related to the fate and transport of oil from the subsurface, such as: the behaviour of oil plume before it reaches the surface; how long it will take for oil to reach the surface; where oil will surface; the amount of oil remaining in the water column and; how oil affects marine wildlife and environmental systems.

There are many parameters in an oil spill model that may affect the prediction of fate/transport of oil. Oil droplet size distribution is one of the most important parameters in oil spill models, determining the prediction results of the fate of oil in marine environments. Oil, released from the subsurface, breaks up into different sizes of oil droplets under the force of ambient conditions (wind, current and wave etc.). The sizes of oil droplets have strong effects on the ultimate fate of oil in the marine environment, such as whether oil will surface, and if so, when and where (Chen and Yapa, 2007; Bradvik *et al.*, 2013; Johansen *et al.*, 2013). A better understanding of how different sizes of oil droplets distribute from subsurface to water surface will help to increase the accuracy of model predictions (Chen and Yapa, 2003). However, there is little knowledge concerning the sizes of droplets formed in the subsurface and limited capability to predict their distribution. Currently, the prediction of oil droplet size distribution in deep water oil spill models is from empirical formulations. For instance, a field study called “DeepSpill” measured droplet sizes from deep water (of 844 metres).This data was widely used to validate the available droplet size distribution approaches, such as Maximum Entropy Formalism (MEF) (Johansen *et al*., 2003; Chen and Yapa, 2007).

Oil droplet size distribution formed in the subsurface can also be significantly affected by the application of subsurface chemical dispersant. The first time use of large amounts of subsurface chemical dispersant was in the DWH incident, and the dispersant

was directly injected into the wellhead at significant depth (around 1500m), with an aim to break the oil into small droplets, so the amount of oil that may have surfaced would be reduced to protect the sensitive shoreline (Thibodeaux *et al*., 2011 and Kujawinski, *et al*., 2011). According to the Federal Interagency Solution Group's report (2010), around 7,000m^3 of dispersant were used in the DWH incident. As expected, the results showed that subsurface chemical dispersants caused a significant reduction on the area of oil slick, and the volume of small droplets was increased over a large water column (Louis *et al*., 2011). However, the effects of chemical dispersant on oil droplet size distribution are not fully understood, and the existing laboratory and field studies on oil droplet size distribution from subsurface oil release are insufficient. Prior to this study, an available mesoscale laboratory experiment on distribution of oil droplet size, with and without chemical dispersant, was conducted by Brandvik *et al*. (2013) in a Tower Tank. More details about the results of measured oil droplet size for Brandvik *et al.* (2013) Tower Tank experiment is reviewed in Chapter 2.

Based on the Tower Tank experimental data (Brandvik *et al*., 2013), the Modified Weber Number (MWN) approach was developed to predict droplet size distribution. The MWN approach has been considered practical for predicting oil droplet size distribution, with and without the application of chemical dispersant, in a deep water oil blowout model (Johansen *et al.*, 2013). This Tower Tank experimental data (Brandvik *et al*., 2013), together with "DeepSpill" experimental data (Johansen *et al.*, 2001), was also used to validate other available subsurface oil droplet size approaches, such as VDROP-J approach and Droplet Size Distribution (DSD) approach (Zhao *et al*., 2014a; Nissanka and Yapa, 2015). However, Zhao, *et al*. (2016) doubted that the "DeepSpill" experimental data was accurate, due to the challenges in controlling the field environment and experimental conditions. In terms of droplet size distribution data gained from Tower Tank, only a light crude oil (Osebeg Blend) was used for experiments, and thus, the set of experimental data for oil and dispersant interaction was limited (Brandvik *et al*., 2013). In these experimental studies, the oil droplet size distribution of different types of oil and the effects of chemical dispersant on droplet size distribution were limited. These may limit the applicability of droplet size distribution approaches to other oils. Therefore, extensive experimental data on various types of oil, with and without chemical dispersant application, is urgently

needed to evaluate the performance of droplet size distribution approaches, and consequently, support the decision-making for subsurface dispersant application, over a range of oil types.

The objective of this study was to have a better understanding of droplet size distribution of different types of oil, with and without the effect of chemical dispersant, by conducting a series of experiments. Eventually, a more general approach in decision-making for subsurface dispersant application may be provided. The **specific objectives** of this study were to:

1. Conduct subsurface oil release experiments in a mesoscale test facility to measure droplet distribution of two different types of oil, with and without the chemical dispersant application.
2. Assess an existing approach for predicting oil droplet size distribution and improve the approach to achieve a better prediction of oil droplet size distribution from subsurface oil releases, with and without chemical dispersant.
3. Apply the improved droplet size distribution approach to study the effects of chemical dispersant application on the fate and transport of oil from a hypothetical subsurface release on the Scotian Shelf and provide support to decision-making for subsurface dispersant application.

To provide fundamental background information relating to subsurface oil release in marine environments, Chapter 2 reviews the information related to general fate of spilled oil, as well as the effect of chemical dispersant on spilled oil. Existing experimental studies and prediction approaches on oil droplet sizes, with and without application of dispersant, are also reviewed in this chapter. In Chapter 3, the experimental facilities and materials, as well as procedure on oil droplet size measurements, are described in details. The results and discussion of experiments are presented in Chapter 4, which include the effects of water temperature and dispersant on measured oil droplet size distribution, evaluation of the Modified Weber Number approach, and the proposal of using the Reynolds Number scaling for prediction of droplet size distribution. In Chapter 5, the sensitivity studies of oil spill model (OSCAR model) on droplet size distribution are presented, followed by case studies of the effects of chemical dispersant application on the fate and transport of oil from

subsurface release on the Scotian Shelf, by using the Reynold Number scaling approach. In Chapter 6, a summary of this research is provided, followed by the research contribution and recommendations.

CHAPTER 2. LITERATURE REVIEW

2.1 Fate of spilled oil in marine environments

The fate of spilled oil in the marine environment has been studied since oil transport and exploration activities began in the marine environment. A better understanding of the fate of oil in the marine environment can help to determine active responses for the most effective oil spill treatment. The most common oil spill incidents, in the marine environment, are caused by tanker incidents or oil loading and discharging activities, which result in medium or large sized spills occur in water surfaces or shallow water depths (ITOPF, 2016). Following an oil spill on the water surface, several oil weathering processes (Figure 2-1), such as: spreading, evaporation, natural dispersion, dissolution, emulsification, photo-oxidation, sedimentation, and biodegradation, occur immediately. These processes determine the ultimate fate of oil in the marine environment.

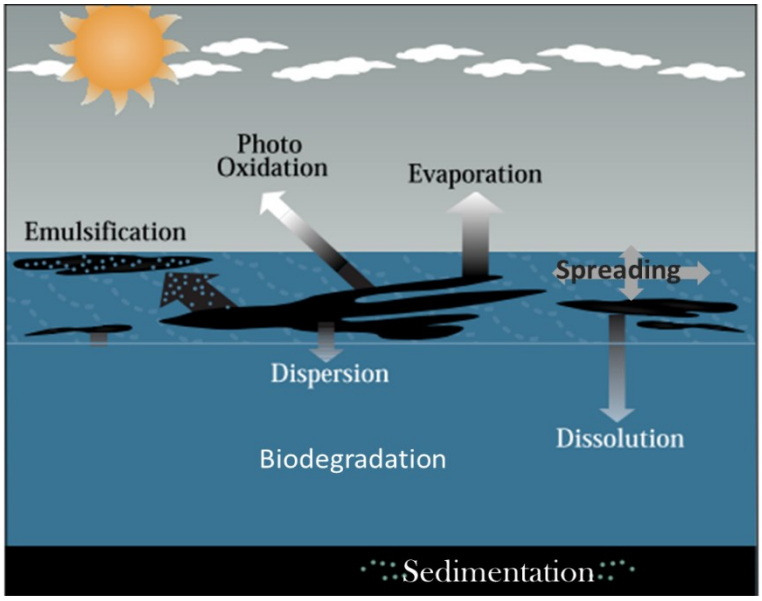

Figure 2-1: The weathering processing of spilled oil in the marine environment (Modified from NOAA, 2015)

These weathering processes occur continuously as time goes on. Spreading of oil occurs in the earliest stage of a spill, and it is a short term process. Once a volume spillage of oil occurs on water surface or near the water surface, the released oil can spread rapidly to a large area in form of oil slicks, this process is called spreading. Spreading process plays

a role in determining the thickness of oil slick, and also affects the performance of other processes (Reed, *et al.,* 1999). When oil spreads on the water surface, the light, and volatile compounds within oil mixture will evaporate to the atmosphere, this process is called evaporation process (ITOPF, 2014). The very surface layer of oil slick can react with oxygen causing photo-oxidation process. In this process, oil can be broken into soluble products or persistent compounds; but this is a slow process, and needs strong sunlight condition. Under the force of winds and ocean surface currents, oil slick can be broken into small oil droplets and dispersed into the water column, which is called natural dispersion. Dispersed oil (droplets) can have greater surface to volume ratio which boost the occurrences of other processes, such as dissolution, emulsification, biodegradation and sedimentation. Therefore, dispersion process is an important process which play a critical role in the fate/transport of the oil. Some dispersed oil in the marine environment can take up water, forming a stable water-in-oil emulsion. This emulsion can persist crude oil on the sea surface or shoreline, and have impacts on the response options. When oil dispersed into the water column, the light aromatic hydrocarbon compounds of dispersed oil can be dissolved. During oil spill, microorganisms, in the marine, consume nitrogenous and sulfur compounds of oil as their nutrient sources, helping to partially or completely degrade oil to water soluble compounds, this process is called biodegradation. The compounds of oil which is indigestible and non-dispersible, can associate with some heavier suspended solid in the water column and form sediment particles or organic matter compounds sink into seabed. This is called sedimentation. If oil released away from the seabed, sedimentation may not occur.

Oil property, as one of the most critical factors, affect these weathering processes. This includes viscosity, density, API gravity, surface and interfacial tension and multicomponent composition and so on. For instance, the effect of oil viscosity on weathering processes had been previously studied. When the viscosity is low, the rate of spreading is generally high, resulting in a larger spilling area and reduced thickness of oil slick (Reed, *et al*., 1999). Moreover, low viscous oil can also be dispersed easier, which is easier for other weathering process occurs. If oil contains a high fraction of water-soluble compounds (e.g. benzene, toluene), more oil can be dissolved. If oil spill on water surface, these water soluble compounds (are also volatile compounds) can be reduced

faster by evaporation than dissolution, and consequently the total amount of the remaining oil can be reduced as well (Fingas, 2011). The properties of oil also affect the biodegradation rate. Oil may be more degradable when oil contains large compounds of nitrogen and phosphorus (ITOPF, 2016).

Besides oil properties, weathering processes also depend on the marine environmental conditions (ambient temperatures, winds, currents, and waves). In general, the rate of weathering will be increased under the increasing ambient water temperature, forcing of winds, currents and wave. Under the relatively strong current and wave action, the spreading rate of oil can be increased, moving to large area; as well strong current and wave also can break the oil into different droplet sizes quickly, which can help oil be dispersed, dissolved and biodegraded (ITOPF, 2002). The high wind speed and ambient temperatures can help to increase the evaporative loss of oil (Cappello *et al.*, 2004) and the ambient temperatures can also affect the biodegraded rate of oil through increasing the activity of microorganisms (Venosa and Zhu, 2003). The effects of oil properties and environmental conditions on weathering processes have been well studied and reported in several papers (Huang, 2005; Lehr, 2001; Reed *et al.*, 1999; ASCE, 1996; Sebastiao and Soares, 1995; Spaulding, 1988; Fay, 1971).

The behaviours of oil from the subsurface or deep water release (water depth greater than 500m) are even more complex than that from the surface or shallow water depth, meaning that the fate of oil from subsurface oil release is different from the surface oil release. In addition to that of the transport process of surface oil spill, the transport of subsurface oil release can be divided into two behaviours: underwater behaviour, and water surface behaviour (Faaneløp and Sjøen, 1980). In the underwater behaviour, high pressure and low water temperature in the underwater environment can result in different states of oil/gas, for example, gas hydrate may be formed which could affect the fate of release oil.

Figure 2-2 shows the underwater behaviours of oil/gas in a deepwater oil/gas blowout. The trajectory of released oil are different at the near-field process and the far-field process. In the near-field, four phases of oil and gas, including oil, water, gas and gas hydrate, may exist (Yapa *et al.*, 2012). In the early stage of a blowout (near-field process), the oil plume saturates with gas/gas hydrate rising as conical in shape. The overall buoyancy of oil plume

is increased with the increasing gas volume (Yapa *et al.*, 2001; Chen and Yapa, 2012). Due to the force of cross-current flow and buoyancy, the oil and gas plume rise to natural buoyancy level. In this stage (near-field), the oil and gas (or gas hydrate) plume will be bent if the cross current is strong enough. Gas/gas hydrate could be separated from this bent plume. The separated gas dissolves into water or rise along to water surface, and gas hydrate could be decomposed. Oil droplets move from the near-field to the far-field (Cooper *et al.*, 1990; Rye *et al.*, 1996). In the far-field stage, the trajectory of oil would be different due to the separation of gas/gas hydrate, this separation can significantly change the buoyancy of plume and eventually, affect the behaviour of oil (Chen and Yapa, 2004a).

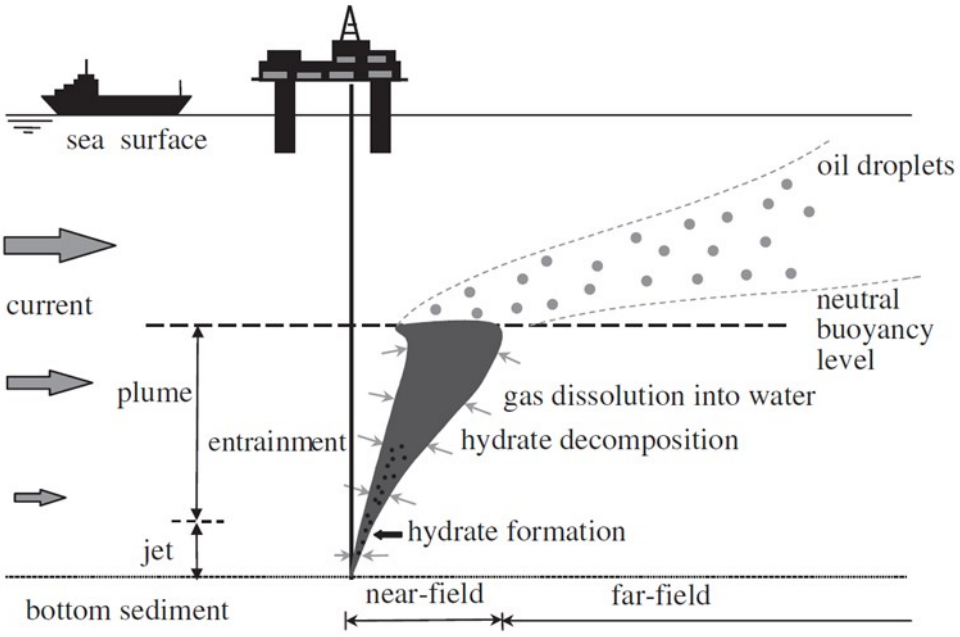

Figure 2-2: Deep water oil/gas blowout (Zheng *et al.*, 2002)

Based on the deepwater oil blowout studies (Yapa and Zheng, 1997; Yapa *et al.*, 2001; Zheng *et al.*, 2003; Johansen, 2003), several oil spill models were developed to simulate the behaviour of oil/gas from deepwater blowout since the late of 1990's, such as Clarkson Deepwater Oil and Gas model (CDOG) (Yapa and Chen, 2004), DEEPBLOW model (Johansen, 2000), and TEXAS A&W Oilspill Calculator (TAMOC) (Socolofsky *et al.*, 2015). In these models, the behaviours of different phases (oil, water, gas and gas hydrate) from deepwater blowout are performed. These models assist in overall oil spill prediction models, such as OILMAP DEEP model (RPS ASA, 2017) and Oil Spill

Contingency and Response (OSCAR) model (SINTEF Marine Modeling Group, 2015), to provide rapid prediction of the trajectory of released oil from deep water, quantify the impact of release oil and help on decision-making of contingency planning.

2.2 Effects of chemical dispersant

In order to significantly reduce the damage of a large amount of oil spill on surface-dwelling organisms (e.g. seabird) and sensitive coastline (coastal habitats and facilities), several countermeasures, such as booms, in-situ burning, skimming and chemical dispersant, are taken. Booms, in-situ burning and skimming are mechanical containments, which can be easily applied on surface oil spill to reduce the area of oil slick, but application of these methods has requirement on sea surface condition, for example, the idea condition for skimming is applied to a fairly calm sea surface for reducing thick oil slicks.

Chemical dispersant, as chemical containments, can be sprayed on oil slick to disperse oil into water columns. The role of chemical dispersant, applying on an oil spill, is to enhance the rate of dispersion through significantly reducing interfacial tension (IFT) between oil and water, which can effective to break oil droplets into small sizes and result in significant reduction of oil slick on water surface (Wells and Harris, 1980; Wells, 1984; Anderson *et al.*, 1985; NRC, 1988; Caneveri *et al.*, 1989; TFISG-OBCSET, 2010). The application of chemical dispersant on affected sea surface area has less requirement on sea condition, which could be easier applied to reduce the oil slicks on water surface, in addition to reduce the effect of oil on sensitive shorelines and coastal habitats.

Over time, the application of chemical dispersant can help to greatly reduce the surface oil, and the rates of some weathering processes (e.g. dissolution, biodegradation) can also be increased. According to the National Research Council report in 1989, chemical dispersant can be a main response option for a large amount of oil released in rough sea or subsurface/deep water through increasing the rate of dispersion and dissolution of oil into water columns, and it could eventually reduce the damage of oil on the water surface and coastline. In terms of chemical dispersant apply on subsurface release, a well-known example dispersant was in the DWH incident. The application result showed a significant reduce on the forming area of oil slicks (Lee, 2012). On the previous chemical dispersant research, most of them focused on the effect of chemical dispersant on the surface oil slick,

but the effectiveness of chemical dispersant, applied on subsurface oil release, still has not been well understood. Currently, exist researches of effects on the effectiveness of chemical dispersant were mainly focus on oil properties, marine environmental factors and the types of chemical dispersant.

Experiments indicated that the interfacial tension (IFT) between oil and water decrease with the application of chemical dispersant, which the value can significantly drop with the increasing dosage of dispersant (Khelifa and So, 1998). Generally, oil with high viscous tend to be more difficult to disperse than those with low viscosities (Strøm-Kristiansen *et al*., 1997). On an ocean surface testing, the measurement of oil droplet sizes showed that the number of small droplet sizes (<70μm) with chemical dispersant application was larger than that without chemical dispersant application (Lunel, 1993 and 1995). In addition, the effectiveness of dispersant is higher for fresh oil than weathered oil, which is mainly affected by the formation of emulsions (NRC, 1988). Strøm-Kristiansen *et al*. (1997) also stated that other properties (e.g. wax and asphaltene content) also affect the oil weathering, further influence the effectiveness of chemical dispersant.

Except the effect of oil properties and weathering process, the environmental factors (e.g. temperature, mixing energy and salinity) also affect the performance of dispersant (Lunel, 1993). In order to understand the effects of environmental conditions on chemical dispersants, several researches were conducted. A research had investigated the impact of salinity and mixing energy on the effectiveness of dispersant (Chandrasekar, *et al*., 2006). The results showed that salinity, mixing energy have effect on the dispersant effectiveness. Mixing energy has pronounced positive effect on dispersant efficiency, the effect of mixing energy is also reported in other studies (Chandrasekar *et al*., 2005; Ma *et al*., 2008, Li *et al*., 2009a). Chandrasekar, *et al.* (2006) also reported that the effect of salinity plays an important role on the dispersant effectiveness at higher temperature. Except these, in Li *et al*. (2009a) research, they studied the effects of different energy dissipation rate (regular non-breaking wave, low-energy spilling wave and plunging breaking wave) on dispersant effectiveness. The result showed that higher energy dissipation rate can help to increase the amount of small droplet sizes, as well, increase oil concentration in the water column. It indicated that energy dissipation rate plays a crucial role in the effectiveness of dispersant and the size of dispersed droplets. (Li *et al*., 2009a).

In several chemical dispersant researches, some research pointed out the effectiveness of different types of chemical dispersant can be different to treat different types of oil. For example, In Li *et al.*, (2009b) study, two dispersants, oil-based dispersant (Corexit 9500) and water-based dispersant (SPC1000), were used to disperse two oils with different wave conditions. The results showed that both dispersants can significantly reduce the oil droplet sizes, but the effectiveness of Corexit 9500 is 48% while that of the SPC1000 is 26%. According to the studied done at SINTEF, Corexit 9500 was confirmed effectiveness on high viscosity (> 17,600cP) oil (Daling, 1996). These studies' results indicated that the effectiveness of chemical dispersant can be affected by the chemical dispersant types. Properly selection of chemical dispersant can help to improve the efficiency of oil dispersion.

On these experimental testing of the effectiveness of chemical dispersant, it has been suggested that oil droplet sizes distribution is an important measurement for the performance of dispersant, as well affects the estimation of the fate of the oil (Chapman *et al*., 2007; NRC, 2005; Masutani & Adams, 2000; Socolofsky & Adams, 2000). For example, study by Li *et al*. (2009b) evaluated the effectiveness of dispersant by measuring oil droplet sizes distribution data. In their experiment, a large amount of small oil droplets (<70μm) was measured throughout the entire experiment under the effect of dispersant (Corexit 9500). With increased time for dispersion, more droplet sizes were dispersed into smaller sizes, leading to higher dispersant effectiveness. However, these studies and measurements are mainly focused on water surface. Since the DWH incident occurred, the effects of chemical dispersant on the fate of oil (oil droplets) from the subsurface oil spill, especially in deep water, attracted more attentions.

There were limited laboratory studies conducted to investigate the effect of chemical dispersant applying on a subsurface oil releases after the DWH incident. Brandvik *et al.* (2013) conducted a mesoscale experiment to investigate the effect of release conditions and dispersant on the subsurface oil release through measuring droplet sizes. The results indicated the increased dispersant to oil ratios (DORs) help to significantly increase the amount of smaller droplet sizes. However, this experiment only used a light viscous crude oil as experimental oil, how the chemical dispersant affect the heavy viscous crude oil was

not indicated in study. It needs more experiments to investigate the effect of dispersant on different oil types.

Better understanding of the effectiveness of chemical dispersant on different oil types and the sizes of dispersed oil droplets in different testing conditions can support the guideline of the application of chemical dispersant on both water surface and subsurface oil release and reduce potential risks of oil in the marine environment. So far, it is still not well understood the effect of dispersant on oil droplet size form in subsurface/deepwater with limited experimental and field droplet size data.

2.3 Oil droplet sizes from subsurface/deep water oil release

It was stated in previous oil release studies that the fate of oil in the marine environment is strongly affected by the size of oil droplets. Oil/gas released from deep water, oil droplets can be separated from the oil and gas/gas hydrate mixture under the effect of surrounding marine environmental factors. The separated oil transport laterally over the sea from deep water for a prolonged period which can result in the sizes of droplets formed in subsurface oil release tend to be smaller than those form in surface oil release (Paris *et al.*, 2012; Johansen *et al.,* 2003; Zheng *et al.*, 2002; Rye *et al.*, 1996; Cooper *et al.*, 1990). Small or finer oil droplets ($d \leq 100\mu m$) could be dissolved into water columns, while relatively large oil droplets ($d > 100\mu m$) could rise to the water surface with different surfacing time and locations. Generally, from a deep water oil blowout incident, droplets, size larger than 500µm, move faster to the water surface, while droplets, size from 100µm to 500µm, may take days or weeks to the surface. Overall, in a subsurface/deep water oil blowout, the size of droplets have significant influence on the dissolution of oil in the water column, rising velocity of oil droplets, the underwater vertical transport time of oil, oil surfacing time and the behaviour of surface appearance (slick formation), sizes of droplets play a role in determining the effect of oil on the marine or sensitivity coastal environments (Rygg and Emilsen, 1998; Li and Garrett, 1998; Johansen, 1999; Grisolia-Santos and Spaulding, 2000; Yapa and Chen, 2004a; Ryerson *et al.*, 2012).

A well-known example of chemical dispersant injected into deep water is in DWH, around 7 million litres of dispersant were applied to reduce the impacts of spilled oil (Lehr, *et al*., 2010). The consequence of the application of subsurface chemical dispersant showed

a significant reduction in the area of oil slick after 11 hours' injection, inhibiting the emulsions and preventing oil spread over a large area on the water surface. In addition, the impact of spilled oil on coastal or marine habitats was also reduced (Kujawinski, *et al*., 2011). However, the effect of chemical dispersant on the fate of the oil was not fully understood. More researches still need to be conducted to trace the ultimate fate of different oil droplets.

In the study of how the fate of oil changed when chemical dispersants were applied in deep water, "Under water plumes", as a common term, was presented (Yapa *et al.*, 2012). This term means the relative small droplets sizes or fine droplet sizes stay submerged for a long time forming underwater plumes. Yapa *et al.* (2012) utilized experimental data from the "DeepSpill" experiments (Johansen *et al.*, 2003) to estimate the droplet sizes by adding dispersant. The result presented that the volume of droplet sizes ranged from 7 to 8mm has dropped significantly, while the volume of droplet sizes ranged from smaller sizes (0-2mm) has increased after chemical dispersant was applied. There was only a few small laboratory scale studies have been done to investigate of oil droplet size distribution from subsurface oil release (Masutani and Adams, 2001; Tang and Masutani, 2003). The reliability of experimental data from these small-scale experiments convert into the real world still need to be verified. Furthermore, the effect of chemical dispersant on droplet size distribution is also limited, in these oil droplet size distribution studies. A recent study, the Tower Tank experiment, was conducted to investigate oil droplet size distribution from subsurface oil release with subsurface dispersant injection (Brandvik *et al.*, 2013). Different dispersant to oil ratios (DORs) were used to test the effect of dosage of dispersant on droplet size distribution. The droplet size data illustrated that the application of the higher dosage of chemical dispersant has a significant effect on increasing the amount of small droplet sizes.

According to previous studies, oil droplet sizes form from deep water oil blowout play an important role in determining the prediction of oil surfacing situation. Therefore, well predicted droplet size distribution, with and without application of chemical dispersant, can improve the performance of an oil spill model on simulation of the fate/transport of oil in deep water and support the decision-making of valid countermeasure for different oil spill.

2.4 Experimental studies of subsurface oil droplet sizes

The studies on simulating the behaviours of oil from subsurface/deepwater oil spill have been conducted for several decades (Bandara and Yapa, 2011; Dasanayaka and Yapa, 2009; Chen and Yapa, 2004a; Johansen, 2003; Fanneløp and Sjøen, 1980). Most of studies were mainly focused on the thermodynamics and hydrodynamics of oil jet/plume. Only limited experimental studies were conducted to record the subsurface oil droplet size distribution. The earliest work was laboratory oval cross section tank experiments which were done by Topham Topham (1975). After two decades, several experiments on measuring oil droplets size were conducted by several researches and reviewed as follows (Masutani and Adams, 2001; Johansen *et al*., 2003; Brandivik *et al*., 2013; Zhao, *et al*., 2016).

2.4.1 Field experiment

2.4.1.1 "DeepSpill" experiment

The "DeepSpill" experiment is a field deep water oil release experiment. It was operated in the coastal Norway, where oil and gas were discharged from a water depth of 844 metres (Johansen *et al*., 2001). There was a total of four releases conducted: nitrogen gas and sea water; diesel and LNG; crude oil and LNG (liquefied natural gas); and LNG and sea water. Two Remotely Operated Vehicles (ROVs) were used to capture the image of oil droplet size distribution and plume formation. This designed field experiment help to reveal physical processes of the trajectory of oil in water columns and provide baseline data for model validation, improving the accurate prediction of different methods. The results related to droplet size from the "DeepSpill" experiment were concluded:

- During these four experiments, the particle size distribution of diesel was observed at different depths from the release point, and the overall size range of diesel droplet was from 1 to 10 mm. The droplet sizes of crude oil were not presented.
- The droplet size data was also compared with the simulation results from DeepBlow model. The model results showed a good agreement with the observations.

Currently, this experiment was only one performing a deep water oil release in a realistic ocean environment. However, due to the limited observation of droplet size data,

the study did not answer the question whether the DeepBlow model would have a good agreement with crude oil droplet size data. As well, this experiment did not study the effect of subsurface chemical dispersant on droplet size.

2.4.2 Laboratory experiments

2.4.2.1 Oval cross section tank experiment

Oval cross section tank experiment probably was the earliest laboratory study, investigating the behaviour of oil/gas from subsurface oil/gas release (Topham, 1975). This study utilized two different crude oils, the Norman Wells crude oil and the Swan Hills crude oil, in an oval cross section tank with 1.5m water depth and 68 L of water capability to study the oil droplet sizes. Gas and oil were released from different pipe sizes (0.64 cm, 2.2 cm, 7.6 cm, and 14.7cm) with different gas exit velocity (1.9 m/sec and 14 m/sec) in fresh water and sea water. Droplet sizes were analyzed from photographs. The oil droplets size results showed that:

- In large pipe diameter (7.6 cm and 14.7 cm), the flow velocity was higher than smaller pipe size (0.64 cm and 2.2 cm), which produced relative smaller droplet size (seem to less than 0.5mm). However, due to the limitation of the apparatus, it was hard to analyze how small it was.
- In general, the measured sized of a large amount of oil droplets was ranged from 0.5 to 1.0mm for both oils in both sea water and fresh water.
- For the employed microscopic photography, the peak droplet size diameter for Swan Hills crude oil was 15 μm under the small pipe size (2.2 cm) with gas exit velocity of 1.9m/s.
- Swan Hill crude oil may form stable emulsions on water surface while the Norman well crude oil form stable emulsions.

In this oval cross section tank study, the effect of exit diameter on different oils were presented through droplet sizes measuring. However, due to the limitation of apparatus, oil droplet sizes were not fully measured for both oils. A better measuring apparatus was required for later study.

2.4.2.2 Jet Breakup experiment

The Jet Breakup experiment is a part of experimental studies of multi-phase plumes of oil/gas from deep water oil spill, conducted by Masutani and Adams (2001) at the University of Hawaii (UH) in collaboration with Massachusetts Institute of Technology (MIT). These lab-scale experiments investigated the behaviour of oil/gas released from the deep water and the resulting dispersed droplet size. An open water tank with atmospheric pressures was used in this experiment and four different crude oils (Genesis, MarTLP, Neptune SPAR and Plateform Gail) were selected. In addition, pure silicone fluid was selected as stable fluid to supplement the crude oil results. The experimental water tank can be filled up with 400L of water. Three orifice diameters (1, 2 and 5mm) were used in their study. Oil was discharged vertically upward from the bottom of the tank. A digital video camera and PDPA (Phase Doppler Particle Analyzer) measured the oil droplet size, respectively. Two cameras were installed to record the jet structure. The experiment was conducted under very low or high flow rate. The length of jet breakup and size of larger droplets can be directly measured from the resulting images. The results are summarized as followed:

- When oil injected from 2 mm diameter orifice, different instability regimes were observed with the increasing oil discharge velocity. Larger droplet sizes were observed near the discharge nozzle with lower discharge velocity. With the increasing of velocity, sinuous instability plume was generated. A higher velocity can result in a poly-dispersion of droplets and the fraction of fine droplets also increased.
- For Neptune SPAR crude oil, fewer droplet sizes less than 3mm were detected through a 2mm of diameter orifice. Even though the jet velocity was increased, the number of smaller droplet size were still not detected.
- Through the observation of silicone fluid experiment, multi-modal distribution was observed and more volume fraction of fine droplets (less than 500μm) was detected with the increasing velocity.

Although the Jet experiment was a small scale, it provided the concept of different plume types and also supported a general the development of prediction of droplet size. However, the measurement of droplet sizes data was limited, no data was measured with

the application of chemical dispersant, and due to the experiment was small lab scale, the result may not suitable to extrapolate to full size deep water oil blowout. It was recommended that meso- or large scale test facility should be utilized to simulate the deep water oil spill in real world. The techniques for full measuring droplet size distribution data also needed to be improved.

2.4.2.3 Tower Tank experiments

Tower Tank experiment was a mesoscale experiment conducted recently in a water tower basin with a volume of 40m^3. Oil droplet breakup from a subsurface oil release was studied in this experiment (Brandivik *et al*., 2013). Compared with previous studies, the effect of chemical dispersant on droplet size distribution was considered in here. Only one type of oil (Oseberg Blend) with and without the injection of dispersant (Corexit 9500) was used in their experiment. The effect of various factors, such as release nozzle diameter (ranged from 0.5 to 3mm), dispersant to oil ratio (DOR from 0 to 1:25) and release flow rate (from 0.2 to 5 L/min) were studied. Oil droplet size distribution and data was measured by LISST-100X. The main findings of this experiment includes:

- The measured oil droplet size in this experiment ranged from 5 to 500μm for cases with and without chemical dispersant.
- A large volume fraction of smaller oil droplet size was observed with higher oil flow rate when the same nozzle diameter was used. Under the same flow rate condition, a smaller nozzle diameter can help to break down large oil droplet size to smaller one.
- When flow rate was 1.2 L/min, dispersant with DOR of 1:1000 and 1:500 has neglect effect on the droplet size. However, higher DOR (1:100, 1:50 and 1:25) can significantly reduce the larger droplets to smaller sizes.
- The data from different release conditions without the injection of dispersant in the experiment was apparently fit to Weber Number approach. However, when dispersant was involved, the data did not fit Weber Number approach very well. Instead, it fit to a new droplet breakup method—Modified Weber Number (MWN) approach (Johansen *et al.,* 2013). The Modified Weber Number approach provided a better fit to both experimental data with and without injection of dispersant.

Based on the Tower Tank experimental data, a modified approach was proposed to predict oil droplet size distribution, with and without the injection of chemical dispersant, which also help to improve the oil droplet size distribution prediction in a realistic subsea oil blowout. However, the Tower Tank experiments only utilized a light crude oil (Oseberg Blend) to validate the effectiveness of the modified approach, whether MWN approach also is applicable to other oil types (medium or heavy oil type) need to be studied. Based on the Tower Tank experiments, different oil types experiments are suggested in the future study.

2.4.2.4 Ohmsett wave tank experiments

Most recently, a larger underwater oil release experiment was conducted in the Ohmsett wave tank facility. This tank is the largest facility for oil spill research in North America with the dimension of 203m ×20m ×2.4m (Zhao, et al., 2016). Oil release from a horizontal underwater release nozzle (d=25.4mm). A fuel oil, JP5 with density of 820kg/m^3, was used in the experiment. Experiment utilized LISST-100X and GoPro to collect the droplet size distribution data and record the oil plume. Experiment focus on measuring the trajectory and velocity of oil plume and oil droplet size distribution. The resultant data was used to validate the prediction models, JETLAG and VDROP-J. The findings relevant to oil droplet size distribution are:

- Two peak volume droplet sizes were observed at 280μm and 460μm.
- Under a good predicted initial droplet size (700μm), the droplet size distribution data predicted by VDROP-J model showed a good match to the observed data, but the predicted d_{50} (320μm) was slightly different to the observed d_{50} (240μm).

To some extent, the droplet size distribution data from this large scale underwater oil release experiment provided much closer to an actual underwater oil release. However, the experiment only used fuel oil as experimental oil and how the effect of chemical dispersant on the oil release was not presented. In addition, there is not available model for predicting initial droplet size exist, which could be a challenge for using the resultant data to validate the VDROP-J model.

2.5 Prediction Approaches for droplet size distribution

According to the limited experimental data on oil droplet size distribution data, up to date, several approaches have been developed to predict subsurface oil droplet size distribution. The Maximum Entropy Formalism (MEF) approach (Chen and Yapa, 2007) and the Modified Weber Number approach (Johansen *et al.*, 2013) are two empirical approaches. While the VDROP-J approach (Zhao *et al*., 2014a) and the Droplet Size Distribution (DSD) model (Nissanka and Yapa, 2015) are two dynamic approaches developed from numerous mathematics. These available oil droplet size distribution approaches have been validated by using the limited "Deepspill" experimental data (Johansen *et al.*, 2001) and Tower Tank experimental data (Brandvik *et al.*, 2013). However, these models still have shortcomings on the estimation of oil droplet size distribution, especially that with chemical dispersant application.

2.5.1 Empirical approaches

2.5.1.1 Maximum Entropy Formalism (MEF) approach

In order to predict droplet size distribution, Probability Density Function (PDF) (e.g. Rosin-Rammler or Nukiyama-Tanasawa distribution), as established corrections, are used. However, these corrections require more theoretical foundations to predict droplet size distribution. The MEF approach was proposed by Chen and Yapa (2007) to provide a good estimate of PDF, and then provide best estimation on droplet size distribution.

Several Characteristic sizes (e.g., δ_{max}, δ_{30} or δ_{32}) are used to connect with probability density function (PDF) for estimating droplet size spectrum. According to Karabelas (1978) and rye *et al*. (1996), the diameter of the nozzle (*D*) and Weber number (*We*) can be used to determine the maximum droplet size δ_{max}:

$$\delta_{max} = kDWe^{-0.6} \quad (1)$$

Where *k* is a coefficient, and it will be influenced by different effects (such as oil properties and the presence of gas)

$$We = \rho U^2 D/\sigma \quad (2)$$

Where:

We: weber number

D : Release nozzle size

ρ: Density of liquid in the jet

U: Exit velocity

σ: Interfacial tension

The mass mean volume equivalent (δ_{30}) and the Sauter mean (Volume surface) diameter (δ_{32}) can be easily calculated, by knowing δ_{max} and f:

$$\delta_{30} = (\int_0^{\delta max} f \cdot \delta^3 \, d\delta)^{1/3} \quad (3)$$

$$\delta_{32} = (\int_0^{\delta_{max}} f \cdot \delta^2 d\delta)^{-1} \delta_{30}^3 \quad (4)$$

The form of the probability density function (PDF) f is:

$$f = 3\delta^{*2} \exp [-\lambda_0 - \lambda_1 \delta^{*3} - \lambda_2 \delta^{*3} u^* - \lambda_3 (\delta^{*3} u^{*2} + \delta^{*2} B)] \quad (5)$$

Where:

δ^* : Non-dimensional droplet diameter

u*: Non-dimensional droplet velocity

λ_i : The Lagrangian multiplier

The estimated droplet size distribution data by using the MEF approach has been compared with the "DeepSpill" field data (droplet size range from 1 to 10 mm). The result of the simulation showed a good agreement with the limited observed data. Although MEF model was concluded as a promising method with the least amount of bias on the estimation of oil droplet size distribution, it was only validated with "DeepSpill" experiment. The effects of oil properties and chemical dispersant on oil droplet size have not been considered. Further studies are required to overcome the limitations.

2.5.1.2 Modified Weber Number Approach

As reviewed previously, the MEF approach has not considered the effect of chemical dispersant on droplet size distribution. However, the application of chemical dispersant, is one of the response. For example, a well-known subsurface application of chemical dispersant was on the DWH incident. The subsurface application of chemical dispersant showed a high efficiency method on reducing the surface oil slicks from subsurface oil blowout. Therefore, in order to have better understanding on predicting droplet size distributions with the chemical dispersant application, there is an urgent need to have approach with the consideration of the effect of chemical dispersant on droplet size distribution prediction.

To predict oil droplet sizes with and without the injection of chemical dispersant, Johansen *et al.* (2013) had proposed the Modified Weber Number (MWN) (Eq. (6) approach based on their Tower Tank experimental data. The Modified Weber Number scaling (Eq. (7) was developed to predict volume median droplet size for subsurface oil and gas releases.

$$We^{*}=We/\left[1+0.8\,Vi(d_{50}/D)^{1/3}\right] \tag{6}$$

Where:

We^{*}: Modified Weber number

We: weber number, Eq.**Error! Reference source not found.**

d_{50}/D: The relative droplet size

d_{50} : Median droplet diameter

D : Release nozzle size

Vi: Viscosity number

The Modified Weber number scaling can be simply expressed as

$$d_{50}/D = \mathrm{AWe}^{*-3/5} \quad (7)$$

Where *A*, an empirical coefficient with a value of 15, was estimated by the gained experimental droplet sizes data, with DORs ranging from 0 to 1:50 (Brandvik, *et al*., 2013; Johansen *et al*., 2013).

Once the d_{50} was determined from Eq.(7), the statistic droplet size distribution can be estimated using either lognormal distribution or Rosin-Rammler distribution (Eq.(8). Compared these two distribution functions, neither of the distribution functions provided a perfect fit to experimental data. Generally, Rosin-Rammler distribution has a better overall fit to the experimental data than the lognormal distribution with spreading parameter α=1.8 (Johansen *et al*., 2013).

$$\mathrm{V}(d)=1\text{-}\exp\left[-0.693\left(\frac{d}{d_{50}}\right)^{\alpha}\right] \quad (8)$$

Where:

$V(d)$:Cumulative volume fraction

d/d_{50}: Relative droplet diameter

α: Speading parameter

Compared with the MEF approach, the MWN approach integrated with Rosin-Rammler distribution is expected to have more accuracy on the prediction of oil droplet size distribution with the consideration of chemical dispersant application. However, the empirical coefficients were determined by using limited Tower Tank data, and there was no evidence showing that empirical coefficients will not change to other content for different oil types or higher DORs. The approach need to be validated against more experimental data to investigate the applicability of empirical coefficients on different oil types.

2.5.2 Dynamical approaches

Except the empirical approaches (the MEF approach and the MWN approach) proposed from experimental data, there were two population dynamic approaches were

develop for the droplet size distribution. These dynamic approaches were composed of differential equations numerically, the details are presented in the following.

2.5.2.1 VDROP-J approach

VDROP-J is a numerical approach, extended from VDROP model, was developed to predict droplet sizes for both low and high viscous oil in the subsurface fluctuating turbulent (Zhao *et al*., 2014a; Zhao *et al*., 2014b). For predicting oil droplet formation processes in a liquid-liquid dispersion system, the population balance (Eq.(9)) was proposed in this approach:

$$\frac{\partial n(d_i,t)}{\partial t} = \underbrace{\sum_{j=i+1}^{n} \beta(d_i,d_j)\, g(d_j)\, n(d_j,t) - g(d_i)\, n(d_i,t)}_{\text{droplet breakup}} + \underbrace{\sum_{j=1}^{n}\sum_{k=1}^{n} \Gamma(d_j,d_k)\, n(d_j,t)\, n(d_k,t) - n(d_i,t)\sum_{j-1}^{n} \Gamma(d_i,d_j)\, n(d_j,t)}_{\text{droplet coalescence}} \tag{9}$$

Where:

d_i: Diameter (m) of droplet i

n: Number concentration of droplets of diameter d_i at a given time t (number of droplet/m^3)

β (d_i,d_j): The breakage probability density function (dimensionless) for the creation of droplet of diameter d_i due to breakage of droplets of a larger diameter d_j

$g(d_j)$: The breakage frequency of droplet diameter d_j

$\Gamma(d_k,d_j)$: Droplet coalescence rate(m^3/s)

The breakage rate $g(d_i)$ is defined as:

$$g(d_i)=K_b\int_{n_e} S_{ed}\ (u_e^2 + u_d^2)^{1/2}\ BE(d_i, d_e,t)dn_e \quad (10)$$

Where:

S_{ed}: Collisional cross section of eddy and droplet (m^2)

u_e: Turbulent velocity of an eddy (m/s)

u_d: Droplet velocity (m/s)

n_e: Number concentration of eddies (number of eddies/m^3)

The system-dependent parameter of droplet breakage k_b was calibrated to fit the experimental data, the best fit of k_b is given by:

$$K_b=3.57(\rho U^2 D)^{-0.63} \quad (11)$$

The breakage efficiency $BE(d_i, d_e,t)$ is given by:

$$BE(d_i, d_e, t) =\exp\left[-\frac{1}{1.3}\left(\frac{E_c+E_v}{e}\right)\right] \quad (12)$$

Where:

E_c: Average excess of surface energy

E_v: Resistance energy due to viscous forces with the droplet (J)

e: Energy of the turbulent eddy

In a deep water oil/gas blowout, gas release with oil also affects the sizes of droplets, and subsequent has influence on the fate/transport of oil droplets. In the VDROP-J approach, the change of gas bubble size, due to gas expansion and dissolution, with time during oil blowout based on the real gas law (zhao *et al.*, 2016):

$$\frac{\partial d}{\partial t} = \frac{zRT\left[-k_{bub}A\left(\frac{P_B}{H_{henry}}-C_0\right)\right]+NRT\frac{\partial N}{\partial t}-\frac{\pi}{6}d^3\rho_w g\frac{\partial H}{\partial t}}{\frac{\pi}{2}d^2\left(P_A+\rho_w gH+\frac{4\sigma}{d}\right)-2/3\pi d\sigma} \quad (13)$$

Where:

k_{bub}: The mass transfer coefficient of the bubble (m/s)

A: The surface area of gas bubble

P_B: The internal bubble pressure

P_A: The atmospheric pressure

H: Water depth

H_{henry}: The Henry's constant (Pa m^3/mol)

C_0: The ambient concentration of dissolved gas (mol/m^3)

N: The number of moles in the bubble

R: The universal gas constant (8.3145 m^3Pa/ (K mod))

T: The absolute temperature (^{o}K)

z: In linear relationship with 1/T

ρ_w: Ambient water density (kg/m^3)

g: Gravitational acceleration (m/s^2)

$\frac{4\sigma}{d}$: The Laplace pressure due to interfacial tension

Two data set: Tower Tank experimental data (Brandvik *et al*., 2013) and "Deepspill" experimental data (Johansen *et al*., 2003), has been used to validate the VDROP-J approach. Figure 2-3 showed the simulation results of oil droplet size distribution with and without chemical dispersant using VDROP-J model, and experimental data from Tower Tank experiments were also presented in this figure. The measured IFT with different DORs of 0, 1:50 and 1:25 were 15.5, 0.05 and 0.09, respectively (Brandvik *et al*., 2013). To match the experimental data, the simulations fit the data by estimating dispersant efficiencies of 10% and 80% for the case of DOR=1:50 and 1:25, respectively. The results showed good agreement between experimental data and VDROP-J model.

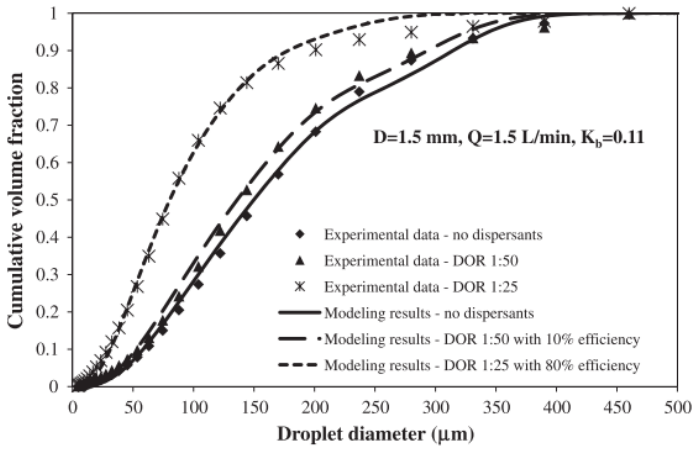

Figure 2-3: Oil droplet size distribution between modeling results and experimental data for the case with and without the addition of chemical dispersant (Zhao *et al*., 2014a).

The simulation results for the case of seawater and gas release showed a good agreement with the corresponding "DeepSpill" experimental data with the k_b ranging from 0.17 to 0.25. However, the simulation for diesel and gas release, result exhibited a larger variation than that for seawater and gas release experiment, but the author stated that this difference was caused by the large variability of field experiments. Although VDROP-J model has reasonable fit to experimental data, further studies are still required to improve the correlation, especially for the cases of stimulating oil droplet size distribution with chemical dispersant injection. As well, the simulation results of the change of gas bubble size module is difficult to validate due to the limited relevant experimental or field data can be used to support. The model still need more experimental data for empirical correlation.

2.5.2.2 Droplet Size Distribution (DSD) model

The DSD model was developed by Nissanka and Yapa (2015), which was based on the bubble size distribution (BSD) model. The details of the BSD model were presented in Bandara and Yapa's paper (2011). The DSD model improved the theoretical method for energy dissipation, droplet breakup and coalescence rate from various underwater release conditions, and further improve the capability of model in calculating a wide range of droplet sizes with different release condition. The population balance equation (PBE) (Eq.(14)) was used to model the oil droplet evolution.

$$\frac{\partial V(v,t)}{\partial t} = \frac{1}{2}\int_0^v \Gamma(v-v', v')V(v-v', t)V(v', t)dv' - \int_0^\infty \Gamma(v, v')V(v)V(v')\,dv' + \int_v^\infty \beta(v, v')\gamma(v')V(v', t)dv' - \gamma(v)V(v, t) \quad (14)$$

Where:

$V(v', t)$: Total volume of each volume v bubble at given time t

$\beta(v, v')$: Probability density of daughter bubbles Eq.(16)

v: Probability of forming bubbles size

v': Bubble breakage volume

$\gamma(v)$: Breakage rate of bubble

$\Gamma(v, v')$: Coalescence rate of bubbles

Study only considered the effect of turbulent fluctuation, the main effect on droplet breakup, on the oil droplet breakup model. Based on the study of Bandara and Yapa (2010), a daughter droplet size (Eq.(15)) was introduced to close the kernel of droplet breakup.

$$d_{min} = \sigma/\rho(\varepsilon\lambda_j)^{2/3} \quad (15)$$

The distribution function for daughter bubble can be expressed as:

$$\beta(v_i, v_j) = \frac{E_{min} + [E_{max} - E_i(d_i)]}{\int_0^{d'} \{E_{min} + [E_{max} - E_i(d_i)]\}\delta d_i} \quad (16)$$

Where:

E_{min}: The minimum energy required

E_{max}: The maximum energy required

E_i: Energy required to create a droplet size class d_i

Oil droplet breakup efficiency (P_B) can be presented as:

$$P_B = \int_{\bar{E}(d)/\bar{e}(\lambda_j)}^{\infty} \exp(-e(\lambda_j)/\bar{e}(\lambda_j))dx = \exp(-\bar{E}(d)/\bar{e}(\lambda_j)) \quad (17)$$

Where:

λ_j: Turbulent velocity of an eddy of size

$e(\lambda_j)$: Kinetic energy of an eddy turbulent

$\bar{e}(\lambda_j)$: Mean kinetic energy of an eddy turbulent

$\bar{E}(d)$: Surface energy increased during the breakup

d_i: Droplet diameters of size class

For droplet coalescence, study considered the effect of turbulent fluctuation and different droplet rise velocities for droplet colliding in the droplet coalescence model. The droplet coalescence efficiency (P_{ij}^{C}) are defined as:

$$P_{ij}^{C} = exp(-\theta \frac{[0.75\,(1+{\xi_{ij}}^{2})(1+{\xi_{ij}}^{3})]^{0.5}}{(\frac{\rho_d}{\rho_c}+\gamma)(1+\xi_{ij})^3} We_{ij}^{0.5}) \quad (18)$$

Where:

We_{ij}: Density of continuous phase

θ: Constant value, 0.4

A key characteristic in predicting the DSD is the energy dissipation rate (Eq.(19)). It relates to both droplet breakup and coalescence.

$$\varepsilon = c_d \frac{\left||V| - V_a'\right|^3}{R_J} \quad (19)$$

Where:

$|V|$: Velocity of control volume

V_a': Projection of ambient velocity in the direction of velocity of control volume

R_J: Radius of the buoyant jet

c_d : Costant value (=2.0 in this study)

The value of c_d was found relate to the different release conditions. However, only very limited experimental data (the "DeepSpill" experiment and Tower Tank experiment) was used to correlate it, more studies are needed for this correlation.

In order to validate the DSD model, experimental data from "DeepSpill" experiments (Johansen *et al*., 2003) and Tower Tank experiments (Brandvik *et al*., 2013) were both used. The model simulated droplet size distributions from two different depth ranges (840 to 839m and 830 to 822m), which were showed in the "DeepSpill" experiment. The validation results showed a good agreement with field data. In terms of simulation of the Tower Tank experimental data, the simulation was divided into two groups: with and without chemical dispersant. The modelling droplet size distribution was well fit with the experimental data, without the application of chemical dispersant. However, for the chemical dispersant cases, the model was only fit with data of lower dispersant cases. The deviation for higher dispersant cases may be due to the reduction of oil viscous caused by chemical dispersants (Nissanka and Yapa, 2015). The improvement of the model is still an on-going work, further study will investigate the applicability of model in the cases with a higher dosage of dispersant.

2.6 Summary

In general, the fate of oil in the marine environment can be affected by several factors, such as oil properties and other environmental conditions. The fate of oil released from subsurface/deep water is different from that released on water surfaces or shallow water depth. Oil droplet size distribution formed in subsurface/deepwater oil release is very important, because of their direct influence on the fate and transport of oil in the marine environment. Well prediction of oil droplet size distribution can help to improve the performance of oil spill model and upgrade spill response plans to reduce the negative effects of oil spill on the environment.

Several available subsurface oil droplet size experimental studies were reviewed in this chapter. "DeepSpill" experiment was the only available field experiment can be used to validate droplet size distribution approaches in a very limited diesel droplet sizes range (Johansen *et al*., 2001). Oval cross section tank experiment studied the effect of diameter of release nozzles and flow velocities on oil droplet sizes (Topham, 1975). The number of smaller oil droplets was increased with higher flow velocities in Jet Breakup experiment (Masutani and Adams, 2001). More recently, Tower Tank experiment gained new experimental data for oil droplet sizes formed in subsurface oil release cases. The

application of chemical dispersant in this study showed a significant effect on reducing oil droplet sizes. These oil droplet size distribution data with and without chemical dispersant application have played an important role in the further validation of droplet sizes distribution approaches (Brandivik *et al*., 2013). In addition, a larger Ohmsett wave tank experiment provided supplemental underwater oil droplet size distribution data for the future study (Zhao, *et al*., 2016).

In general, these exist experimental data provide oil droplet size distributions data for several oil droplet size distribution prediction approaches validation. Compared two empirical approaches: the MEF approach and the MWN approach, the MWN approach has took consideration of the effect of oil properties and chemical dispersant, thus, the prediction of droplet size distribution by using the MWN may be more accurate than that predicted by the MEF approach. For the two dynamical approaches: the VDROP-J approach and the DSD model, exist experimental data show better fit to the VDROP-J approach than the DSD model, and the improvement of DSD model is required for further application.

Although these prediction approaches are of a different level of complexity, two or three tuning coefficients are required to perform these approach. The Modified Weber Number approach showed less complexity than other approaches. Therefore, the Modified Weber Number approach, as preliminary, was seen to be easier to integrate into several deep water oil spill models. For example, the Oil Spill Contingency and Response (OSCAR) model updated the existing oil plume model by integrating with Modified Weber Number approach.

Even though the MWN approach was obtained in the state-of-the-art deep water oil spill model, this approach still need further validation with more droplet size distributions data of different types of oils. As previously mentioned, this approach was developed from limited Tower Tank experimental data. Thus, the determination of empirical coefficients value and spreading parameter did not consider the effects of different types of oil. Similarly, other available approaches were also validated by using very limited experimental data. More extensive experimental data are needed to improve the accuracy of each approach. In order to support the applicability of oil droplet size distribution

approaches over a range of oil types, extensive experimental data on different types of oil is urgently needed. In this study, a series of experiments for two viscosities of oils at different release conditions are conducted to fill this gap. Based on the new gained experimental data, the further validation of prediction approach (Modified Weber Number approach is used in this study) is assessed in this study, and results are presented in the Chapter 4.

CHAPTER 3. MATERIALS AND METHOD FOR MEASURING OIL DROPLET SIZE DISTRIBUTION

3.1 Experimental facilities and materials

To provide more droplet size distribution data of oils for further studies on investigating the applicability of the approaches for other oil types, with and without application of a chemical dispersant, a series of experiments was designed to measure oil droplet size distribution of two different types of oil, with and without the application of chemical dispersant. Oil droplet size distribution data was measured by a particle size analyzer. In this chapter, detailed descriptions of apparatus, selected oil and chemical dispersant, DORs, and procedure are provided.

3.1.1 Flow-through wave tank facility

All experiments in this study were conducted in a wave tank with an underwater oil release system at the Center for Offshore Oil, Gas and Energy Research (COOGER), Bedford Institute of Oceanography (BIO), located in Dartmouth, NS. Li *et al*. (2009b) stated that a meso-scale testing facility is more realistic to study the effectiveness of chemical dispersant. In this study, the same meso-scale wave tank testing facility as Li *et al*. (2009b) was used. A schematic of the wave tank is presented in Figure 3-1. The dimensions of the tank are 32m×0.6m×2m (length×width×depth), and the average water depth was 1.5m with a water holding capacity of 28,800L. The oil injection nozzle (D=2.387mm) was installed near the bottom of the tank, at 8.4m away from the inflow pump. Seawater in the tank was taken from the Bedford Basin through a serial filtration system and entered the wave tank via the inflow pump. The current flow rate in the wave tank was controlled by a computer system at a constant rate of 600 gallons per minutes (gpm) for all experiments. The outflow pump was located at the opposite side of the inflow pump.

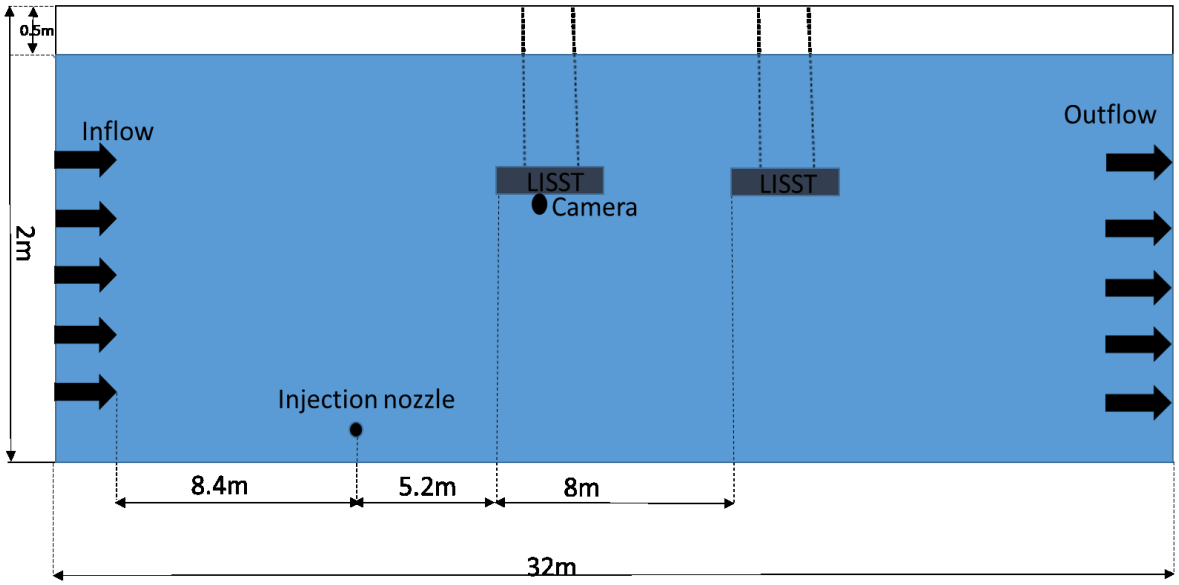

Figure 3-1: Schematic of the cross section of the wave tank facility.

3.1.2 Particle size analyzer

A laser diffractometer analyzer—Laser In-Situ Scattering and Transmissometry (LISST-100X) instrument was used to measure the oil droplet size distribution data in the wave tank (Sequoia Scientific, Inc., 2012). The advantage of using LISST-100X is that the laser diffraction is not affected by the particle composition because of the multiple, small forward angles of observation of scattering of laser light, providing an accuracy record on particle size distribution. The application of this instrument can be found in several researches (Johansen *et al*., 2013; Li, *et al*., 2009 a; Li, *et al*., 2009b; Li *et al*., 2007; Serra *et al*., 2002; Gartner *et al*., 2001).

Figure 3-2 shows the sketch of LISST-100X. The specially constructed multi-ring detector is utilized to record scattering intensity over a range of small angles (Sequoia Scientific, Inc., 2012). It can measure particle sizes ranging from 2.5µm to 500µm. Equal logarithmic intervals are made for the diameters, and the same increment is used for the diameter size: $d_n = 1.18 * d_{n-1}$ (where d_n is the top value of each bins and d_{n-1} is the top value of previous bins). Output to each bin are given as the median diameter (d_m), expressed as $d_m = (d_{n-1} * d_n)^{1/2}$. The LISST-100X captures dynamic particle size every 3 seconds (Li *et al*., 2007), the particle size distribution is presented as the average volumetric concentration.

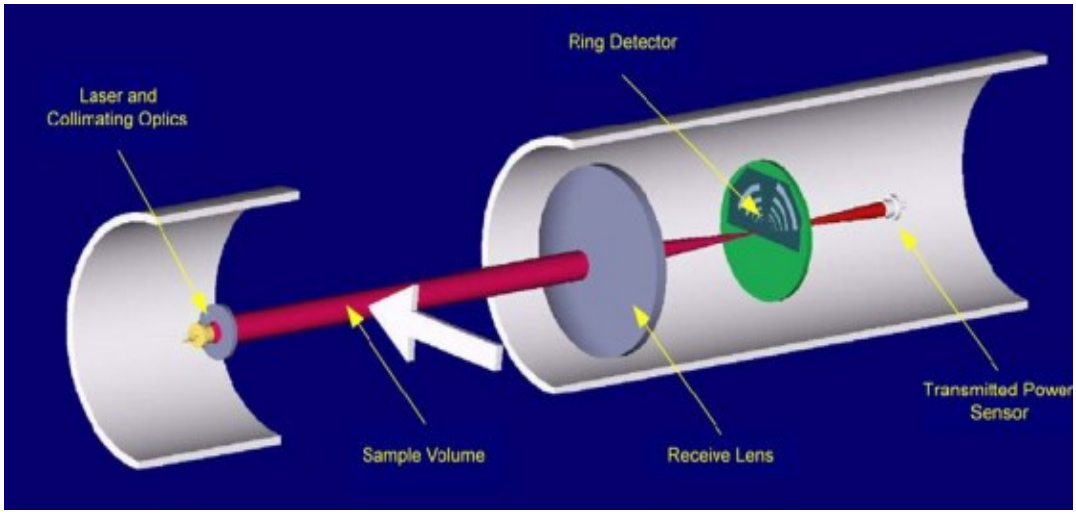

Figure 3-2: The sketch of the structure of LISST-100X (Sequoia Scientific, Inc., 2012).

Two LISST-100X devices were installed in the wave tank (Figure 3-1) at 5.20m and 13.20m away from the oil injection nozzle, respectively. Both LISST-100Xs were connected to a computer, where the droplet size data was directly saved for future analysis. However, one limitation of LISST-100X is that it cannot detect any particles sizes out of the LISST-100X detected range, the movement of oil plume after release was recorded, using a high-resolution camera installed in the tank.

3.1.3 Selection of oils and chemical dispersant

As reviewed in Chapter 2, oil viscosity and chemical dispersant can have effects on the fate of oil. The experiment, conducted by Brandvik *et al.* (2013), used one crude oil, Norwegian Oseberg Blend crude oil, a light viscosity crude oil. In this study, two different types of oils were utilized: one was a medium viscosity crude oil (Alaskan North Slope, ANS) and the other was a heavy viscosity crude oil (Intermediate Fuel Oil 120, IFO-120). The properties of ANS and IFO-120 were measured at COOGER: density and viscosity were measured by the Anton Paar SVM3000 instrument, and BTEX content was analyzed with a gas chromatography/mass spectrometer. The properties for these two oils are presented in Table 3-1. Due to different chemical compositions and properties of these two oils, the droplet size distributions and dispersant effectiveness were expected to be different. To simulate the oil temperature in a realistic deep water oil blowout, both oils were heated to 80 °C, then injected into the wave tank from a high-pressure container.

Table 3-1: Properties of ANS and IFO-120.

Properties	ANS	IFO-120
Density*(g/mL)	0.8777	0.9587
Dynamic viscosity*(mPa·s)	18.9	2481.5
API gravity	29.72	16.96
BTEX content (% total)	2.30	0.20

**:at 15 ℃, 0% evaporation.*

The dispersant used in this study was Corexit 9500, a commercial dispersant, which has been stored as an option of oil spill countermeasure. This chemical dispersant has been used in really deepwater oil blowout accident (the DWH incident). In this experimental study, this dispersant was mixed with oil, and held in a nitrogen pressurized container, ensuring the oil was dispersed sufficiently.

3.2 Description of experimental procedures

The experimental procedure is described below and summarize in Figure 3-3:

- The wave tank was filled with the seawater from the Bedford Basin of Halifax Harbor.
- The instruments (LISST-100X and camera) were installed at the corresponding locations, as described in earlier sections, and connected to a computer for automatic measurements of particle size and movement of oil plume (Figure 3-1).
- The wave tank conditions, such as water and air temperature, salinity and weather conditions, were recorded prior experiment and the current flow rate was controlled at 600gpm.
- Preparation of oil: for each experiment, the amount of pre-heated oil (80 °C) was weighed and recorded, and then held in a nitrogen pressurized container by itself or premixed with different dosages of chemical dispersant.
- Initiation of experiment: oil or oil/dispersant mixture was injected into the wave tank from the injection nozzle and the particle size of the droplets was analyzed by the LISST-100Xs. Based on varied experimental conditions, the experimental injection pressure ranged from 40 to 62 psi (pounds per square inch) and the injection time ranged from 5 to 10 seconds depending on experimental conditions.

- Movement of oil plume and oil droplet size distribution data was recorded for around 12 minutes, then the experiment was stopped.

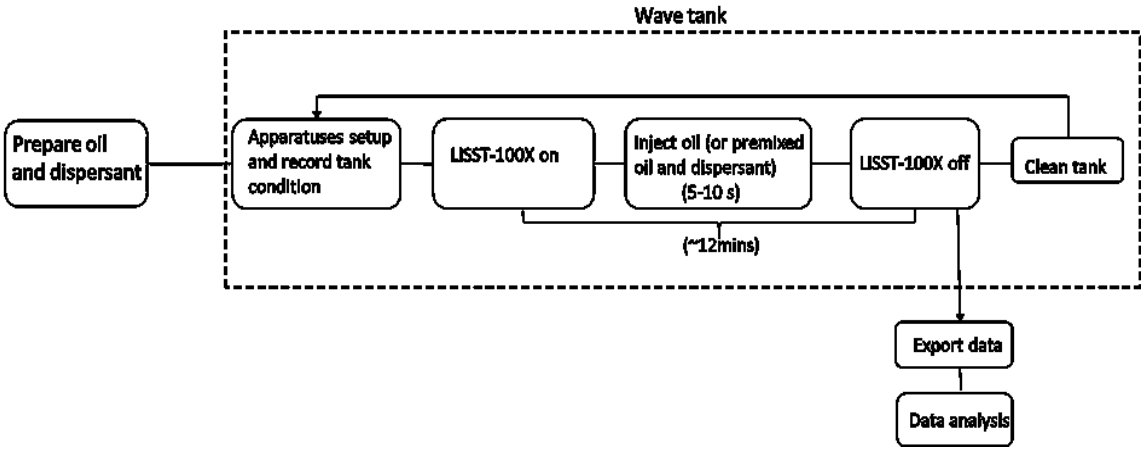

Figure 3-3: Flowchart of the experimental procedure.

3.3 Experimental conditions

In the study performed by Brandivik *et al.* (2013), the effects of DORs, which ranged from 1:1000 to 1:25, were studied. Three relative high dispersant to oil ratios (DOR =1:200, 1:100 and 1:20) were performed in this study. In addition, the experiments without dispersant injection (DOR=0) were conducted for comparison purpose. For each DOR, triplicated experiments were conducted in both warm and cold water conditions for each oil, as shown in Table 3-2 and Table 3-3. This gave a total number of 24 combinations for each oil. Experiments, with DOR=0, 1:200, 1:100 and 1:20, done in cold water were numbered from 1 to 12, and experiments, with these DORs, done in warm water were recorded in No.13-24. Additional experiments, with DOR of 1:50 for ANS, were conducted to fill the gaps between DOR=1:100 to DOR=1:20, but they were no conducted for IFO-120, due to the unavailability of the experimental facility. The experiments, with DOR=1:50 for ANS, were numbered from No. 25 to 27.

Table 3-2: Experimental conditions for ANS.

No.	Factor	Measurements				
	DOR	Date	Oil Amount (g)	Water Temperature (°C)	Injection Time (sec)	Injection pressure (psi)
ANS-1	0	Date	208.0	11.4	4	40
ANS-2	1:250	22-May-14	280.0	10.6	5	40
ANS-2R	1:200	23-May-14	290.5	6.4	5	40
ANS-3	1:100	02-Dec-14	284.5	11.2	5	40
ANS-4	1:25	23-May-14	283.0	8.4	5	40
ANS-4R	1:20	26-May-14	287.2	6.8	5	40
ANS-5	0	03-Dec-14	279.3	8.4	5	40
ANS-6	1:250	26-May-14	279.7	7.7	5	40
ANS-6R	1:200	30-May-14	335.0	6.1	5	40
ANS-7	1:100	02-Dec-14	276.3	8.5	5	40
ANS-8	1:25	30-May-14	277.4	9.4	5	40
ANS-8R	1:20	02-Jun-14	297.2	7.0	5	40
ANS-9	0	03-Dec-14	281.4	9.7	5	40
ANS-10	1:250	02-Jun-14	281.0	10.3	5	40
ANS-10R	1:200	06-Jun-14	344.5	5.4	5	40
ANS-11	1:100	17-Dec-14	276.8	10.7	5	40
ANS-12	1:25	06-Dec-14	280.6	12.5	5	40
ANS-12R	1:20	09-Jun-14	295.7	7.3	5	40
ANS-13	0	10-Dec-14	303.7	17.7	5	40
ANS-14	1:200	05-Sep-14	295.2	16.0	5	40
ANS-15R	1:100	08-Sep-14	304.3	13.8	5	40
ANS-16	1:20	10-Sep-14	291.9	14.7	5	40
ANS-17	0	10-Sep-14	299.6	18.1	5	40
ANS-18	1:200	05-Sep-14	297.7	16.2	5	40
ANS-19	1:100	08-Sep-14	283.4	15.3	5	40
ANS-20	1:20	09-Sep-14	289.6	14.1	5	40
ANS-21	0	11-Sep-14	297.1	15.1	5	40
ANS-22	1:200	08-Sep-14	281.8	14.2	5	40
ANS-23	1:100	09-Sep-14	284.4	13.4	5	40
ANS-24	1:20	10-Sep-14	285.8	13.6	5	40
ANS-25	1:50	06-Nov-15	299.6	11.1	6	40
ANS-26	1:50	06-Nov-15	330.6	11.1	6	40
ANS-27	1:50	06-Nov-15	304.3	11.1	6	40

Note: R indicates repeated experiments.

Table 3-3: Experimental conditions for IFO-120.

No.	Factor	Measurements				
	DOR	Date	Oil Amount (g)	Water Temperature (°C)	Injection Time (sec)	Injection Pressure (psi)
IFO-1	0	9-Jun-14	145.2	13.0	5	40
IFO-2	1:250	20-Jun-14	199.6	12.2	7	60
IFO-2R	1:200	04-Dec-14	208.2	6.7	7	60
IFO-3	1:100	20-Jun-14	213.9	13.2	7	62
IFO-4	1:25	11-Jun-14	179.1	12.8	9	40
IFO-4R	1:20	05-Dec-14	219.6	5.6	10	30
IFO-5	0	17-Jun-14	275.1	12.0	7	62
IFO-6R	1:200	04-Dec-14	215.6	6.6	8	60
IFO-7R	1:100	10-Dec-14	239.3	7.5	8	60
IFO-8	1:25	11-Jun-14	255.8	13.2	9	40
IFO-8R	1:20	05-Dec-14	243.3	5.4	10	60
IFO-9	0	17-Jun-14	359.6	12.7	7	62
IFO-10R	1:200	04-Dec-14	221.7	6.6	8	60
IFO-11R	1:100	17-Dec-14	N/A	4.9	10	60
IFO-12	1:25	16-Jun-14	354.8	12.5	9	62
IFO-12R	1:20	10-Dec-14	204.8	6.8	9	60
IFO-13	0	12-Sep-14	256.8	14.9	7	60
IFO-14	1:200	15-Sep-14	279	13.5	8	60
IFO-15	1:100	16-Sep-14	336.2	14.0	8	60
IFO-16	1:20	17-Sep-14	315.9	14.7	7	60
IFO-17	0	12-Sep-14	293.3	14.7	8	60
IFO-18	1:200	15-Sep-14	331.8	13.8	8	60
IFO-19	1:100	16-Sep-14	353.8	14.7	7	60
IFO-20	1:20	17-Sep-14	345.6	15.2	7	60
IFO-21	0	12-Sep-14	303.6	15.2	8	60
IFO-22	1:200	15-Sep-14	363.3	14.0	8	60
IFO-23	1:100	16-Sep-14	352.6	14.7	7	60
IFO-24	1:20	17-Sep-14	380	16.0	7	60

Note: R indicates repeated experiment.

As shown in Table 3-2 and Table 3-3, experiments, for ANS and IFO-120, were mostly done during the year of 2014. Some experiments were scheduled in spring (May 2014-June 2014), but not conducted due to abnormal weather conditions with rising water temperature were rescheduled and conducted in late Dec. 2014. The experiments with DOR=1:50 for ANS were conducted in Nov. 2015. These experiments with the "R" marked indicated repeated experiments. Additionally, it also represented the repeated experiments with slightly adjusted DOR conditions (e.g., Adjust DOR=1:250 to DOR=1:200). A total of 33 experiments using ANS and 28 experiments using IFO-120 were conducted in this study. Other parameters (e.g. oil amount, injection time, and injection pressure) were recorded for each experiment and listed in the tables in details.

The effect of water temperature on droplet sizes (relative cold and warm water) was also investigated in the wave tank. The water temperature was recorded depending upon the ambient weather conditions. Cold water experiments were conducted during the spring of 2014 (May 2014-June 2014) and warm water experiments were conducted during the summer of 2014 (September 2014). Generally, the cold water experiments (in the spring condition) were conducted under slightly low water temperatures (around from 8 to 13 °C). In contrast, the warm water experiments (in the summer condition) were conducted at around from 15 to 20°C water temperature.

CHAPTER 4. EXPERIMENTAL RESULTS AND THE REYNOLDS NUMBER SCALLING APPROACH

4.1 Experimental results

A total of 61 experiments were performed to study oil droplet size distribution, with and without the effect of dispersant, at different ambient water temperatures for two oils. The volume fraction of each droplet size bin, median volume diameter (d_{50}) and peak volume diameter (d_p) were calculated for each experiment, based on the measured data. The effect of water temperature and the effect of chemical dispersant at different DORs on droplet size distribution for both ANS and IFO-120 were discussed. Some experimental data were excluded from data analysis due to limited observation range of LSST, and abnormal peak probably due to unknown measuring error(s).

4.1.1 Effects of water temperatures

According to ambient water temperature measurement, the experimental temperature was classified as two conditions: the spring (relative cold water temperature) and the summer (relative warm water temperature). Examples of the droplet size distribution of IFO-120 and ANS, with DOR=0 under spring and summer conditions, are presented in Figure 4-1 and Figure 4-2, respectively.

Figure 4-1 illustrates the normalized oil droplet size distribution for IFO-120, with DOR=0 in summer and spring conditions. Experiments No. 1, 5 and 9 were performed under the spring condition, with water temperatures around 12.6 °C (distributions shown in blue). The results showed that Experiments No. 1 and 5 had the same peak diameter (d_p =259μm), but slightly differed on d_{50} (258.36μm for No.1 and 176.59μm for No.5). The concentration measured in No. 1 is relatively smaller than the other two cases. The d_{50} and d_p for Experiment No. 9 were both smaller than those of the other two experiments (d_{50} = 99.63μm; d_p =186μm). For summer conditions, Experiments No. 13, 17 and 21 were conducted at water temperature around 15 °C (distributions shown in orange). Experiments No. 13 and 21 have the same d_p (391μm) and similar d_{50} (263.27μm and 263.95μm, respectively), while the Experiment No. 17 had a slightly smaller d_{50} and d_p (d_{50}=192.71μm, d_p=293μm).

Based on the measurements of experimental conditions in Table 3-3, the different results of these experiments may have been affected by both water temperature and injection pressure. It was indicated that oil droplets can be dispersed into much smaller sizes with the effect of higher release pressure (Grammeltvedt, 2014). In spring condition, Experiment No.1, with the lowest injection pressure (40psi) and the highest water temperature (13 °C), showed larger value of d_{50} (258.36μm), while in Experiment No. 5, with the slightly lower water temperature (12 °C) and higher injection pressure (62psi), the d_{50} (176.59μm) decreased. In these two experiments, the results showed that injection pressure may have effects on droplet size distributions of IFO-120, together with water temperature. However, for the spring cases of IFO-120 alone, the significant of temperature on the oil droplet sizes was not determined. Considering the experiments (No.13, 17 and 21) in summer conditions, with the same injection pressure (60psi), the normalized volume fractions of each size bin were similar in all three experiments, and the values of peak volume diameter (d_p) and median volume diameter (d_{50}) hardly changed as temperature increased. Overall, compared with water temperature, the injection pressure presented a greater effects on droplet size distribution of IFO-120.

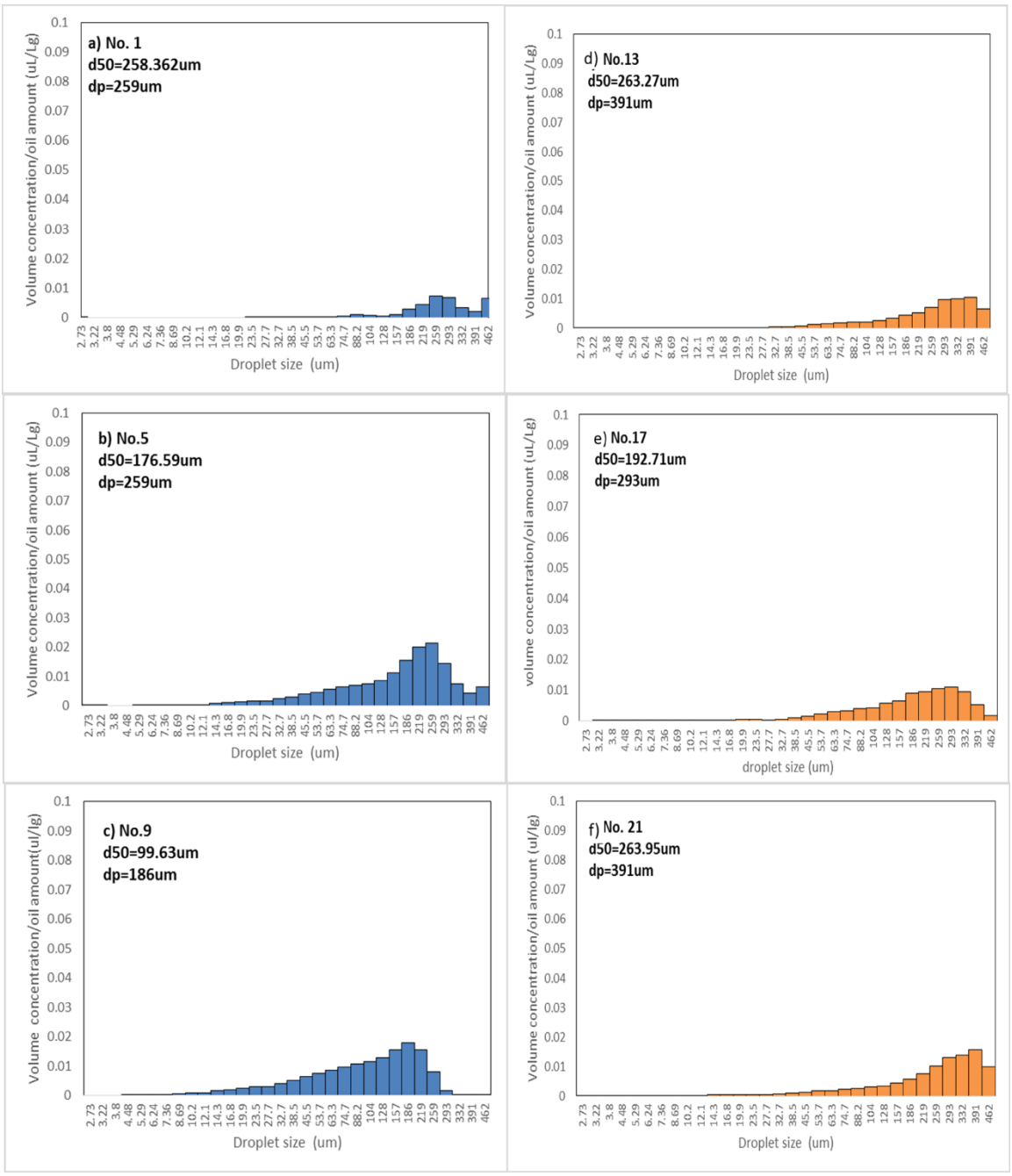

Figure 4-1: Experimental droplet size distribution of IFO-120 with DOR=0 from experiments: Spring conditions: a) No. 1, b) No. 5, and c) No.9

Summer conditions: d) No. 13, e) No. 17, and f) No. 21

(Left column with ~12.6 °C water temperature; Right column with ~ 15.0 °C water temperature)

For ANS, the injection pressures were all the same, set at 40 psi. For the case of DOR=0, the d_{50}s and d_ps for ANS were overall smaller (d_{50}<102μm; d_p<128μm) than that of IFO-120 in both spring and summer conditions. As shown in Table 3-2, the water temperature for Experiment No.1 (11.4°C) was slightly higher than that for Experiment No.9 (9.7°C). The values of d_p for both experiments were the same (88.2μm), but the d_{50} for Experiment No.1 was 81.9μm, which was slightly higher than that for Experiment No.9 (68.13μm). Compared with the distribution in spring conditions, experiments in summer conditions (water temperatures>15 °C) had a large quantity of relatively large oil droplets sizes. The d_p (>100μm) and d_{50} (>80μm) for Experiments No.13, 17 and 21 were generally higher than those in spring conditions (d_p<100 μm; d_{50}<80 μm).

The effect of water temperature on oil droplet size distribution of both IFO-120 and ANS, with the presence of chemical dispersant, showed differences from those without the presence of chemical dispersant. Figure 4-3 and Figure 4-4 show examples of the normalized droplet size distribution of ANS and IFO-120 with DOR=1:20, respectively.

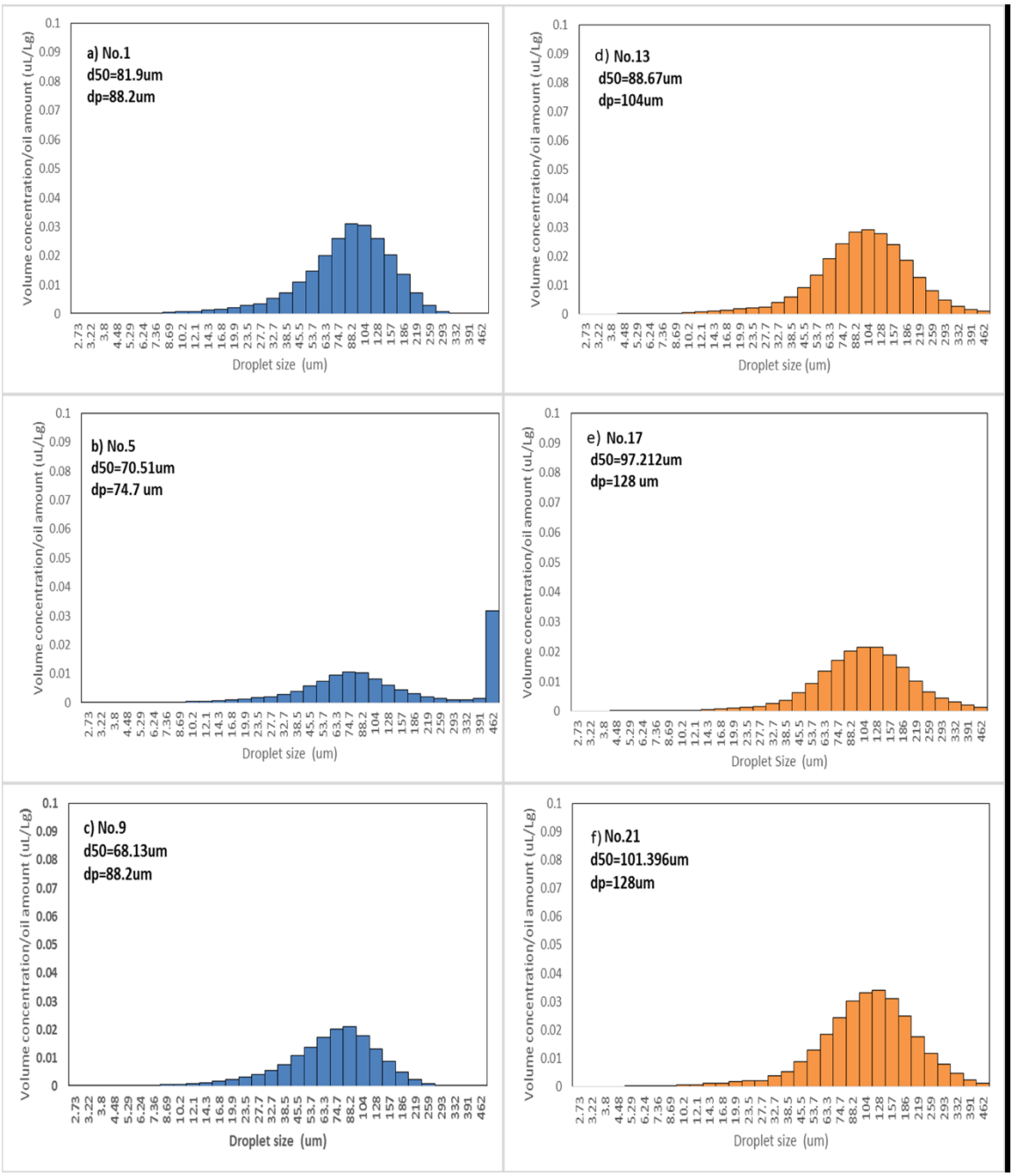

Figure 4-2: Experimental droplet size distribution of ANS with DOR=0 from experiments: Spring conditions: a) No. 1, b) No. 5, and c) No.9

Summer conditions: d) No. 13, e) No. 17, and f) No. 21

(Left column with under 12 °C *water temperature; Right column with higher than 15* °C *water temperature)*

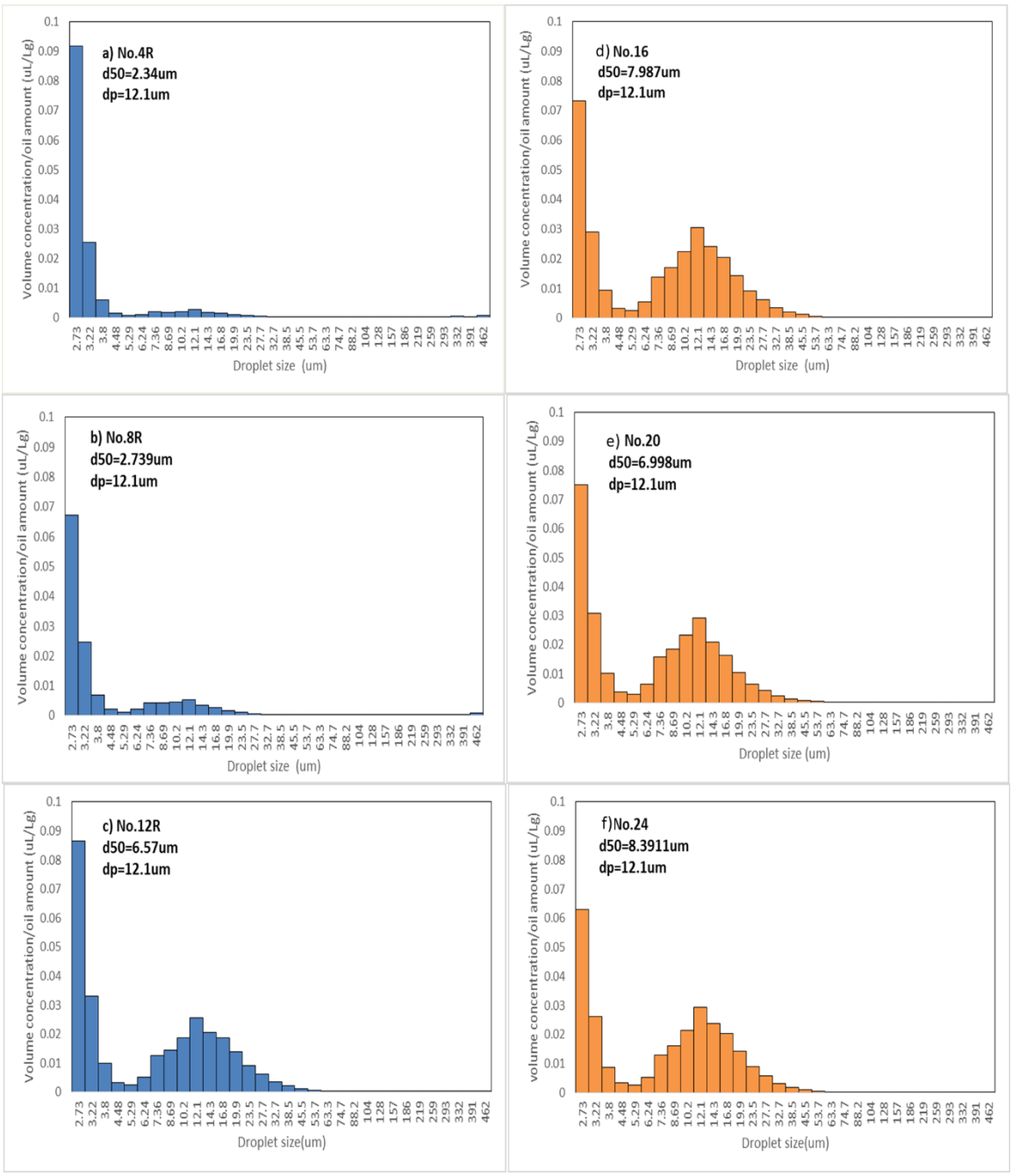

Figure 4-3: Experimental droplet size distribution of ANS with DOR=1:20 from experiments: Spring conditions: a) No. 4R, b) No. 8R, and c) No. 12R

Summer conditions: d) No. 16, e) No. 20, and f) No. 24

(Left column with around 7 °C water temperature; Right column with higher than 14 °C water temperature)

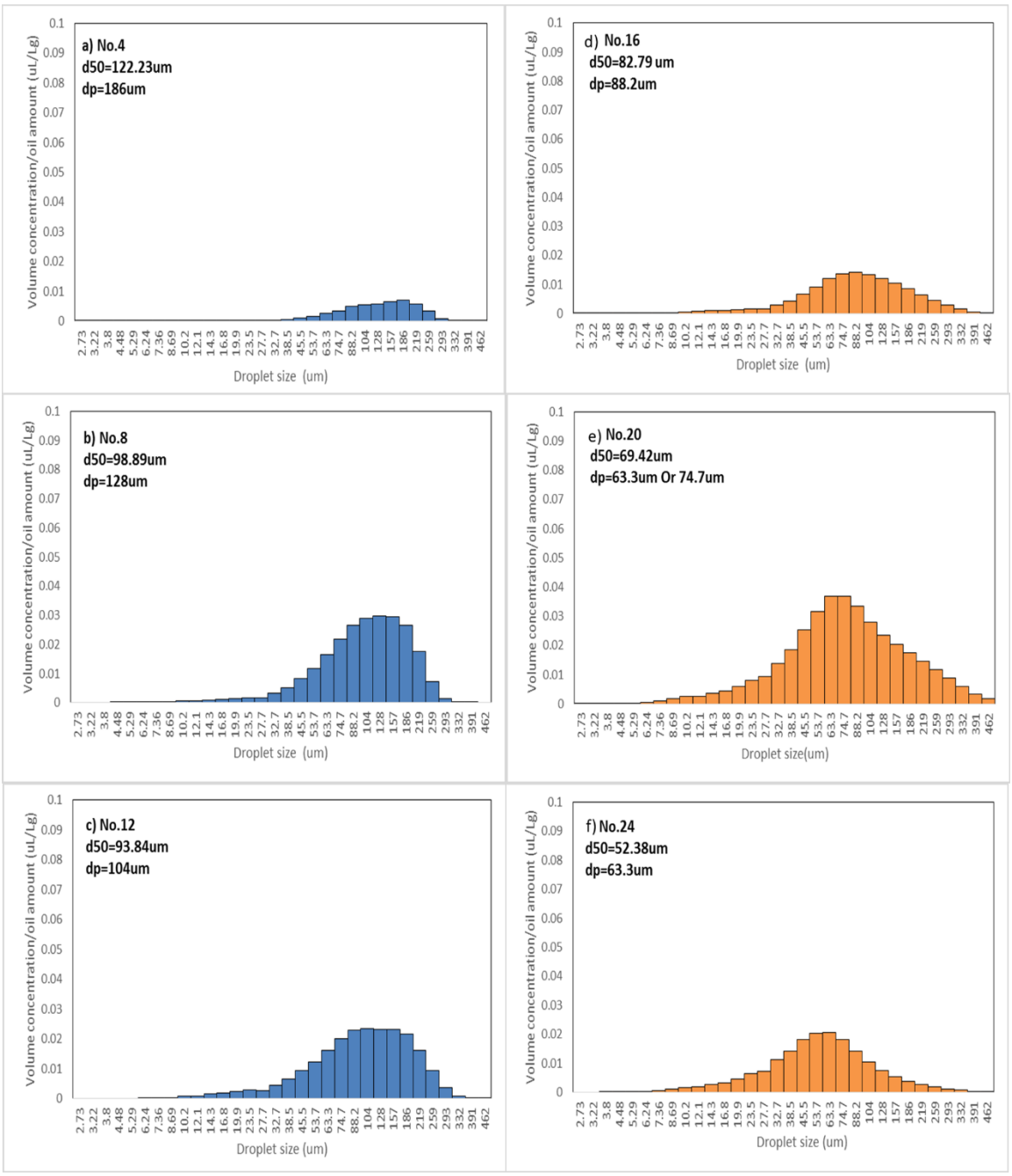

Figure 4-4: Experimental droplet size distribution of IFO-120 with DOR=1:20 from experiments: Spring conditions: a) No. 4, b) No. 8, and c) No. 12

Summer conditions: d) No. 16, e) No. 20, and f) No. 24

(Left column with around 12.5 °C water temperature; Right column with higher than 15 °C water temperature)

The values of d_p for ANS, with DOR=1:20, in both spring and summer conditions, were the same (d_p =12.1μm), but the values of d_{50} appeared to be influenced by the water temperature (d_{50}>7μm in summer conditions, d_{50}<7μm in spring conditions) (Figure 4-3). However, for other DOR cases (DOR=1:200 and 1:100), the effects of water temperature on d_p and d_{50} were not evident. In terms of droplet size distributions of IFO-120, with DOR=1:20, the effect of water temperature on droplet size distribution showed a different situation (Figure 4-4). When the water temperature rose, the resulting d_{50} and d_p tended to decrease (d_{50}<70μm in summer conditions; d_{50}>70μm in spring conditions). In these two cases, chemical dispersant played a role in reducing droplet sizes, but the effect of water temperature on d_{50}s were not consistent due to limited experimental data.

In the analysis of the effect of water temperature on droplet size distributions for both ANS and IFO-120 with and without chemical dispersant application, the effects can be well observed in the case of ANS (medium crude oil) without chemical dispersant application. Compared with the effect of injection pressure on droplet size distribution of IFO-120, the water temperature may have less effect on the droplet size distribution of IFO-120 (heavy crude oil). Compared both oils, the experimental data showed that water temperature may have greater effects on droplet size distributions of medium crude oil (ANS) than on that of heavy crude oil (IFO-120). In the cases with chemical dispersant application (DOR=1:20), high water temperature increased the values of d_{50} of ANS, but this effect was not presented in other DOR cases (DOR=1:200 and DOR=1:100). On the contrary, the values of d_{50} of IFO-120 with DOR=1:20 showed a decrease with an increase in water temperature. Overall, for both oils, compared with injection pressure and chemical dispersant, study cannot clearly address the relationship between water temperature and droplet size distribution, due to the uncontrollable water temperature. Further study is needed to better understand how water temperatures affect the distribution of droplet sizes for different types of oil, with and without the application of chemical dispersant. Consequently, this would assist the decision-making process when applying chemical dispersant under different water conditions.

4.1.2 Effects of dispersant to oil ratios (DORs)

In spring conditions, experiments with DOR=1:200 (1:250) and 1:20 (1:25) were carried out for ANS and IFO-120. In our experimental design, it was designed to have experiments with DOR=1:200 and 1:20, but due to some mistakes, experiments with DOR=1:250 and 1:25 for ANS and IFO-120 were conducted. Compared the measured droplet size distribution data, the data with DOR=1:250 showed similar results to that with DOR=1:200 for both oils, similar results appeared in the distribution with DOR=1:25 and DOR=1:20. Drawing a conclusion from these data, minor changes in the dosage of dispersant have less effect on the amount of dispersed oil droplet sizes. The data, with DOR=1:250 and 1:200, yielded almost identical results. For the purpose of presentation, both data sets are presented as one set of data (e.g. DOR=1:200). This is also done for data with DOR=1:25 and 1:20 (e.g. DOR=1:20).

Examples of the effect of DORs on oil droplet size distribution for ANS and IFO-120 under spring and summer conditions are compared in Figure 4-5 and Figure 4-6. Figure 4-5 (a) is an example of droplet size distribution of ANS, with different DORs, in spring condition. This figure shows that increased DOR resulted in increased volume fraction of smaller droplets and consequently decreased the values of d_{50} and d_p. The data set of ANS was significantly shifted toward smaller droplet sizes with increased DOR (from 0 to 1:20). For distribution of IFO-120 (Figure 4-5b) in spring conditions, not only the chemical dispersant had little effect on decreasing droplet sizes from DOR=0 to DOR=1:100, but also there was a slight rise in the number of large oil droplets observed from DOR=0 to 1:100; based on present knowledge, this may be affected by several factors, such as environment conditions, chemical effectiveness or mixing energy. However, the proportion of small oil droplets was cleanly elevated when the DOR increased to 1:20. The results indicate that dispersant can reduce oil droplet sizes of heavy crude oil (IFO-120), but has less effect for low dose of chemical dispersant.

In terms of the summer conditions (c and d in Figure 4-6) for both oils, the droplet size distributions were similar to the spring conditions. Oil droplet sizes of ANS were reduced as the DORs increased. Regarding droplet size distributions of IFO-120, the noticeable effects of dispersant were observed in a higher ratio of dispersant to oil

(DOR=1:20). Lower ratio (DOR=1:200 and 1:100) appeared to have very little effect on droplet sizes of heavy crude oil (IFO-120). Overall, relatively high dosage of chemical dispersant (1:50 and 1:20) greatly reduced the oil droplet sizes of medium (ANS), and for heavy (IFO-120) crude oils, the dosage of chemical dispersant of DOR=1:20 showed great reduce on the droplet sizes. The effectiveness of chemical dispersant on the reduction of droplet sizes also showed a difference with varying types of oils. Generally, chemical dispersant appeared to be more effective for medium crude oil (ANS, low viscosity) release than for heavy crude oil (IFO-120, high viscosity), under the same environmental conditions.

A bimodal droplet size distribution was observed in the all experiments of ANS, with DOR=1:20, in both summer and spring conditions (Figure 4-5a and Figure 4-6c). In our study, this bimodal distribution was considered as normal.

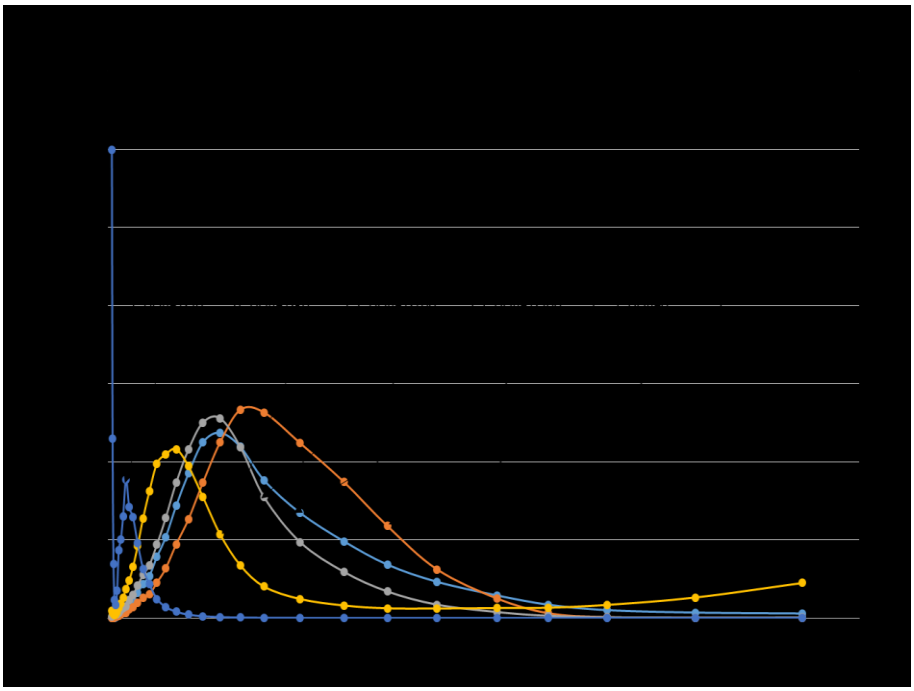

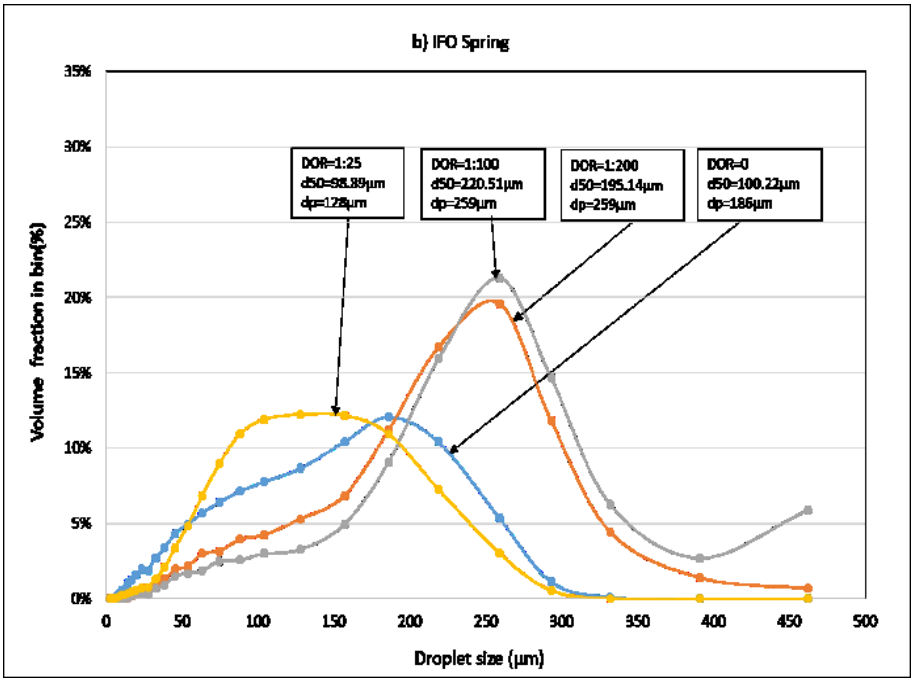

Figure 4-5: Examples of volume fraction in each size bin (%) as a function of DOR with ANS and IFO in spring seasonal conditions a) ANS, spring condition; b) IFO, spring condition.

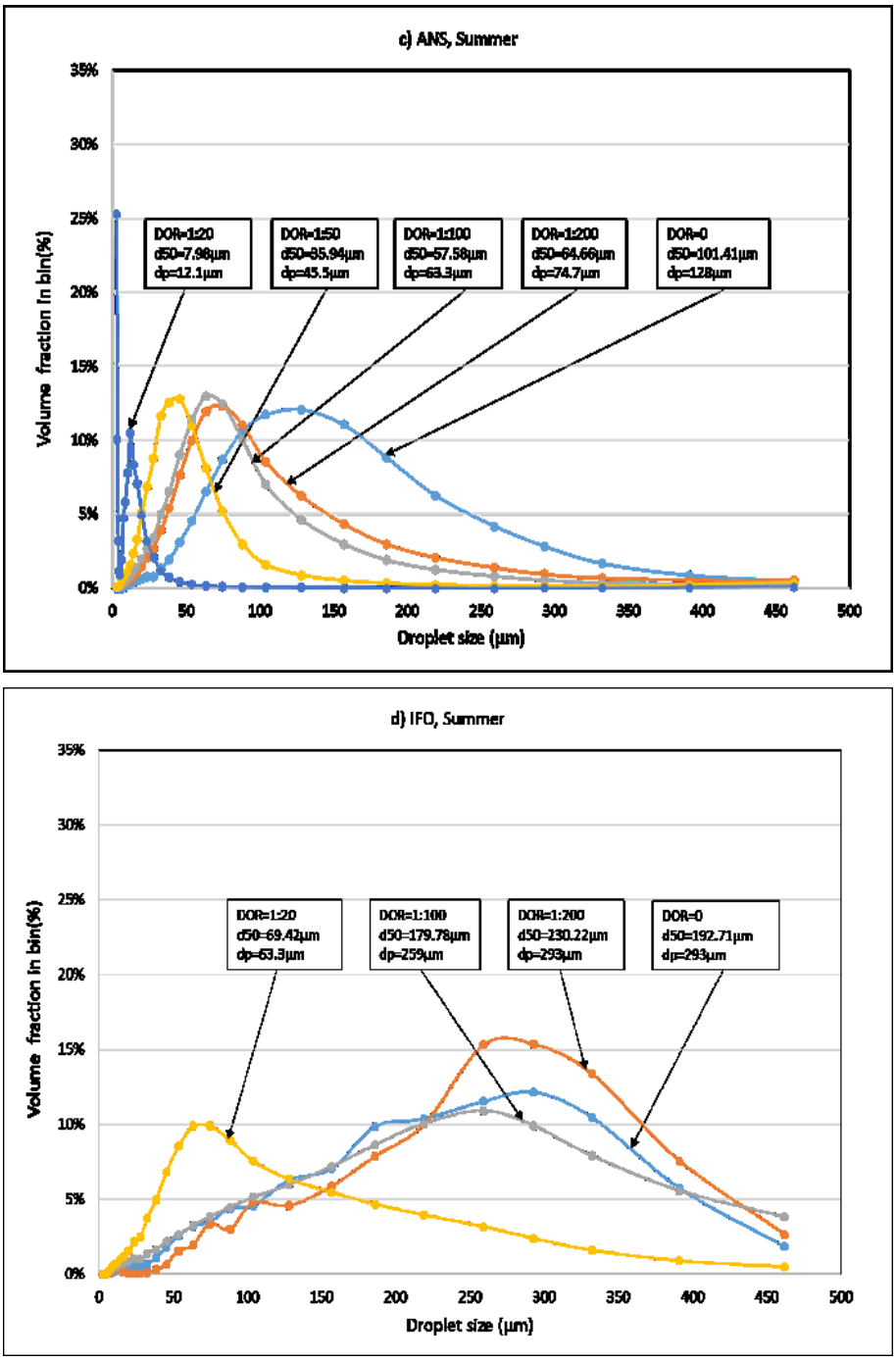

Figure 4-6: Examples of volume fraction in each size bin (%) as a function of DOR with ANS and IFO in summer seasonal conditions: c) ANS, summer condition; d) IFO, summer condition.

In general, chemical dispersant played an important role in reducing droplet sizes for both oils. The effectiveness of chemical dispersant on reducing droplet size distribution was higher for ANS (medium crude oil) than for IFO-120 (heavy fuel oil). The droplet size distributions of ANS, with different DORs in spring conditions, were similar to the corresponding distributions in summer conditions. The effect of water temperature was clearly demonstrate in this study with limited experimental data. Therefore, the effect of water temperature is not considered in the later data analysis.

4.2 Prediction of median volume diameter (d_{50})

4.2.1 Issues of the Modified Weber number scaling approach

As mentioned in the research objectives, the experimental data is to be used to assess and improve existing oil droplet size approaches, for better prediction of oil droplet size distribution from subsurface oil releases. Comparing the available oil droplet size distribution approaches (Chapter 2), the Modified Weber Number (MWN) approach is easier to be implemented in oil spill models because of its robustness and efficiency. Therefore, the MWN approach was selected in this study to fit the new experimental data. In this section, the comparison of MWN scaling, using Brandvik *et al.* (2013) Tower Tank data and experimental data, was presented and the challenge of using the Modified Weber Number approach in this study was discussed.

4.2.1.1 The performance of the MWN scaling for experimental data

The data from Brandvik *et al.* (2013) Tower Tank, using Oseberg oil as experimental oil, is plotted in the relation of the MWN (We^*) and relative median droplet size (d_{50}/D) (Figure 4-7). The MWN scaling fit the Tower Tank data well, with empirical coefficients A=15.0 for both untreated and treated oil (0≤DOR≤1:100) (Brandvik *et al.*, 2013). The scaling also fit to the data with DOR=1:25 when the empirical coefficient A was reduced to 8.7. In order to establish the MWN scaling for experimental data of ANS and IFO-120, more parameters, such as viscosity and interfacial tension (IFT), were also measured at COOGER. Using these data, the values of MWN (We^*), Viscosity number (Vi) and Reynolds number (Re) were calculated. These measured parameters and calculated values for ANS and IFO-120 are presented in Table 4-1 and Table 4-2, respectively.

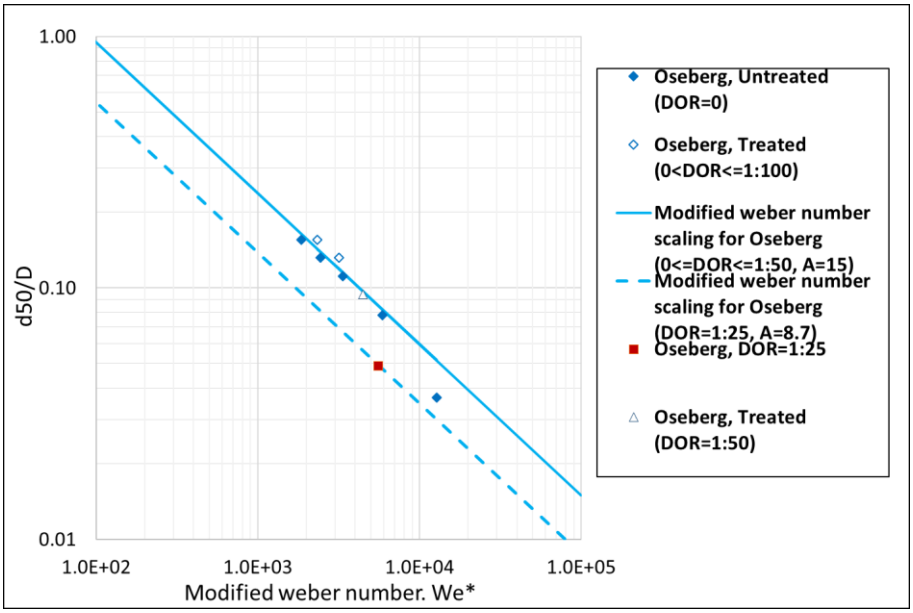

Figure 4-7: Data regression from modified weber number (We^*) and relative median droplet size (d_{50}/D) from Brandvik *et al*. (2013) Tower Tank experiments for untreated oil and oil with premixed dispersants (Regenerated from Johansen, *et al*., 2013).

Table 4-1: Data analysis for droplet size distribution of ANS.

No.	Factor	parameters						
	DOR	Dynamic Viscosity (mPa·s)	d_{50} (μm)	d_p (μm)	IFT (mN/m)	*Vi*	We^*	*Re*
1	0	7.2	81.9	88.2	63.97	1.52	4.19×10^3	3852.38
2#	1:250	8.2	398.780	462	60.52	1.97	3.83×10^3	3642.77
2R	1:200	8.2	65.750	74.7	60.52	2.04	6.79×10^3	3779.38
3	1:100	8.3	56.875	74.7	55.94	2.19	6.17×10^3	3656.72
4#	1:25	7.6	9.534	10.2	42.07	2.64	8.09×10^2	3972.47
4R#	1:20	7.6	2.340	12.1	42.07	2.69	1.12×10^3	4031.43
5#	0	7.2	70.512	74.7	63.97	1.63	4.8×10^3	4138.34
6	1:250	8.2	62.961	74.7	60.52	1.96	6.44×10^3	3638.87
6R	1:200	8.2	64.140	74.7	60.52	2.35	8.50×10^3	4358.32
7	1:100	8.3	55.487	74.7	55.94	2.12	5.91×10^3	3551.38
8#	1:25	7.6	3.095	12.1	42.07	2.6	8.23×10^3	3893.87
8R#	1:20	7.6	2.739	12.1	42.07	2.78	9.41×10^3	4171.8
9	0	7.2	68.131	88.2	63.97	1.64	4.88×10^3	4169.46
10	1:250	8.2	66.325	74.7	60.52	1.97	6.44×10^3	3655.78
10R#	1:200	8.2	212.55	462	60.52	2.42	8.68×10^3	4481.91
11	1:100	8.3	57.589	74.7	55.94	2.13	5.90×10^3	355.76
12	1:25	7.6	6.301	12.1	42.07	2.63	7.98×10^3	3938.78
12R	1:20	7.6	6.570	12.1	42.07	2.77	8.77×10^3	4150.74
13	0	7.2	88.870	104	63.97	1.77	5.41×10^3	4499.9
14	1:200	8.2	64.661	74.7	60.52	2.07	6.98×10^3	3840.5
15R	1:100	8.3	63.604	74.7	55.94	2.34	6.77×10^3	3911.2
16	1:20	7.6	7.987	12.1	42.07	2.73	8.44×10^3	4097.4
17	0	7.2	97.212	128	63.97	1.75	5.24×10^3	4439.1
18	1:200	8.2	65.183	74.7	60.52	2.09	7.06×10^3	3873
19	1:100	8.3	59.305	63.3	55.94	2.18	6.10×10^3	3642.6
20	1:20	7.6	6.999	12.1	42.07	2.71	8.39×10^3	4065.1
21	0	7.2	101.396	128	63.97	1.73	5.14×10^3	4402.1
22	1:200	8.2	63.747	74.7	60.52	1.98	6.5×10^3	3666.2
23	1:100	8.3	57.583	63.3	55.94	2.19	6.16×10^3	3655.4
24	1:20	7.6	8.391	12.1	42.07	2.68	8.07×10^3	4011.8
25#	1:50	8.1	43.94	45.5	N/A	N/A	N/A	3470.4
26	1:50	8.1	37.44	45.5	N/A	N/A	N/A	3628.5
27	1:50	8.1	35.94	45.5	N/A	N/A	N/A	3339.8

Note: # mark means these data were not considered in the prediction of droplet size distribution due to incomplete measured distribution. N/A means data or value is not available.

Table 4-2: Data analysis for droplet size distribution of IFO-120.

No.	Factor	Parameters						
	DOR	**Dynamic Viscosity (mPa·s)**	d_{50} **(μm)**	d_p **(μm)**	**IFT (mN/m)**	***Vi***	***We****	***Re***
1#	0	44	230	259	46.78	5.27	5.29×10^2	293.5
1R	0	44	265.9	293	46.78	5.52	5.43×10^3	307.4
2	1:250	45	197.3	259	57.84	5.14	6.24×10^2	338.0
2R#	1:200	45	293.510	293	57.84	5.36	9.62×10^2	352.556
3	1:100	42	223.1	259	56.97	5.22	7.01×10^2	388.1
4#	1:25	40	122.2	186	49.09	3.75	4.71×10^2	265.4
4R#	1:20	40	195.310	462	49.09	4.14	4.96×10^2	292.84
5	0	44	176.6	259	46.78	8.56	1.05×10^3	476.4
6R#	1:200	45	312.310	319	57.84	4.86	5.21×10^2	319.451
7R#	1:100	42	341.750	462	56.97	5.11	6.31×10^2	379.893
8	1:25	40	98.9	128	49.09	5.36	8.18×10^2	379
8R	1:20	40	177.920	293	49.09	4.59	5.85×10^2	324.444
9	0	44	100.4	186	46.78	11.19	1.69×10^2	622.7
10R#	1:200	45	408.290	462	57.84	4.99	5.1×10^2	328.489
11R#	1:100	42	370.340	462	56.97	N/A	N/A	N/A
12	1:25	40	93.8	128	49.09	7.44	1.29×10^3	525.7
12R	1:20	40	211.340	293	49.09	4.29	5.14×10^2	303.449
13#	0	44	263.3	391	46.78	7.89	7.77×10^2	444.7
14	1:200	45	230.2	259	57.84	6.28	7.86×10^2	413.4
15	1:100	42	215.2	259	56.97	7.17	1.07×10^3	533.7
16	1:20	40	82.8	88.2	49.09	8.52	1.59×10^3	601.8
17	0	44	192.7	293	46.78	7.99	9.44×10^2	444.5
18#	1:200	45	224	462	57.84	7.47	8.38×10^2	491.6
19	1:100	42	179.8	259	56.97	8.63	1.4×10^3	641.9
20	1:20	40	69.38	74.7	49.09	9.32	1.86×10^3	658.4
21#	0	44	254.6	391	46.78	8.27	8.1×10^2	460.1
22#	1:200	45	245.9	293	57.84	8.18	9.54×10^2	538.3
23	1:100	42	167.8	219	56.97	8.60	1.44×10^3	639.7
24	1:20	40	52.6	63.3	49.09	10.24	2.25×10^3	723.9

Note: # mark means these data were not considered in the prediction of droplet size distribution due to incomplete measured distribution. N/A means data or value is not available.

The relationship between the MWN (We^*) and relative median droplet sizes (d_{50}/D) for ANS and IFO-120 are presented in Figure 4-8 and Figure 4-9, respectively. The MWN scaling for ANS and IFO-120, with different DORs, were established by adjusting the value of empirical coefficients (A). According to the regression analysis for ANS (Figure 4-8), the MWN scaling, with A=5, fits the experimental data of untreated oil and treated oil (0 ⩽DOR≤1:100) reasonably well, but it was not as close as that for the Tower Tank data (Oseberg Blend crude oil). Compared with the A (A=15) for the Tower Tank data with 0⩽ DOR≤1:100, the empirical coefficient A for ANS was much lower (A=5). In the experimental data with DOR=1:20, the regressed value of empirical coefficient (A) for ANS was 0.64, which for Tower Tank data was 8.7. In comparison, the regression results of empirical coefficient A for IFO-120, with different DORs, were also different (Figure 4-9). The MWN scaling, with A=5, is a good fit to the experimental data with 0⩽ DOR≤1:100 of IFO-120, but the scaling, with A=2.45, closely corresponded to the experimental data with DOR=1:20.

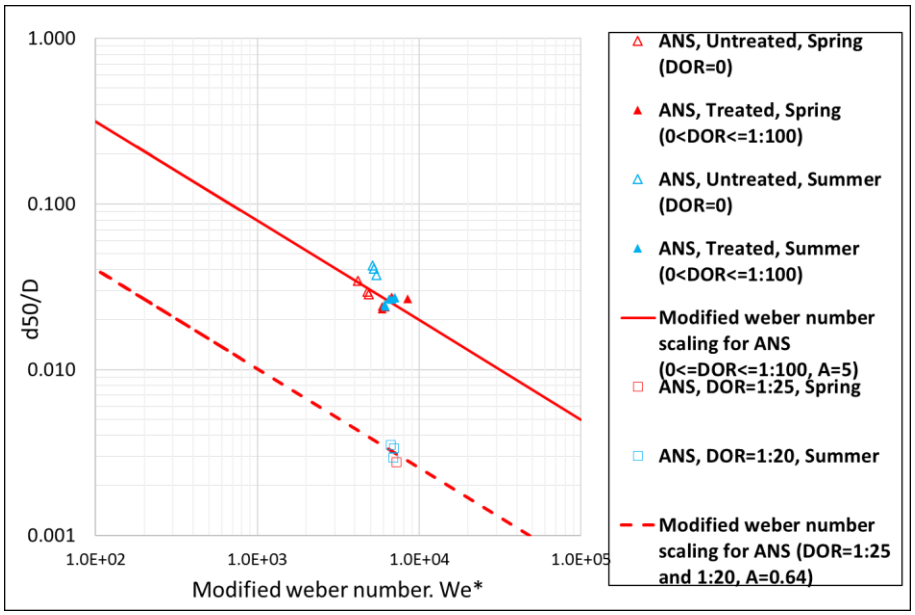

Figure 4-8: Data regression from Modified Weber number (We^*) and relative median droplet size (d_{50}/D) from untreaed oil and oil with premixed dispersants of ANS.

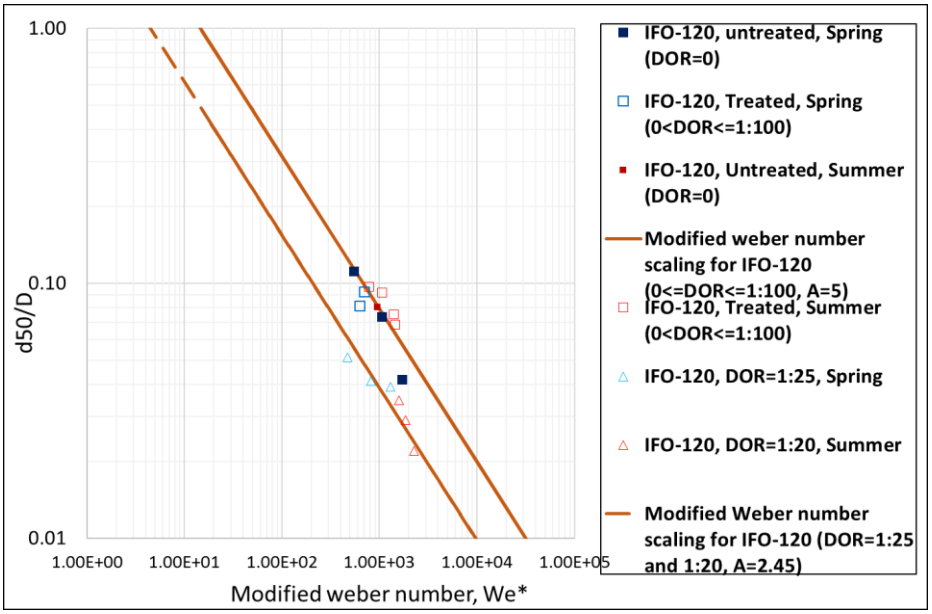

Figure 4-9: Data regression from Modified Weber number (*We**) and relative median droplet size (d_{50}/D) for untreated oil and oil with premixed dispersants of IFO-120 oil.

In general, the MWN scaling fits the experimental data of IFO-120 better than ANS. The regressed *A* value for untreated and treated oil of IFO-120 (0≤DOR≤1:100) was equal to 5, which was the same as for ANS. The regressed *A* value was 2.45 and 0.64 for IFO-120 and ANS with DOR=1:20, respectively. When DOR is increased from less than 1:100 to 1:20, the regressed *A* values have been reduced by 42% for Oseberg oil. This is close to the 51% reduction for IFO-120. However, the reduction of *A* for ANS is at a much higher level of 87%, it was almost doubled in the experimental data of ANS (around 87% reduction). According to the studies by Mackay and Hossain (1982), the reduction of *A* can affect by the amount of dispersant and the volumetric ratio of water to oil. It is necessary to investigate the effect of IFT on the magnitude of reduction of the *A* value.

4.2.1.2 Interfacial tension between oil and water

According to Eq.(2) and (6), the interfacial tension (IFT) of oil-water plays a role in determining the value of MWN, which affects the fitting of MWN scaling to experimental data. However, the measured value of IFT between seawater and crude oil can vary due to the effect of the amount of dispersant, the volumetric ratio of water to oil, and temperature (Mackay and Hossain, 1982). The usage of chemical dispersants can also result in a

dramatic drop in the value of IFT of oil/water and consequently raise the number of small droplets. For instance, according to the study by Khelifa and So (2009), the results showed that the value of IFT for oil-brine can be ultra-low under the effect of higher dosage of chemical dispersant. It was also mentioned by the Johansen *et al.* (2013), the value of IFT on their study were determined from the controllable oil sampling, which can control the oil to water ratio as the same. However, in the in-situ sampling, it is hard to control the oil to water ratio, which can result in different value of IFT, so the measurement of IFT in the real world is impractical and it should be avoided. In order to assess the droplet size approach by using experimental data and determine the value of the empirical coefficient, a different approach without using IFT value should be considered, in our study, Reynolds Number scaling approach is considered.

4.2.2 Reynolds Number scaling approach

As reviewed in Chapter 2, the Modified Weber Number approach was developed from the Weber Number approach. Wang and Calabrese (1986) found that the Weber Number scaling and the Reynolds Number scaling (Eq. 21) can govern droplet breakup for different viscosity numbers: small viscosity number ($Vi \rightarrow 0$) and large viscosity number ($Vi >> 1$), respectively. The dimensionless number, viscosity number (Vi) can be expressed as:

$$Vi = We/Re \tag{20}$$

Comparison between the Modified Weber Number scaling (Eq. (7) and the Reynolds Number scaling (Eq. (21), the latter has an apparent advantage of avoiding the inconsistent IFT measurements and can make a comparison of data from different sources easier. In our study, the viscosity numbers for ANS and IFO-120 are larger than 1, and the values (Vi) for Oseberg oil are also large than 1 (Brandivik, *et al.*, 2013). So, the Reynold Number scaling can be used in our study to present the corresponding relation between Reynold Number (Re) and relative median diameter (d_{50}/D).

$$\frac{d_{50}}{D} = A^{5/4} * 0.8^{3/4} * (Re)^{-3/4} \tag{21}$$

$$Re = \frac{\rho UD}{\mu} \quad (22)$$

Where

Re: Reynolds Number

μ : Dynamical viscosity

4.2.2.1 Data fit with Reynolds Number approach

According to the data from Johansen *et al*. (2013) research, the Reynolds Number (*Re*) for the Tower Tank data were calculated and the relationship between *Re* and relative median diameter (d_{50}/D) is plotted in Figure 4-10. The empirical coefficient (*A*) value for the data, with 0≤ DOR ≤1:100, was equal to 16.8, the coefficient (*A*) for the data, with DOR=1:25, was equal to 8.7. The regressed *A* value decreased by 48.2 % from the data with 0≤ DOR ≤1:100 to DOR=1:25 for Oseberg Blend by using the Reynolds Number approach.

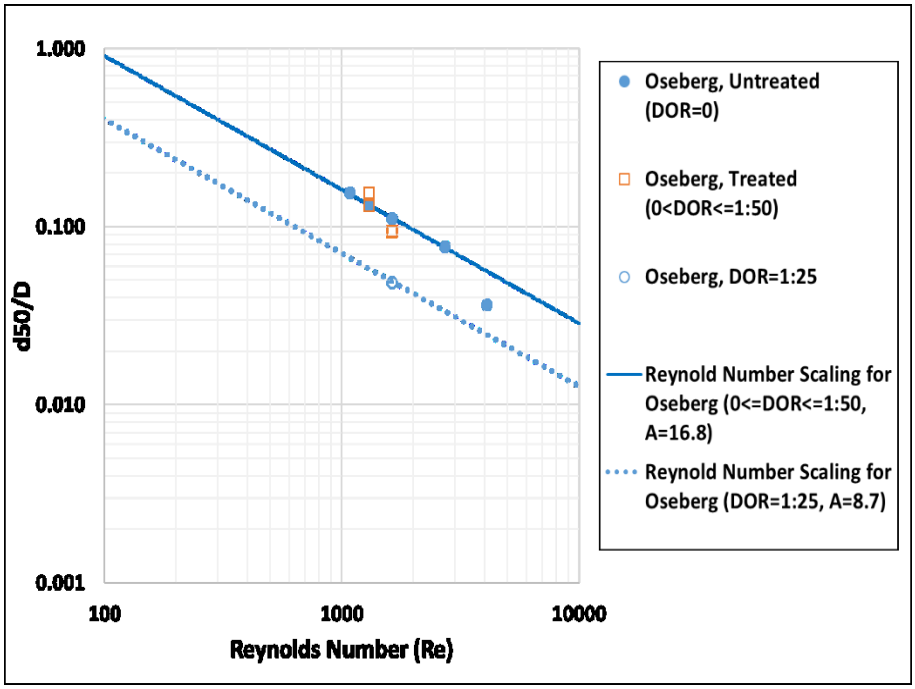

Figure 4-10: Data regression for constant *A* from Reynolds number and d_{50}/D for the data from Brandvik et al. (2013).

The Reynolds Number for experimental data of ANS and IFO-120 were also calculated and presented in Table 4-1 and Table 4-2. The relative median diameters against with Reynolds Numbers for ANS and IFO-120 are plotted in Figure 4-11 and Figure 4-12, respectively. It can be seen that the experimental data of both oils fit the Reynolds number scaling overall well with appropriate empirical coefficients (*A*). The Reynolds Number Scaling was also used to fit the additional data of ANS with DOR=1:50 and is presented in Figure 4-11.

The regressed results, using the Reynolds Number Scaling, for ANS showed that the *A* were decreased with the increasing of DORs. The regressed *A* for the data, with 0≤ DOR ≤1:100, was equal to 9, this value was reduced to 5.35 for the data with DOR=1:50 and it dropped to1.65 dramatically when the DOR was increased to 1:20. Around a 41% reduction of *A* value was observed from 0≤ DOR ≤1:100 to DOR=1:50, but a dramatic reduction was observed from DOR=1:50 to DOR=1:20 (reduced by 69%). Based on the initial data analysis, this great reduction from DOR=1:50 to DOR=1:20 may be caused by an increasing volume fraction of the smallest oil droplet sizes with DOR=1:20, and consequently affect the regression results.

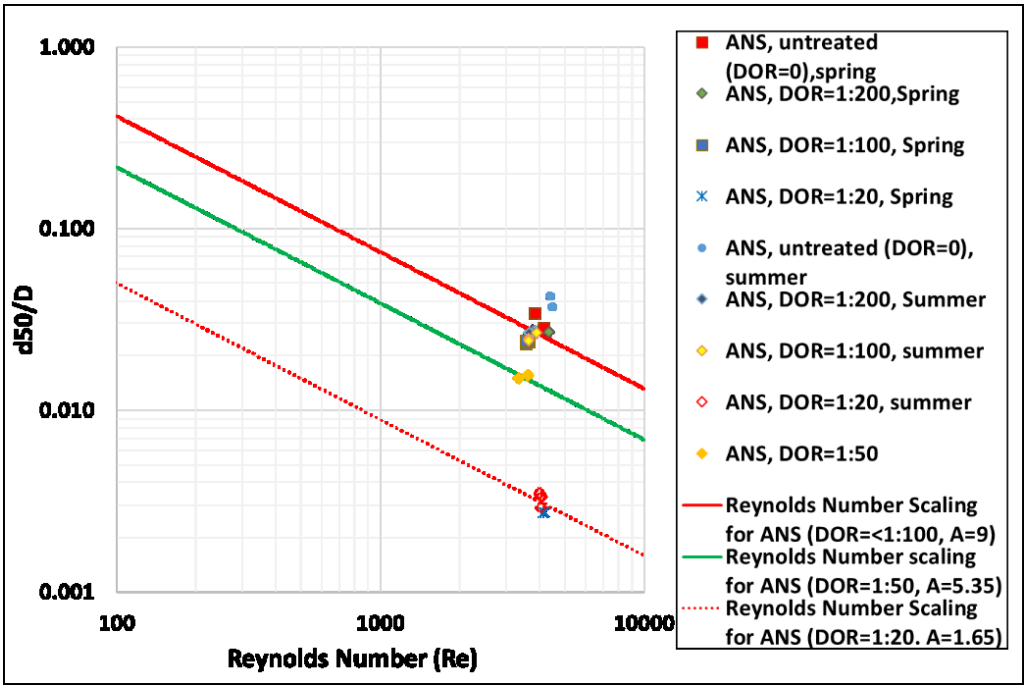

Figure 4-11: Data regression for constant A from Reynolds number and *d50*/D for ANS experimental Data.

Figure 4-12 presents the relationship between relative median diameter and the Reynolds Number for IFO-120. The experiments of IFO-120, with DOR=1:50, were not conducted due to the unavailability of the experimental facility. Therefore, only data with 0≤ DOR ≤1:100 and DOR=1:20 were plotted in this figure. The regressed empirical coefficient *A* values were 6.1 and 3.21 for the data, with 0≤ DOR ≤1:100 and DOR=1:20, respectively. There was around 47.4% reduction of *A* value from 0≤ DOR ≤1:100 to DOR=1:20, which was the same reduction, shown in Brandvik *et al.* (2013). Except the 69% reduction observed in ANS from DOR=1:50 to 1:20, the empirical coefficient (*A*) value for these three oils from lower dosage of dispersant (0≤ DOR ≤1:100) to higher dose of dispersant (DOR=1:20 or 1:50) was ranged from 41% to 50%. This reduction could be used as a effectiveness value of chemical dispersant on droplet size distribution.

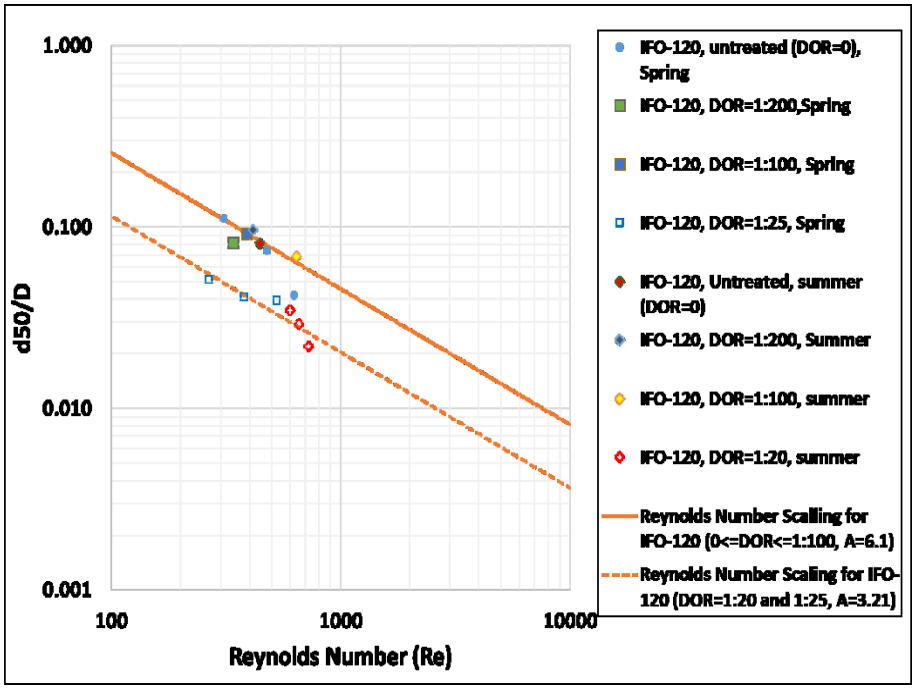

Figure 4-12: Data regression for constant A from Reynolds number and d_{50}/D for ANS experimental Data.

The Reynolds Number scaling for Oseberg Blend, ANS and IFO-120 oils with different DORs are plotted in Figure 4-13 with the regressed *A* values. This figure shows that the empirical coefficients *A* reduced with the increasing of DORs, and the *A* values decreased with the increasing of oil viscosity (Viscosity: Oseberg Blend<ANS<IFO-120).

For example, if the regressed A values for the experimental data with 0≤DOR≤1:100 were only considered, Oseberge Blend (light viscous crude oil) has the highest A value (A=16.8), following by medium viscous crude oil (ANS) with A equal to 9, then the heavy viscous oil (IFO-120) has the smallest A value (A=6.1). The similar reduction was also presented on the case with high DORs (DOR=1:20). It was known that the value of empirical coefficient (A) appears to be influenced by oil viscosity (light, medium and heavy oil). However, due to the limited oil viscosity used in this study, it was hard to determine whether different crude oils with slightly changed viscosity have a great effect on the selection of empirical coefficient. More experimental data using different crude oils are suggested in future study.

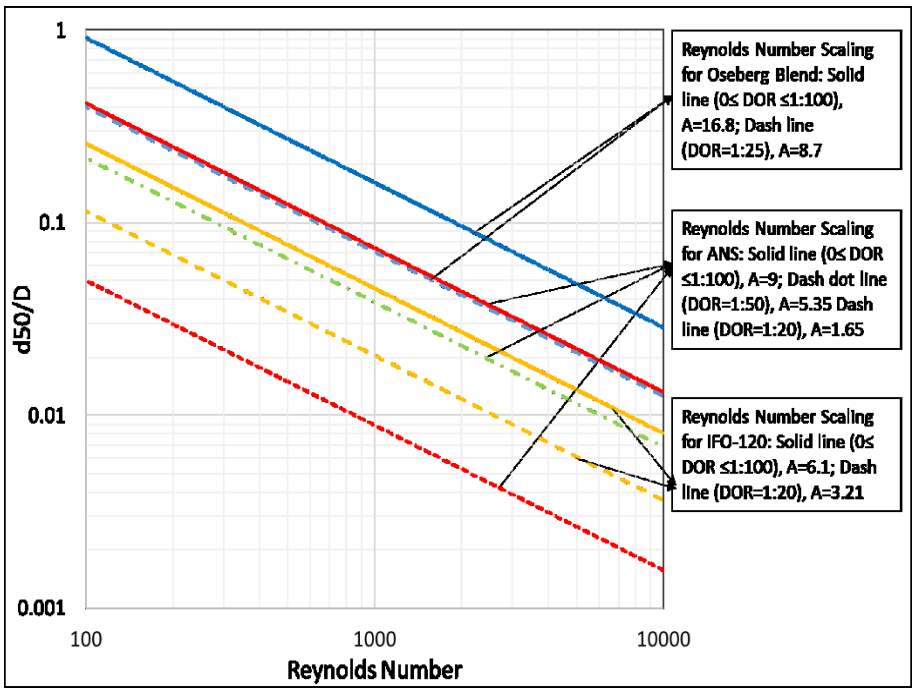

Figure 4-13: Reynolds number scaling for empirical coefficient A of Oseberg Blend oil, ANS and IFO-120.

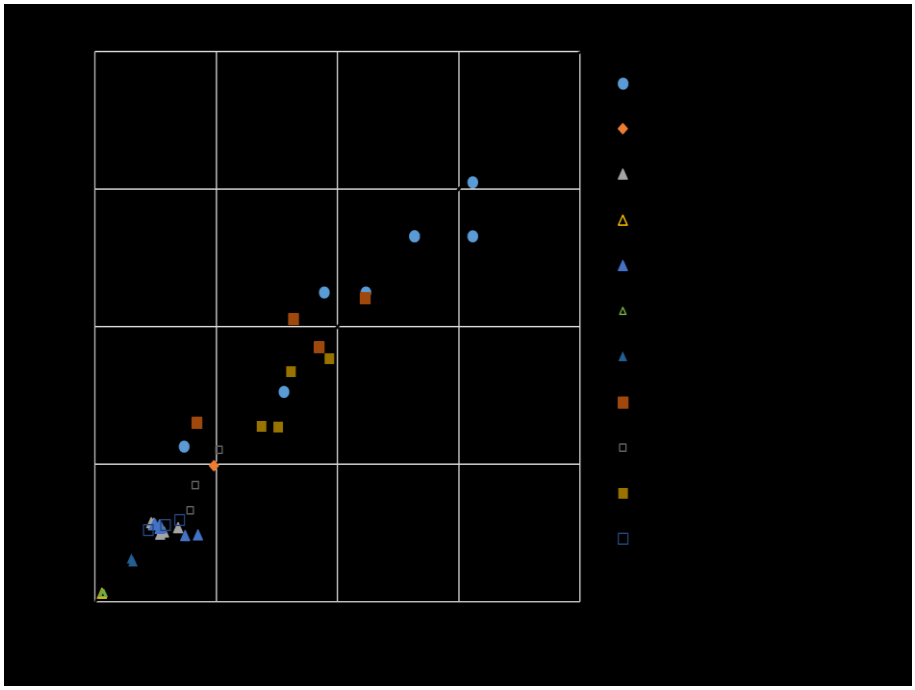

Figure 4-14: Measurement and calculation d_{50}/D from Tower Tank experiments and experiments with ANS and IFO-120.

According to the different regressed values of the coefficient for the experimental data and the Tower Tank (Oseberg Blend crude oil) data, the relative median droplet sizes were computed based on Eq.(21. A correlation curve of measured and computed relative median droplet sizes for the data of Oseberg Blend, ANS and IFO-120 are presented in Figure 4-14. It was shown by the figure that the computed and measured d_{50}/D correlated overall well for three oils, with and without chemical dispersant injection. The use of different coefficient (A) values for different oil types and different DORs can provide a good fit to the data. According to Figure 4-13 and Figure 4-14, the effect of different DORs on the selection of A for different DOR was clearly observed and the analysis of A as a function of DOR was presented in the following section.

4.2.2.2 Correlation between empirical coefficient (A) and DORs

According to the Figure 4-11and Figure 4-12, the regressed A value for the Reynolds Number scaling of ANS with 0≤DOR≤100, DOR=1:50 and DOR=1:20 are 9, 5.35 and 1.65, respectively. As well, the differences in the coefficient values for different DORs were also

presented in IFO-120 (A value for 0≤DOR≤100 was 6.1, for DOR=1:20 was 3.21) and Oseberg Blend (the A value for data with 0≤DOR≤100 was 16.8 and for DOR=1:25 was 8.7). In the study by Johansen *et al.* (2013), the empirical coefficient (A=15) was determined without the consideration of DOR=1:25. However, this study indicated that a high dosage of dispersant (DOR>1:100) can have a great effect on the empirical coefficient value. The results shows a notable reduction with the presence of high DOR (Figure 4-3).

In a realistic oil spill accident of high volume, high dosage of dispersant tends to have a better treatment effect on spilled oil. For example, in the DWH incident, the 1:25 of dispersant to oil ratio was used as a response, and resulted in a dramatic reduction on a large amount of surface oil (Conmy, *et al*., 2013). Hence, the empirical coefficient gained from Johansen *et al.* (2013) study, without consideration of high dosage of dispersant, may not be suitable and practical in the prediction of a large amount of oil spill. In order to increase the accuracy of the droplet distribution approach, it is necessary to study the relationship between DOR and empirical coefficient (A) value, especially for the high ratio of dispersant-to-oil (e.g. DOR=1:20). Furthermore, improving the performance of approach on predicting the fate and transport of oil from subsurface oil release in the realistic ocean environment.

According to the data presented in this study, the empirical coefficient A value for each experimental data was calculated, based on Eq. (21) and listed in Table 4-3 and Table 4-4 for ANS and IFO-120, respectively. Several relational equations were presented in the regression results for the relationship between A and DORs, such as four or five order polynomial equations. In order to have a simple and practical equation for the relationship between A and DOR, an equation with less coefficients is the first choice in this study. The exponential equation (Y=a*exp (b*x)) was considered in this study. Figure 4-15 and Figure 4-16 show the regression results by using exponential equations for ANS and IFO-120, respectively. Only two coefficients (a and b) are needed in this equation. The exponential equations and coefficients R^2 for ANS and IFO-120 are presented in Table 4-5.

Table 4-3: Coefficient (*A*) value for ANS with different DORs.

No.	DOR	*A*-value
SUBANS-1	0	10.91
SUBANS-9	0	9.88
SUBANS-2R	1:200	9.05
SUBANS-6R	1:200	9.66
SUBANS-10	1:200	8.93
SUBANS-14	1:200	9.02
SUBANS-18	1:200	9.12
SUBANS-22	1:200	8.67
SUBANS-6	1:100	8.54
SUBANS-3	1:100	7.90
SUBANS-7	1:100	7.61
SUBANS-11	1:100	7.85
SUBANS-15R	1:100	9.00
SUBANS-19	1:100	8.15
SUBANS-23	1:100	7.98
SUBANS-2TEST	1:50	5.28
SUBANS-3TEST	1:50	5.00
SUBANS-4R	1:20	0.65
SUBANS-8R	1:20	0.76
SUBANS-12R	1:20	1.52
SUBANS-16	1:20	1.76
SUBANS-20	1:20	1.58
SUBANS-24	1:20	1.81

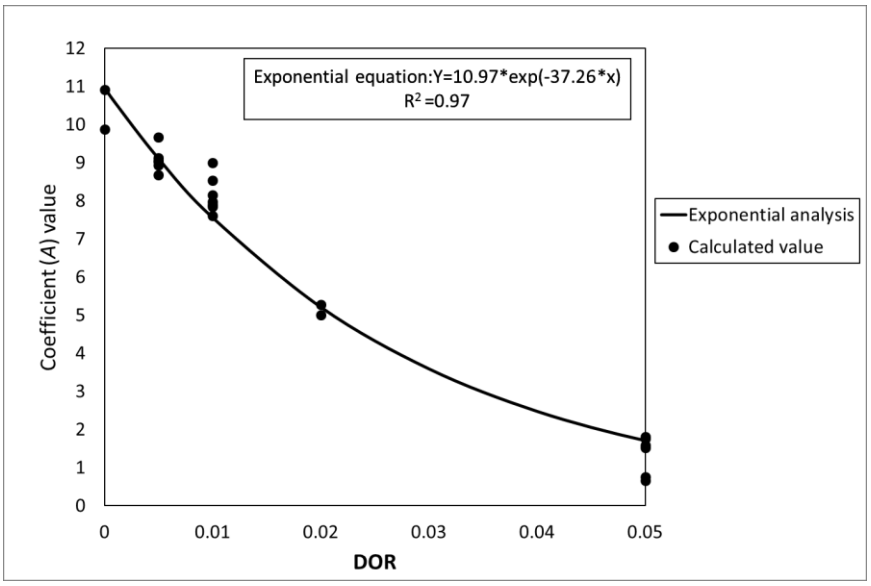

Figure 4-15: Regression analysis of *A* as a function of DORs for ANS.

Table 4-4: Coefficient (*A*) value for IFO-120 with different DORs.

No.	DOR	*A*-value
SUBIFO-9	0	4.30
SUBIFO-17	0	5.92
SUBIFO-2	1:250	5.08
SUBIFO-14	1:200	6.54
SUBIFO-3	1:100	6.08
SUBIFO-23	1:100	6.47
SUBIFO-4	1:25	3.02
SUBIFO-8	1:25	3.16
SUBIFO-12	1:25	3.68
SUBIFO-16	1:20	3.61
SUBIFO-20	1:20	3.31
SUBIFO-24	1:20	2.80

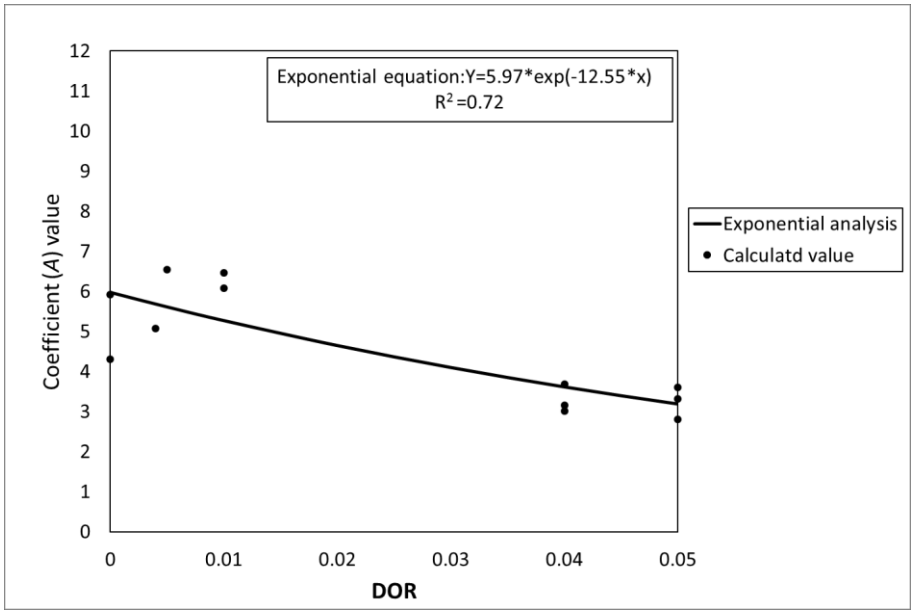

Figure 4-16: Regression analysis of *A* as a function of DORs for IFO-120.

Table 4-5: Regression equations and regression coefficients (R^2) for ANS and IFO-120.

Oils	R^2	Equations	
ANS	0.97	$Y = 10.97 * \exp(-37.26 * X)$	(23)
IFO-120	0.72	$Y = 5.97 * \exp(-12.55 * X)$	(24)

The regression coefficient (R^2) for ANS and IFO-120 differed: 0.97 for ANS and 0.72 for IFO-120. The reason that R^2 was lower for IFO-120 data, may be caused by the limited experimental data, such as the lack of data with DOR=1:50 and less data point for regression. The equation has an overall good fit to the experimental data of ANS (Figure 4-15). Comparing the equations for ANS and IFO-120, the coefficients (*a* and *b*) were different for both oils. There is a negative correlation between absolute coefficients values and viscosities: medium crude oil (ANS) has high absolute coefficient values, while, heavy oil (IFO-120) has small values. However, how the viscosity affected the coefficients was unable to be identified by using these limited datasets. It was suggested that additional

data for different viscosity of oils can be used together with existing experimental data to study the effect of oil viscosities on droplet size distribution approach.

4.3 Prediction of droplet size distribution function

4.3.1 Rosin-Rammler Distribution

Once the estimation of characteristic droplet size (d_{50}) was determined by the droplet size distribution approach, such as the Modified Weber Number from Johansen *et al.,* (2013) or the Reynolds Number used in this study, the corresponding statistical distributions for droplet sizes around the characteristic diameter (d_{50}) can be predicted. There are two distribution functions commonly used in literatures: the lognormal distribution and the Rosin-Rammler distribution (Lefebvre, 1989). Both distribution functions need two parameters. Currently, no additional experiments or studies identified the most appropriate distribution for general application. In the Johansen *et al.* (2013) study, the Tower Tank data were used to fit both distribution functions, and the results showed that the Rosin-Rammler distribution (Eq. (25) fit overall better to their data, with the spreading parameter α=1.8. Besides this, the Rosin-Rammler distribution was also used as the first approximation for the simulation of oil droplet size distribution from deep water blowout scenario (Aman, *et al*., 2015). In this study, the estimation of the statistical droplet size distribution was presented by the Rosin-Rammler distribution.

$$V(d) = 1 - \exp[-0.693\left(\frac{d}{d_{50}}\right)^{\alpha}] \tag{25}$$

Where:

$V(d)$: Cumulative volume distribution function

d/d_{50}: Relative droplet diameters

α: Spreading parameter

The cumulative volume distribution ($V(d)$) and characteristic diameter (d_{50}) for each experimental data of ANS and IFO-120 were calculated from the measured droplet size distribution data. Based on these data ($V(d)$ and d_{50}), the value of spreading parameter (α) for each experiment was calculated and presented in Table 4-6 and Table 4-7 for ANS and

IFO-120, respectively. For ANS, the spreading parameter (α) is much smaller for DOR=1:20. The average value of α for experimental data of ANS (include DOR=1:20) was around 1.79, which was closed to 1.8, while IFO-120 showed a slightly higher α value (1.95). Compared oil properties of these two oils with that of Oseberg Blend oil, the specific gravities (density) of these three oils are 0.8393 for Oseberg Blend oil, 0.8777 for ANS and 0.9587 for IFO-120. Oseberg Blend oil and ANS have similar density, while the density of IFO-120 is slightly higher. More investigations are needed to better understand how different oil types affect the selection of α value.

Table 4-6: Spread coefficient for Rosin-Rammler distribution of ANS.

			All Data			Average			
			Single	**2-Step:**		**Single**	**2-step**		
			α	α_1	α_2	α	α_1	α_2	α_1 and α_2
summer	Untreated	No. 13	1.93	2.32	1.57	1.90	2.30	1.55	1.93
		No. 17	1.87	2.29	1.51				
		No. 21	1.9	2.3	1.58				
	1:20	No. 16	1.12	0.62	1.39	1.14	0.64	1.41	1.02
		No. 20	1.12	0.61	1.34				
		No. 24	1.17	0.68	1.49				
	1:100	No. 15R	1.99	2.24	1.65	2.02	2.23	1.66	1.94
		No. 19	2.05	2.24	1.67				
		No. 23	2.03	2.20	1.66				
	1:200	No. 14	1.96	2.1	1.49	2.02	2.21	1.57	1.89
		No. 18	2.03	2.29	1.61				
		No. 22	2.06	2.25	1.62				
Spring	Untreated	No. 1	2.08	2.00	1.90	2.04	2.01	1.93	1.97
		No. 5#	/	/	/				
		No. 9	1.99	2.02	1.95				
	1:20	No. 4R#	/	/	/	0.98	0.49	1.10	0.80
		No. 8R#	/	/	/				
		No. 12R	0.98	0.49	1.10				
	1:50	No.2-TEST	1.74	2.04	1.6	1.94	2.19	1.775	1.98
		No.3-TEST	2.14	2.34	1.95				
	1:100	No. 3	2.14	2.17	2.11	2.10	2.11	2.09	2.10
		No. 7	2.15	2.13	2.18				
		No. 11	2.00	2.03	1.97				
	1:200 (and 250)	No. 2R	1.87	2.11	1.50	2.01	2.19	1.73	1.96
		No. 6R	1.92	2.16	1.54				
		No. 10	2.23	2.30	2.15				
Average						1.79	1.82	1.65	1.72

"/" indicates that the data is unavailable due to incomplete droplet size distribution from measurement.

Table 4-7: Spread coefficient for Rosin-Rammler distribution of IFO-120.

			All Data			**Average**			
			Single	**2-step**		**Single**	**2-step**		
			α	α_1	α_2	α	α_1	α_2	α_1 and α_2
Summer	Untreated	No.13#	/	/	/	1.86	1.53	2.20	1.87
		No.17	1.86	1.53	2.20				
		No.21#	/	/	/				
	1:20	No.16	1.75	2.13	1.44	1.72	2.04	1.37	1.71
		No.20	1.55	1.95	1.18				
		No.24	1.85	2.05	1.50				
	1:100	No.15	1.96	1.50	2.54	1.71	1.37	2.17	1.77
		No.19	1.57	1.30	2.00				
		No.23	1.59	1.31	1.975				
	1:200	No.14	2.39	1.85	3.10	2.39	1.85	3.10	2.48
		No.18#	/	/	/				
		No.22#	/	/	/				
Spring	Untreated	No.1#	/	/	/	1.60	1.41	1.89	1.65
		No.5	1.66	1.32	2.14				
		No.9	1.54	1.49	1.63				
	1:25	No.4	2.13	2.24	2.10	1.98	2.18	1.85	2.01
		No.8	2.05	2.31	1.83				
		No.12	1.77	1.99	1.62				
	1:100	No.3#	/	/	/	/	/	/	/
		No.7R#	/	/	/				
		No.11R#	/	/	/				
	1:250	No.2	2.39	1.72	3.20	2.39	1.72	3.20	2.46
		No.6R#	/	/	/				
		No.10R#	/	/	/				
Average						1.95	1.73	2.25	1.99

"/" indicates that the data is unavailable due to incomplete droplet size distribution from measurement.

4.3.2 Two-step Rosin-Rammler distribution

Although 1.8 was considered as an approximate value of the spreading parameter in the Rosin-Rammler distribution, which can fit to different oil types with similar oil properties, from the initial data analysis, the distributions of data with $d/d_{50} \leq 1$ and $d/d_{50} > 1$ predicted by the Rosin-Rammler distribution were found to be different. Thus, it would be relatively less accurate to predict the droplet size distribution by only using single spreading parameter. In order to have a more accurate prediction, a two-step Rosin-Rammler approach was introduced by advancing from the Rosin-Rammler approach. Two separate spreading parameters, α_1 for $d/d_{50} \leq 1$ and α_2 for $d/d_{50} > 1$, were used in this proposed approach, providing a better fit of the data in all cases. Table 4-6 and Table 4-7 summarize the spreading parameters (α, α_1 and α_2) for all experiments.

Figure 4-17 shows an example of the cumulative distribution of d/d_{50} and regression results by using both single step Rosin-Rammler distribution and two-step Rosin-Rammler distribution. In Figure 4-17a, the two-step Rosin-Rammler distribution presented a better fit to the experimental data than single step. In Figure 4-17b, the regression coefficients (R^2) for both distribution functions were closed. This analysis indicated either singer step or two step Rosin-Rammler distribution can be used to predict droplet size distribution for both ANS and IFO-120, but the two-step Rosin-Rammler distribution showed an advantage to fit experimental data, presenting accurate prediction result.

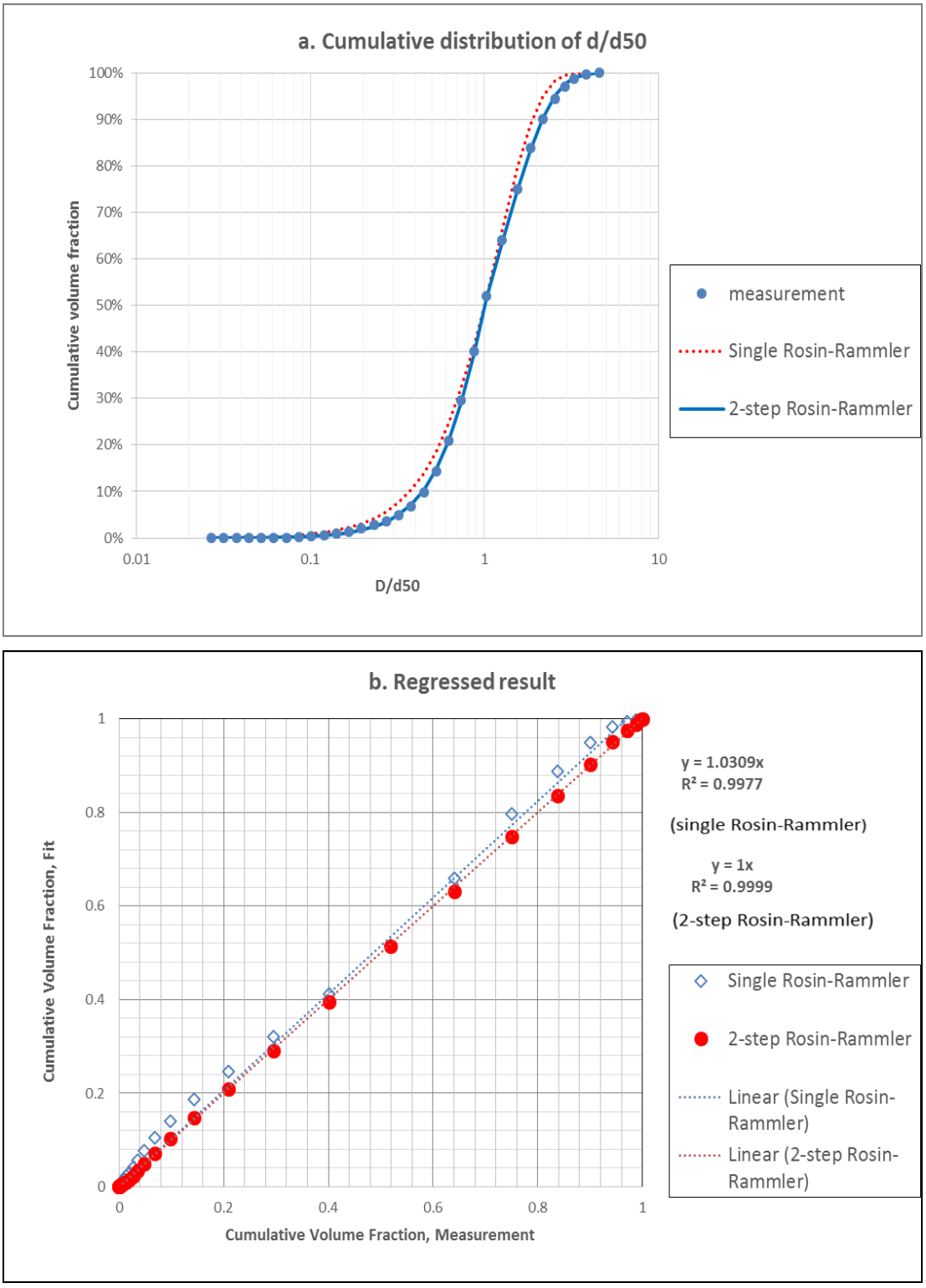

Figure 4-17: Example of the cumulative distribution of d/d_{50} (a) and regression results (b).

In Table 4-6 and Table 4-7, the average α_1 was 1.82 and α_2 was 1.65 for ANS; for IFO-120, the average α_1 was 1.73 and α_2 was 2.25. The average value of α_1 for both oils was close to 1.8 (1.82 for ANS and 1.73 for IFO-120), while the values of α_2 showed a big difference between ANS and IFO-120: smaller for ANS (α_2=1.65) and relatively larger for IFO-120 (α_2=2.25). Although there is a clear difference in terms of α_2, this study did not establish the relationship between α_2 and oil properties due to the limited experimental data. Further studies are needed to investigate the effect of different oil types on the selection of separated spreading parameters. Still, it was believed that the two-step Rosin-Rammler distribution can help to improve the accuracy of the prediction of droplet size distribution.

4.4 Comparisons of the predicted droplet size distribution with experimental data

In the previous sections, the improvement in the Reynolds Number approach and the two-step Rosin-Rammler distribution have been discussed. The approach will be used here to predict DSD and compared with experimental data. The estimated A values for ANS and IFO-120 were calculated based on Eq. (23) and (24), and the VMD (d_{50}) was calculated by using Eq. (21) with corresponding A value. The estimated cumulative volume fractions for ANS and IFO-120 were determined by two-step Rosin-Rammler distribution (α_1 and α_2) based on calculated d_{50} values. The cumulative volume fractions for both oils were also calculated by using the Rosin-Rammler distribution with single α. The selected spreading parameter as described in Table 4-8.

Table 4-8: The spreading parameters for ANS and IFO-120.

	Single Rosin-Rammler distribution	**Two-step Rosin-Rammler distribution**	
	α	**α_1**	**α_2**
ANS	1.8	1.8	1.65
IFO-120	1.8	1.8	2.25

Figure 4-18 and Figure 4-19 are examples of comparison among the estimated results by using the single step Rosin-Rammler distribution, the two-step Rosin-Rammler distribution, and experimental data for cases of ANS and IFO-120 with DOR=1:200,

respectively. For ANS, the results, using the single step Rosin-Rammler distribution and the two-step Rosin-Rammler distribution, showed different fit to the experimental data. In the distribution of $d/d_{50}<1$, the values of α_1 (for two step Rosin-Rammer distribution) and α (for single step Rosin-Rammer distribution) were the same, this results in the distribution are the same for single step and two step Rosin-Rammler distribution. For the size of droplets larger than d_{50}, the distribution estimating by single step and two step Rosin-Rammler are difference with different spreading parameter applied. The estimated cumulative volume fraction (Figure 4-18a) for ANS by using the two-step Rosin-Rammler distribution was closer to experimental data than the single step Rosin-Rammler distribution, it was also showed in the case of IFO-120 (Figure 4-19a). Comparing the volume fraction for each size bin between the Rosin-Rammler distribution and the two-step Rosin-Rammler distribution (Figure 4-18b and Figure 4-19b), the results estimating by the two-step function showed that the volume fraction for the droplet sizes larger than d_{50} appeared to be closer to experimental data than that estimated by the single step Rosin-Rammler distribution. Overall, in our study, the results presented that the two step Rosin-Rammler distribution can make more accurate prediction result.

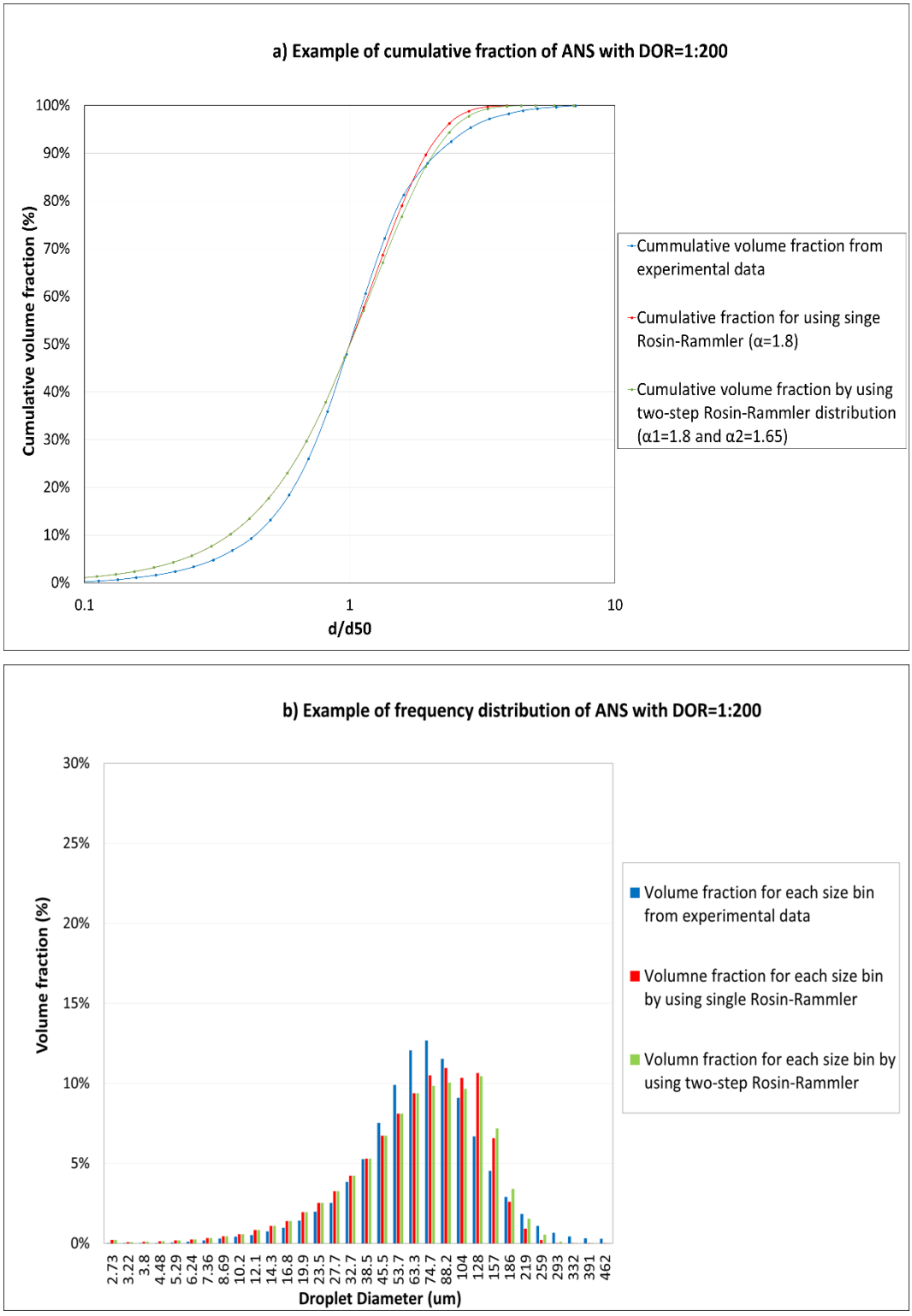

Figure 4-18: Example of the comparison among the Rosin-Rammler distribution and the two-step Rosin-Rammler distribution and measured experimental data; (a) cumulative volume fraction for the case of ANS with DOR=1:200, (b) and volume fraction of each size bin for the case of ANS with DOR=1:200

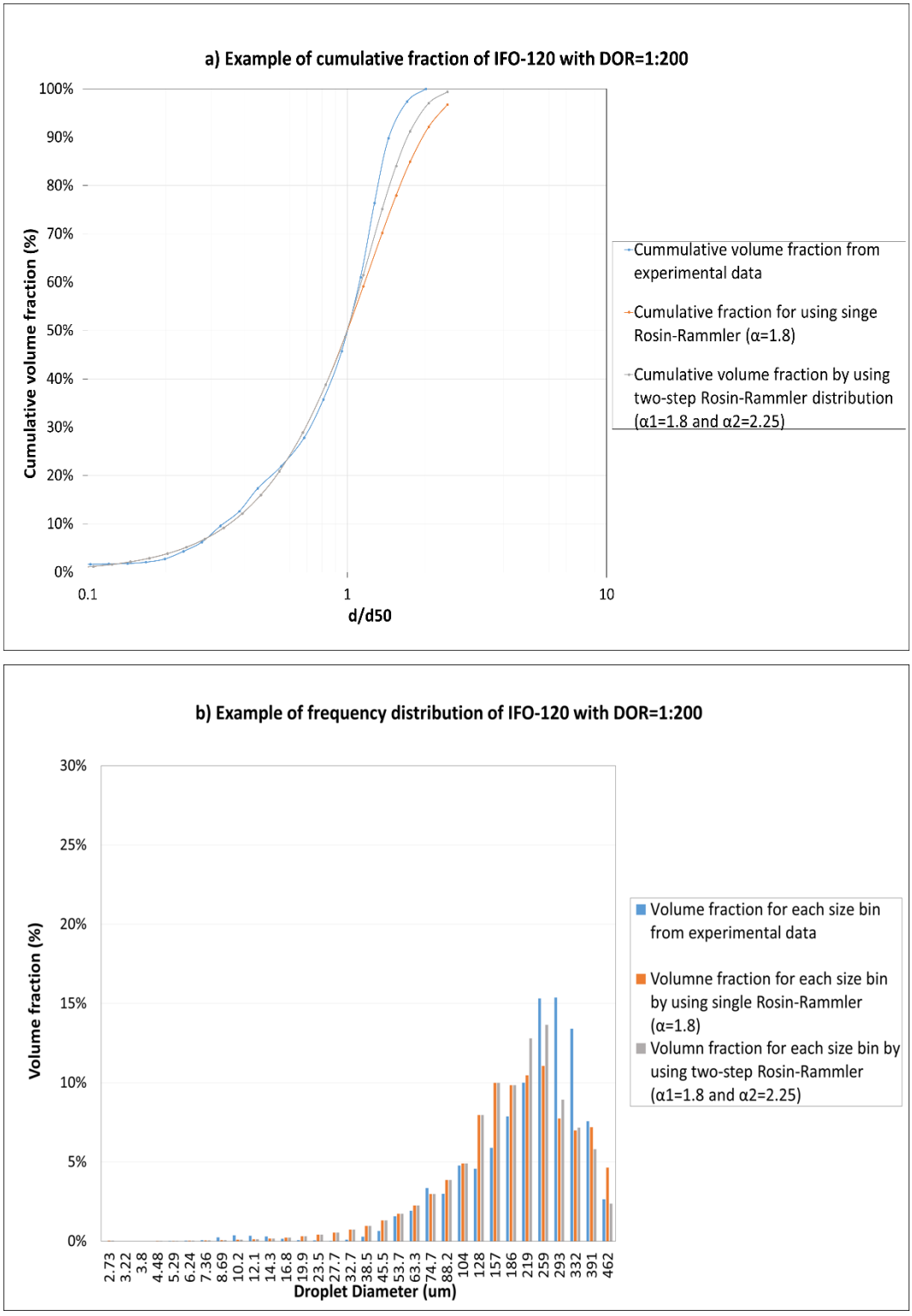

Figure 4-19: Example of the comparison among the Rosin-Rammler distribution and the two-step Rosin-Rammler distribution and measured experimental data; (a) cumulative volume fraction for the case of IFO-120 with DOR=1:200, (b) and volume fraction of each size bin for the case of IFO-120 with DOR=1:200

In summary, the Reynolds Number approach, integrated with the equation of A as function of DOR, provided a good estimation on characteristic diameter (d_{50}), and result in good prediction of cumulative volume fraction. The proposed two-step Rosin-Rammler approach has shown a better fit to experimental data than the single step Rosin-Rammlar distribution, especially for the oil droplet sizes larger than d_{50}. However, this two-step Rosin Rammler distribution were developed to have good fit to the experimental data, whether it can also have better fit than single Rosin Rammler distribution for all oils need to be studied. Except for the effect of oil types, the improved Reynolds Number approach and the Two-step Rosin-Rammler distribution can provide a reliable way to predict droplet size distribution, and ultimately provide support to decision-making for subsurface dispersant application. Further studies about the effect of different oil types on the droplet size distribution approach should be conducted to enable the development of a more generalized prediction approach.

CHAPTER 5. APPLICATION OF IMPROVED DROPLET SIZE DISTRIBUTION APPROACH: A MODELING STUDY

In this chapter, a case study, using the Oil Spill Contingency and Response (OSCAR) model, was conducted to investigate the effect of subsurface chemical dispersant on the fate and behaviour of oil from a hypothetical subsurface oil release on the Scotian Shelf, by using the newly developed equations for droplet size distribution predictions. The same oils used in the experimental study were used in this modeling study.

5.1 Oil spill model

The OSCAR, a three-dimensional particle-based model, was developed by SINTEF (the Foundation for Scientific and Industrial Research) to simulate the fate and transport of oil from surface and subsurface oil releases (Figure 5-1). The model computes dispersed and dissolved oil concentration in the water column, and the evolution of oil on the water surface or along shorelines (Reed *et al.,* 1995b; Aamo *et al.,* 1997; Reed *et al.,* 1999; Reed *et al.,* 2004). There are three key components to the OSCAR: a databased oil-weathering model, an oil trajectory and fate model, and an oil spill strategic response model. More details of the model and its validations have been reported by Reed *et al.,* (1996; 2000).

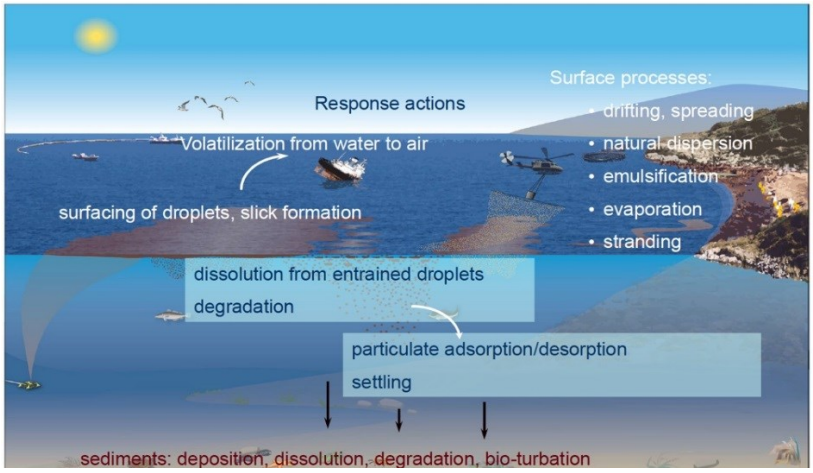

Figure 5-1: Fate/transport processes of oil included in the OSCAR model (Courtesy of SINTEF).

5.2 Study area

The Scotian Shelf is located in the southwest of Nova Scotia (Figure 5-2). The offshore oil and gas exploration in this area has continued for around half a century. The first offshore oil project, Cohasset-Panuke Project, has been exploited on the Scotian Shelf since 1992 (CNSOPB, 2004), and these offshore oil exploration and development activities were expanded to deeper waters recently. For example, the first deep water well drilling off Halifax harbour was the Shelburne Basin Exploration project, which started from 2015 and plan to complete by 2019. The drilling depth ranged from 1500 to 3000m water depth (CEAA, 2015). These oil and gas exploration and development activities increase the potential risk of subsurface oil blowout, which can bring disastrous effects to the ecology of the Shelf.

In the Shelburne Basin Exploration project environmental assessment report, oil spill model simulated oil blowout from deepwater for 30 days. The results showed that oil reached to water surface and shoreline would take 20 to 30 days. In order to test our new approach, the approach can be applied to the oil spill model to investigate the fate and transport of oil in case of a deep water oil blowouts event in this study area, as well, the application of subsurface chemical dispersant is also needed to determine its effects on the oil fate. This study assumes that oil is released off Nova Scotia ($64^0$00'W, $42^0$18'N) at 1700m water depth from a 0.2m of diameter pipe, and the release point is marked as a small square in Figure 5-2 and the domain of the model is in [69^0W, 38^0N] - [59^0W, 46^0N].

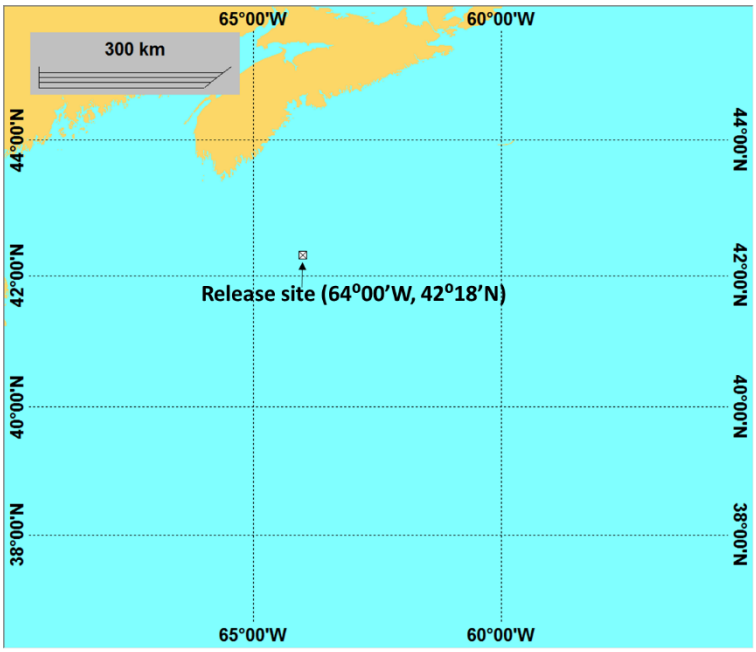

Figure 5-2: Study area and release site (study area: the Scotian Shelf; Release site: located at 1700m under the water surface).

5.3 General input parameters

Environmental data, such as ocean current, wind speeds and directions, are required for the OSCAR model in order to move oil particles from subsurface oil release. The user also needs to specify other model parameters, such as particle number and grid size. In this study, current data and wind forcing on oil spill modeling are the two main environmental parameters.

Hydrodynamic model—NEMO

The regional 1/36° NEMO model simulates high resolution regional currents. It was developed by using NEMO version 3.1 framework (Katavouta and Thompson, 2016). The domain covered by this model is on the Gulf of Maine, the Scotian Shelf and adjacent deep ocean. The horizontal resolution in longitude and latitude is approximately 1/36° (2.8 km average grid spacing) and vertically, it has 52 z-levels, with a spacing that varies from 0.7m closest to the surface to 233m for the deepest level (4000m) (Katavouta and Thompson, 2016). The advantage of this model is that its high resolution can give a better forcing for oil spill simulations.

Wind forcing—CFSR

The wind forcing used in this study was obtained from the global National Centers for Environmental Prediction (NCEP) climate forecast system reanalysis (CFSR). CFSR presents a more comprehensive analysis, including atmospheric, oceanic, sea ice and land surface outputs. These output products are measured at an hourly time resolution and a horizontal resolution of 0.5° latitude × 0.5° longitude (Saha et al., 2010).

Other model parameters

Except the environmental parameters, other model parameters, such as the number of particles (solid and dissolved) and the number of grid cells, are also necessary for model prediction. It was evaluated by Niu & Li (2016) and the results indicated that the values of the number of particles and grid cells can affect the accuracy of model prediction. In this study, the effect of these two parameters on prediction of the fate of oil droplets were not investigated. Thus, the number of particles for solid and dissolved are both set to 9000 and the number of grid cells is set to 1000 × 1000. The reason for using these values for particle number and grid size is because these values can give good details of simulation under the limited load capability of the software. These above configurations were used for all release scenarios in this chapter.

Two more user define droplet size parameters, characteristic diameter (d_{50}) and spreading parameter (α), are also required for accuracy simulating the fate of oil in marine environment. However, currently, these droplet size input parameters, for droplet size distribution simulation in the deepwater oil blowout model, are empirical formulations, which are gained from limited experimental data (Brandvik *et al.,* 2013 & Johansen *et al.,* 2001). In order to determine the effects of oil droplet size distribution parameters on the prediction results of the model, a sensitivity analysis of the model, based on several hypothesis scenarios, were conducted.

5.4 Sensitivity study of oil spill model on oil droplet size distribution

In order to study the effect of model on the prediction of the fate of oil, it is necessary to evaluate the sensitivity of model with various droplet size distribution parameters (d_{50} and α), to droplet size distribution. As shown in Table 5-1, three different characteristic

diameters (d_{50}=8μm, 60μm and 250μm) with the same spreading parameter (α=1.8) and, three different spreading parameters (α =0.5, 1.8 and 3) with the same characteristic diameter (d_{50} =60μm), were considered in this study.

5.4.1 Model scenarios

The input of Environmental data, the number of particles and the number of grid cells have been described previously. For this sensitivity study, only a medium crude oil, ANS, was investigated. This simulation assumed that a continuous release of ANS, at a rate of 298,800 barrels/day for 12 days (the maximum time required by regulation for capping the well) (CNSOPB, 2015). The oil was continuously tracked by the model for 60 days (from Jan. 1st, 2010 at 0:00 am to Mar. 1st, 2010 at 0:00 am).

Based on empirical formulations, the effect of characteristic diameter and spreading parameter on droplet size distribution showed great differences with different characteristic diameters and spreading parameters (Figure 5-3). The figure shows the cumulative volume fraction only had very slight change, when d_{50} increased from 8μm to 60μm, but it changed greatly when increase d_{50} to 250μm. For the different spreading parameters (α), the cumulative volume fractions showed a clear difference among these three values. In order to determine the sensitivity of model to oil droplet size distribution, with different d_{50} and α, five simulation scenarios were considered in this sensitivity study (Table 5-1). According to the wave tank experimental data and Tower Tank experiment (Brandvik, et al., 2013), the input minimum droplet size was 2μm and maximum droplet size was 500μm, which were the same for these five scenarios. The first three scenarios (No. 1, 2 and 3) showed different characteristic diameters (d_{50}), but the same spreading parameter (1.8), which studied to effect of characteristic diameters on the fate of oil; while Scenarios 2, 4 and 5, with the same characteristic diameters (60μm), but different spreading parameters, focused on studying the effect of spreading parameters (α).

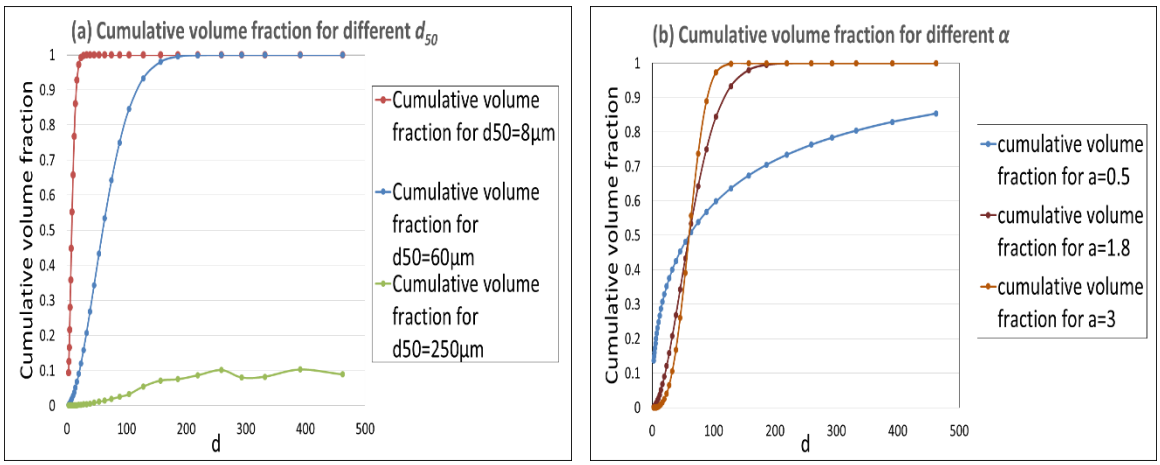

Figure 5-3: Cumulative volume fractions for different d_{50} (a) and α (b) based on the empirical formulations.

Table 5-1: Parameters of simulation Scenarios

No.	Minimum size (μm)	Maximum size (μm)	Characteristic diameter (d_{50}) (μm)	Spreading parameter (α)
1	2	500	8	1.8
2	2	500	60	1.8
3	2	500	250	1.8
4	2	500	60	0.5
5	2	500	60	3

5.4.2 Results and discussions

Figure 5-4 shows that the mass balance changed over the 60 days of the simulation period for scenarios with different d_{50}, ranging from 8 to 250μm. The results indicate that the oil mass fractions in different states were the same for d_{50}=8μm and d_{50}=60μm (Scenario 1 and 2). For both scenarios, the model predicted that no surface oil was left, and about 60.3% of oil remained dispersed in the water column at the end of 60 days, with the remaining oil being biodegraded. With an increase of d_{50} to 250μm (Scenario 3), the mass balance changed significantly. This scenario predicted that 6.4% of the oil was evaporated into the atmosphere at the end of 60 days, 56.1% of the oil was dispersed into the water column and 37.4% of the oil was biodegraded. The fractions of oil, dispersed into the water column and in biodegradation, were reduced in this case, but the evaporated oil was

increased. These simulation results indicated that the model and the mass balances were more sensitive for large d_{50} values (changed from 60µm to 250µm in this case), but less sensitive for small d_{50} values (changed from 8µm to 60µm in this case).

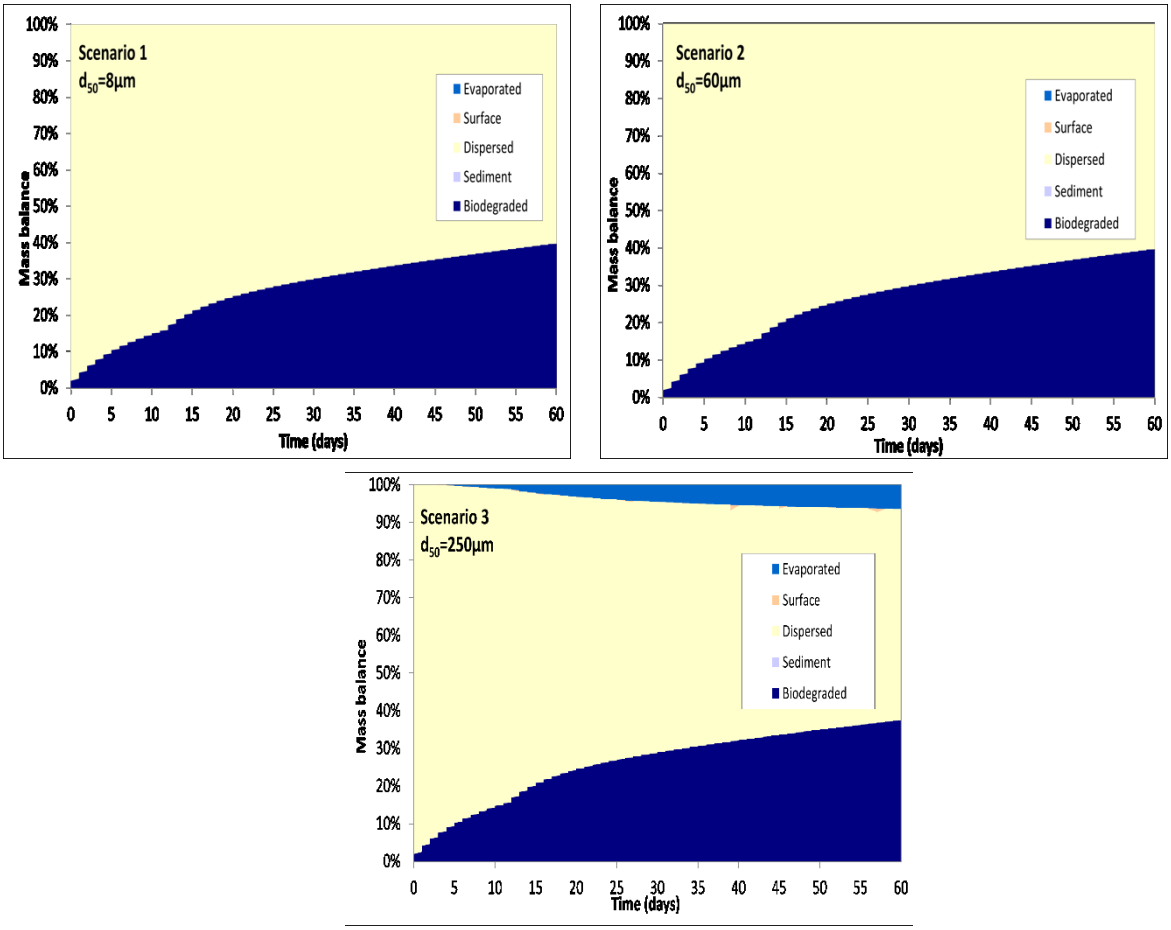

Figure 5-4: Mass Balance for Scenario 1, 2 and 3.

In addition to mass balance, there is a need to study trajectory. The trajectories of oil particles at the end of the 60 day simulation period for these three scenarios are presented in Figure 5-5. When d_{50} was equal to 250µm (Figure 5-5 e and f for Scenario 3), the size of droplets was relatively large. As a result, a great amount of the oil rose to the upper water surface and eventually was carried by stronger surface current to a large area; some parts of oils were transported close to the shoreline. When d_{50} was equal to 8µm (Figure 5-5 a and b for Scenario 1), the number of small droplets was increased (a, c and e in Figure 5-5);

because of the small rising velocity associated with these small droplets, they dispersed mostly at the level similar to the release wellhead (b, d and f in Figure 5-5). When the d_{50} increased to 60μm (Figure 5-5 c and d for Scenario 2), although the mass balance did not change much, as shown earlier, the trajectory of this case was slightly different from that of d_{50} =8μm. When d_{50} increased to 60μm, a large number of oil droplets remained at a level similar to the release, but a noticeable amount of oil droplets with larger diameters started to rise to the upper water column. The horizontal trajectories for Scenarios 1 and 2 are similar because very little oil from Scenario 2 actually reached near to the surface and therefore, was not affected by stronger surface currents.

Besides the sensitivity of d_{50} in the model, the model's sensitivity to the spreading coefficient also needs to be investigated. As analysis in the Chapter 4, a spreading parameter appears to be affected by the type of oils. However, in the OSCAR model, the spreading parameter with default value of 1.8 was used for predicting droplet size distribution, which may lead to an inaccurate prediction. In this case, it is necessary to conduct a sensitivity study of the model with different spreading parameters on the oil droplet size distribution, to determine its effects of spreading parameters on simulation results.

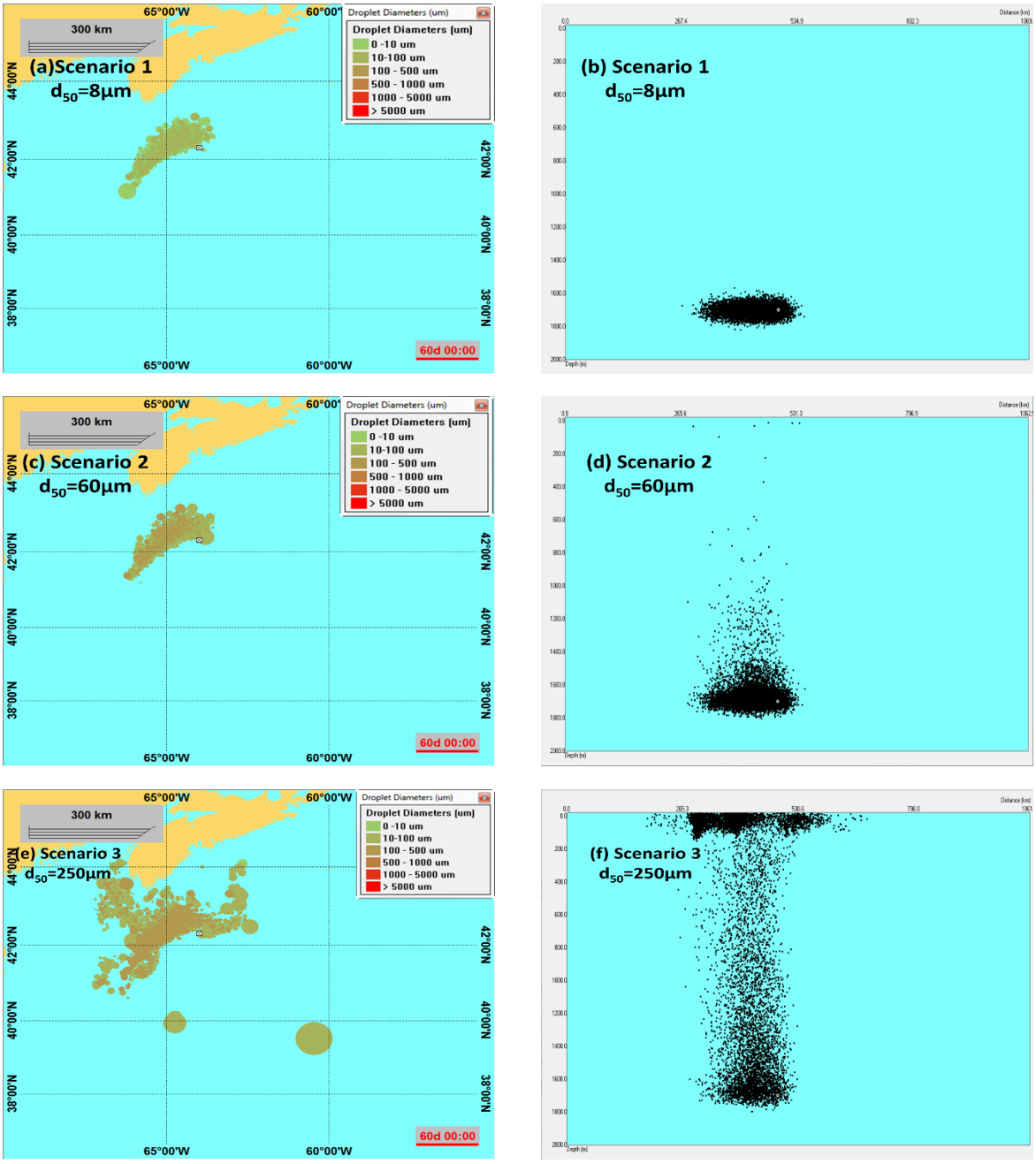

Figure 5-5: Snapshot of dispersed oil droplet size distribution by the end of day 60 (left) and vertical cross section of oil distribution (right) for Scenarios 1, 2 and 3.

To study the effects of the spread parameters on the fate/transport of oil, two additional simulations with the same d_{50} (60µm), but different value of spreading coefficient (α), were conducted of scenarios 2 (α=1.8), 4 (α=0.5) and 5 (α=3.0). The simulated results of mass balances for these three scenarios have been plotted in Figure 5-6.

For the case with smaller spread parameter (α=0.5, Scenario 4), the results showed that 1.8% of the oil was evaporated into the atmosphere, 59.2% of the oil was dispersed into the water column and 39.1% of the oil was in biodegradation. Increasing α to 1.8 (Scenario 2), the evaporated oil fraction was reduced to 0.2%, but the oil fraction in the water column rose slightly to 60.2 % and oil in biodegradation was also increased marginally to 39.6%. When α was further increased to 3 (Scenario 5), the results show that 60.4% of the oil remained in the water column and 39.6% of the oil was biodegraded and no oil was found evaporated to the atmosphere at the end of the simulation period. Overall, the mass balances for these three scenarios were very close. The decreases of α increased oil fraction in evaporation, which indicates that smaller α produced more large droplets which could finally rise to or near to the water surface, and then form oil slick or evaporate to the atmosphere.

Similar to the study of sensitivity to d_{50}, the trajectories from the three scenarios also need to be investigated in order to understand its effect on the model's sensitivity of spreading coefficient. Figure 5-7shows the trajectories of three scenarios (2, 4 and 5) with α changed from 0.5 to 3. In the case of α=0.5 (Scenario 4), there were some relatively large oil droplets presented and rose to the surface, which resulted in more oil evaporated into the atmosphere. This rising of larger droplets to the surface caused a wider spreading of oil over a larger area due to the effects of stronger surface currents. When α was increased to 1.8 (Scenario 2), the number of larger droplets was significantly reduced and the majority of the oil dispersing at the level close to the release depth. Although some larger droplets rose toward the upper water column, they did not reach to the surface. Therefore, they were not affected by the stronger surface currents. In the case of α =3 (Scenario 5), oil droplets mostly presented as small sizes (e in Figure 5-7) and dispersed at a level close the release depth (f in Figure 5-7). These simulation results showed that the model is sensitive to the spreading coefficient, in terms of affecting the prediction of the fate/transport of oil.

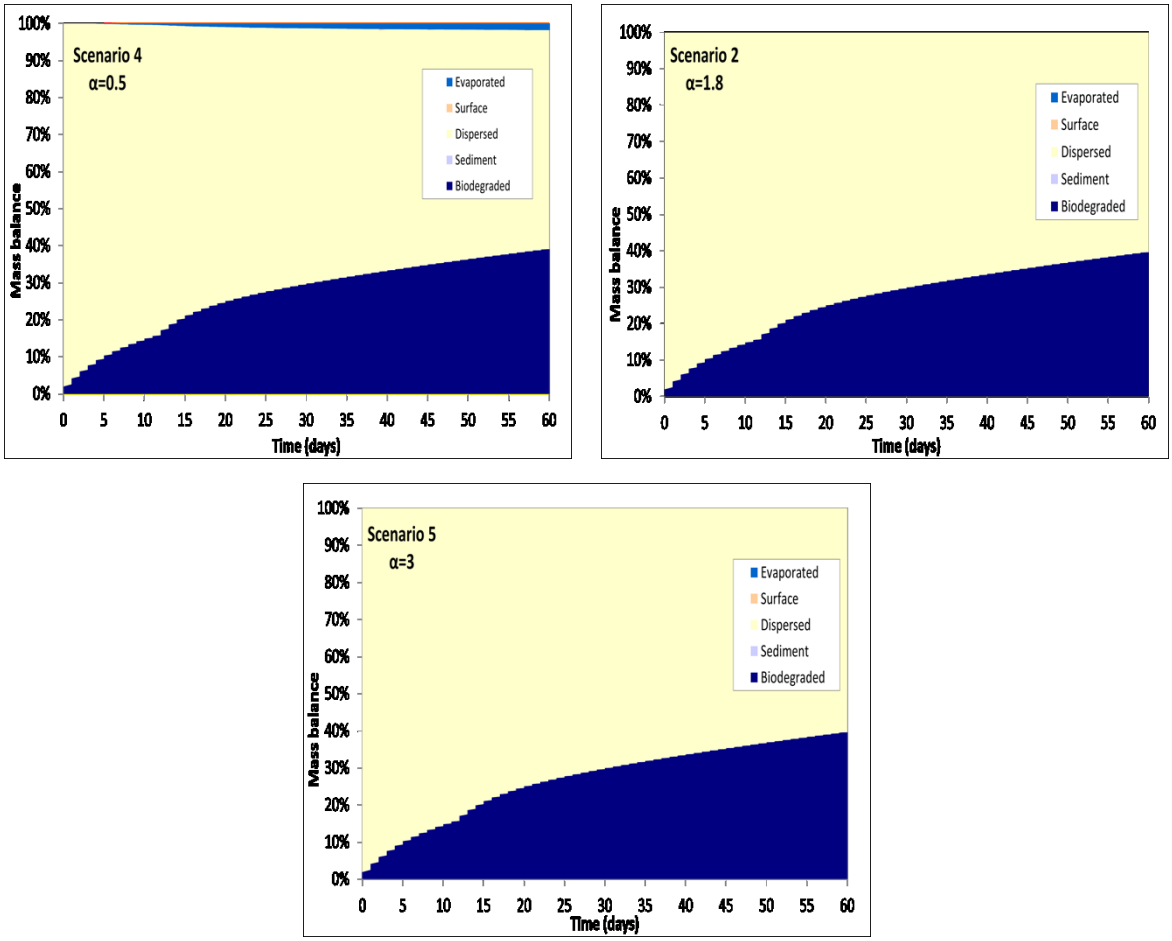

Figure 5-6: Mass balance for Scenario 2, 4 and 5.

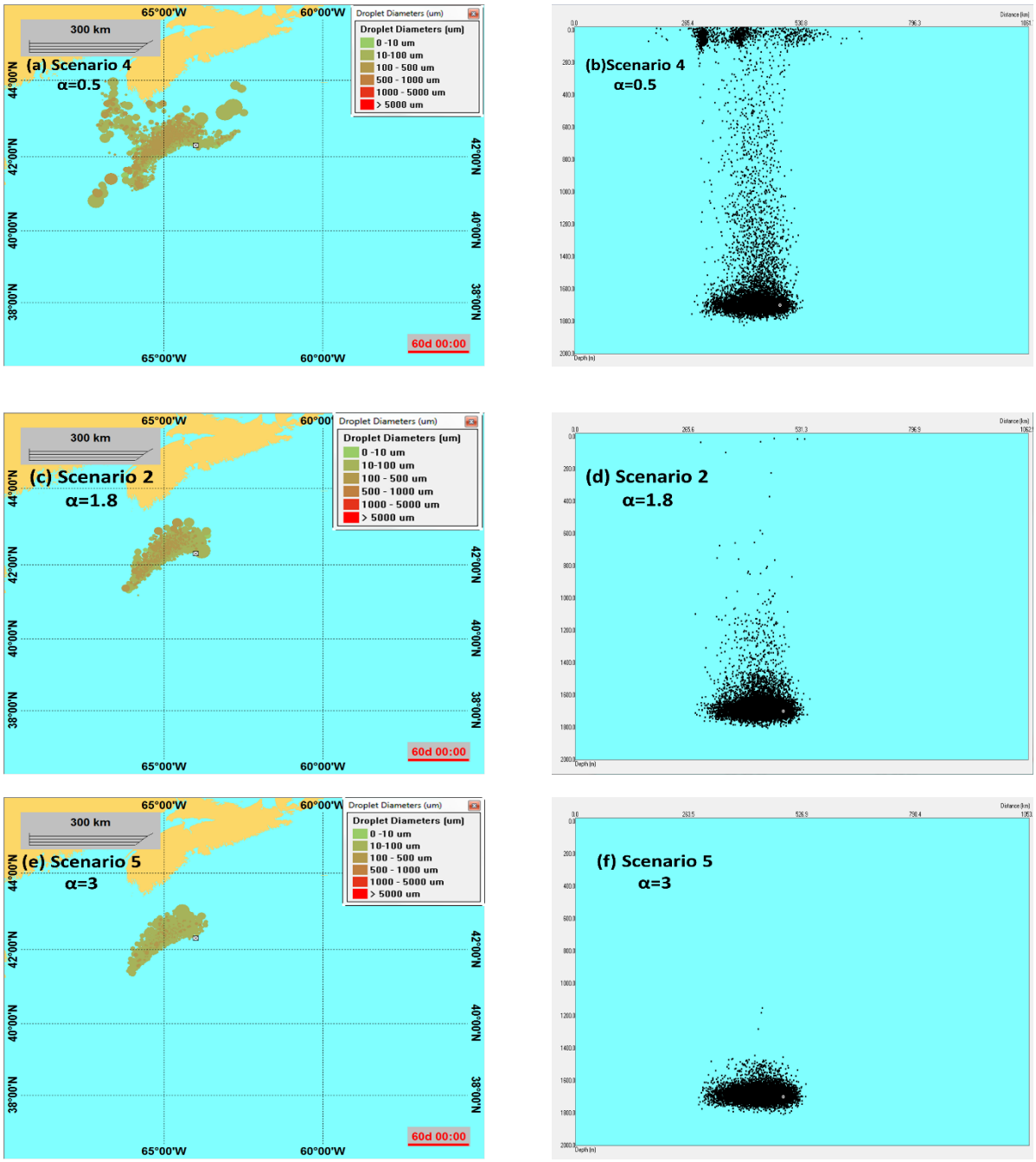

Figure 5-7: Snapshot of dispersed oil droplet size distribution by the end of 60 days (left) and vertical cross section of oil distribution (right) for Scenarios 2, 4 and 5.

5.4.3 Conclusions to model sensitivity study

In conclusion, the model, with different characteristic diameters (d_{50}) and spreading parameter (α), is sensitive to oil droplet size distribution. From the perspective of the mass

balance, the model predicted no surfacing of oil at the end of the simulation period for d_{50}, ranging from 8μm to 60μm; at that time, the fraction of evaporated oil increased from 0% to 6.4% for d_{50}, ranging from 60μm to 250μm. With the same range of d_{50}, the oil fraction in the water column and biodegradation reduced from 60.3% to 56.1% and from 39.7% to 37.4%, respectively. However, the fractions of oil evaporated into the atmosphere (0%), dispersed into the water column (60.3%) and biodegraded (39.7%) were not changed when increasing d_{50} from 8μm to 60μm. For the sensitivity study on the effect of spreading parameters, the results of mass balance at the end of 60 days showed only slight changes. The fraction of oil evaporated into the atmosphere, at the end of the simulation period was reduced from 1.8% to 0% when increasing α from 0.5 to 3, but the fraction of oil dispersed into the water column and biodegradation were increased from 59.2% to 60.4% and from 39.1%to 39.6%, respectively. There was no surface oil left at the end of 60 days in this case.

The sensitivity of the model to oil droplet size distribution is more significant for the trajectory predictions than on the mass balance. When d_{50} was raised from 8μm to 250μm. the number of large oil droplet sizes was increased and rose to the upper water column. Once large oil droplet (d_{50}=250μm) rose to near the surface, droplets were transported, by strong surface currents, close to the shoreline. With the respect of the spreading parameter, when α was small (α=0.5), large droplets rose to near the surface and spread to larger areas and oil may rose to surface or evaporated to the atmosphere. When the value of α increased, the number of large droplets reduced significantly and resulted in a reduction of evaporated oil. A number of small droplets increased and dispersed close to the release depth.

Both the characteristic diameter (d_{50}) and spreading parameter (α) showed significant effects on the fate/transport of oil. In order to have more accurate prediction of oil droplet size distribution, better prediction approaches, such as the Reynolds Number approach, should be used.

5.5 Study the effect of dispersant application on fate/transport of oil using the improved equations

In this section, a case study of the fate/transport of oil from a subsurface blowout on the Scotian Shelf, using the improved droplet size distribution model is presented. The

effects of chemical dispersant application on the fate and transport of oil is addressed in this section.

5.5.1 Model inputs and scenarios

In this hypothetical case study, the release data was the same as that in the sensitivity study. To study the effect of the dispersant, scenarios with and without the dispersant application were conducted for both ANS and IFO-120. Three DORs were considered for both oils: DOR = 0, DOR = 1:100 and DOR = 1:20. Because the research objective is to study the effects of chemical dispersant, the application of dispersant in this study start right after the oil release.

The droplet size distribution was divided into 30 bins of a range of droplet sizes for every scenario. Table 5-2 is an example that shows the data for 30 size bins for ANS crude oil with DOR= 1:20. The oil volume fraction for each size bin was calculated, based on Eq.(21), (24) (25) and Eq. (23 (for ANS) or Eq. (24 (for IFO-120), and two separated spreading parameters were used. The details of parameters for ANS and IFO-120 are shown in Table 5-3. According to the volume fraction of each size bin, oil amount for each size bin was calculated and inputted to the release information. The same calculation method for oil amount was applied to every scenario.

Table 5-2: Example of 30 bins of a range of droplet sizes for ANS with DOR=1:20.

Size bin No.	Size bin range (μm)	Release Amount	Unit
1	2-3	89608.9	barrels
2	3-4	44704.5	barrels
3	4-6	5932.1	barrels
4	6-7	5282.2	barrels
5	7-8	12989.1	barrels
6	8-9	15038.5	barrels
7	9-11	19408.2	barrels
8	11-13	26464.6	barrels
9	13-15	21199.2	barrels
10	15-18	19291.3	barrels
11	18-22	14300.6	barrels
12	22-26	9470.1	barrels
13	26-30	6496.8	barrels
14	30-36	3684.8	barrels
15	36-42	2144.8	barrels
16	42-50	1234.7	barrels
17	50-58	667.2	barrels
18	58-68	368.6	barrels
19	68-82	200.9	barrels
20	82-94	108.5	barrels
21	94-114	63.3	barrels
22	114-142	37.3	barrels
23	142-172	23.8	barrels
24	172-200	16.1	barrels
25	200-238	13.4	barrels
26	238-280	15.1	barrels
27	280-306	17.3	barrels
28	306-358	10.6	barrels
29	358-424	4.4	barrels
30	424-500	3.4	barrels
Total release amount		298800	barrels

Table 5-3: Details of parameters for ANS and IFO-120. The parameters in this table are empirical coefficient A, Reynolds Number Re, medium volume droplet size d_{50}, spreading parameters for $d/d_{50} \leqslant 1$ α_1, and spreading parameters for $d/d_{50} > 1$ α_2.

	ANS			IFO-120		
	DOR=0	DOR=1:100	DOR=1:20	DOR=0	DOR=1:100	DOR=1:20
A	10.97	7.55	1.70	5.97	5.27	3.19
Re	4169.50	3911.20	4097.40	444.45	388.08	658.38
d_{50}	77.69	51.14	7.66	194.66	184.21	66.17
α_1	1.80	1.80	1.80	1.80	1.80	1.80
α_2	1.65	1.65	1.65	2.25	2.25	2.25

5.5.2 Results and discussion

Table 5-4 shows the results of mass balance of each scenario for ANS and IFO-120 at the end of 60 days of the simulation period. The results indicate that the oil fractions in different states can be affected by chemical dispersant, even though the effect are very small on both oils, it is relatively higher on IFO-120.

For ANS, in the case without chemical dispersant application (DOR=0), there was no oil slick left on the water surface after the 60 days. At the end of the simulation period, a total fraction of 0.5% of the oil was evaporated into the atmosphere at the end of the simulation period, about 60.0% of the oil was dispersed into the water columns and 39.5% of the oil was biodegraded. In the case of ANS with DOR=1:100, the fraction of oil in the atmosphere was reduced to 0% at the end of the simulation period, compared with that in the case with DOR=0. The fraction of oil on the water surface and the fraction biodegraded increased slightly from 60.0% to 60.4% and from 39.5% to 39.6%, respectively. When the DOR increased to 1:20, the mass balance of the different states of oil were similar to the case of DOR=1:100. No oil was found on the surface or evaporated to the atmosphere at the end of 60 days. A large amount of oil was dispersed into water columns (60.3%), with the remaining oil (39.7%) being biodegraded. In this case, chemical dispersant appeared to prevent the oil (ANS) from rising to near the water surface and accelerated oil dispersion into the water column and biodegradation. In the case of IFO-120 with DOR=0, the results show that 1.6% of oil was left on the water surface and 2.1% was evaporated into the atmosphere at the end of the simulation period. A total of 72.7% of oil was dispersed into the water column and 23.4% of oil was biodegraded. There was 0.5% of oil transported outside the simulation area at the end of 60 days. With the increasing of dosage of chemical dispersant to DOR=1:100, the amount of surface oil was reduced by 0.3% (from 1.6% to1.3%), but the amount of evaporation was the same. The fraction of dispersed oil rose slightly to 72.7 % and the fraction in biodegradation was also increased slightly to 23.3%. The fraction of oil which stayed outside the simulation area was not reduced. In comparison, the mass balances of different states for IFO-120 changed significantly when a higher dosage of chemical dispersant (DOR=1:20) was applied. The fractions of surface oil and evaporated oil significantly reduced from 1.3% to 0% and from 2.1% to 0% when the DOR increased from DOR=1:100 to DOR=1:20, respectively. The fraction of dispersed

oil increased by 3.3% (from 72.7% to76%) in this DOR range, and the fraction of biodegraded oil rose by 0.7% (from 23.3% to 24.0%). Chemical dispersant also reduced the fraction of oil which travelled outside of the simulation area (reduce from 0.5% to 0%). These mass balance results indicated that chemical dispersant significantly affects the fate of oil, raising the oil fraction that is biodegraded and that is in the water column. The effect of chemical dispersant on the mass balance of oil is greater in the high dosage of chemical dispersant (DOR=1:20) as well as higher on IFO-120 than ANS.

Table 5-4: The mass balance in the last simulation day (60-day) for ANS and IFO-120 based on improved oil droplet size distribution model.

	ANS			IFO-120		
	DOR=0	**DOR=1:100**	**DOR=1:20**	**DOR=0**	**DOR=1:100**	**DOR=1:20**
Surface	0%	0%	0%	1.6%	1.3%	0 %
Atmosphere	0.5%	0%	0%	2.1%	2.1%	0%
Water column	60.0%	60.4%	60.3%	72.4%	72.7%	76.0%
sediments	0%	0%	0%	0%	0%	0%
biodegraded	39.5%	39.6%	39.7%	23.4%	23.3%	24.0%
outside	0%	0%	0%	0.5%	0.5%	0 %

Although the mass balance results showed that chemical dispersant has little effects on the fate of oil, it is still necessary to study how chemical dispersant affects the trajectories of oil on the Scotian Shelf. Figure 5-8 to Figure 5-13 show the trajectory results of oil droplet distribution with different DORs for ANS and IFO-120 scenarios at the end of 60 days of the simulation period. Comparing the horizontal trajectories figures (a in Figure 5-8, a in Figure 5-9 and a in

Figure 5-10) of ANS with different DORs (0, 1:100 and 1:20), there was a larger amount of dispersed oil droplets in the scenarios with DOR=0 and DOR=1:100 transported to a large area, and closer to the shoreline compared with that of DOR=1:20. The number of large dispersed oil droplets appeared to be higher in the case with DOR=0 than with DOR=1:100. However, the droplets in the case with DOR=1:20 were relatively small and stayed in the water column near the release nozzle. The vertical oil droplet size trajectories between these three cases also changed. The change was mostly noticeable in the case with

DOR=1:20 (c in Figure 5-8; c in Figure 5-9 and c in Figure 5-10). Some oil rose to the upper water columns and near the water surface in the cases with DOR=0 and DOR=1:100. The amount of rising droplets was observed to be larger in the case with DOR=0, than that with DOR=1:100. A large amount of oil droplets presented as small size droplets and were observed to stay at the level close to their release location for these three scenarios. In the case with DOR=1:20, oil mostly dispersed near the wellhead because of the small rising velocity of small droplets. In these three figures, there was no oil slick left at the end of 60 days (b in Figure 5-8, b in Figure 5-9 and b in Figure 5-10). Overall, the results indicated that the higher dosage of chemical dispersant (DOR=1:20) had more significant effects on the trajectory of ANS, preventing dispersed oil transport to a large area and the shoreline.

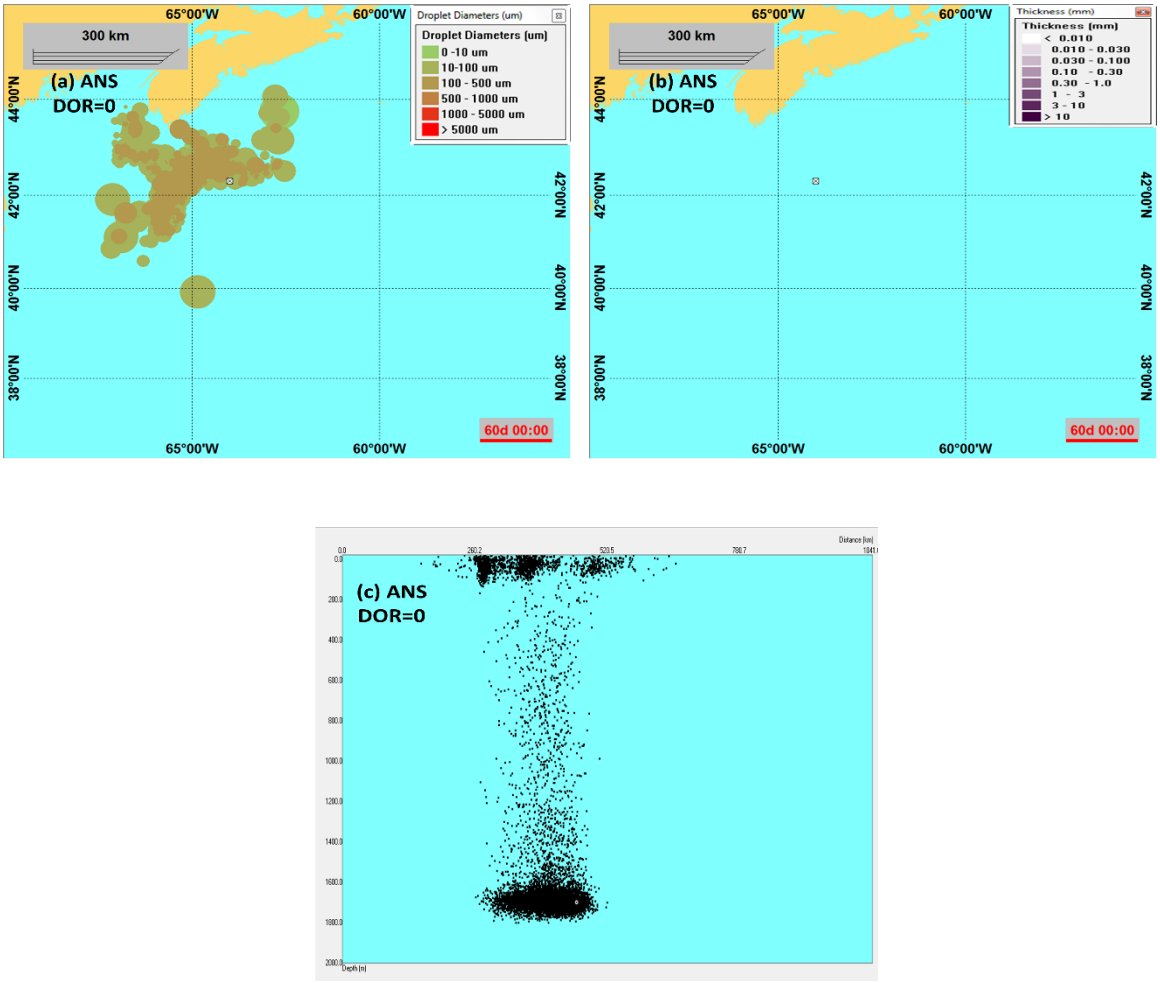

Figure 5-8: The distribution of droplet size over water column with and without chemical dispersant injection (a), oil slick on water surface (b) and vertical oil droplet size trajectory (c) for ANS with DOR=0 at the end of 60 days.

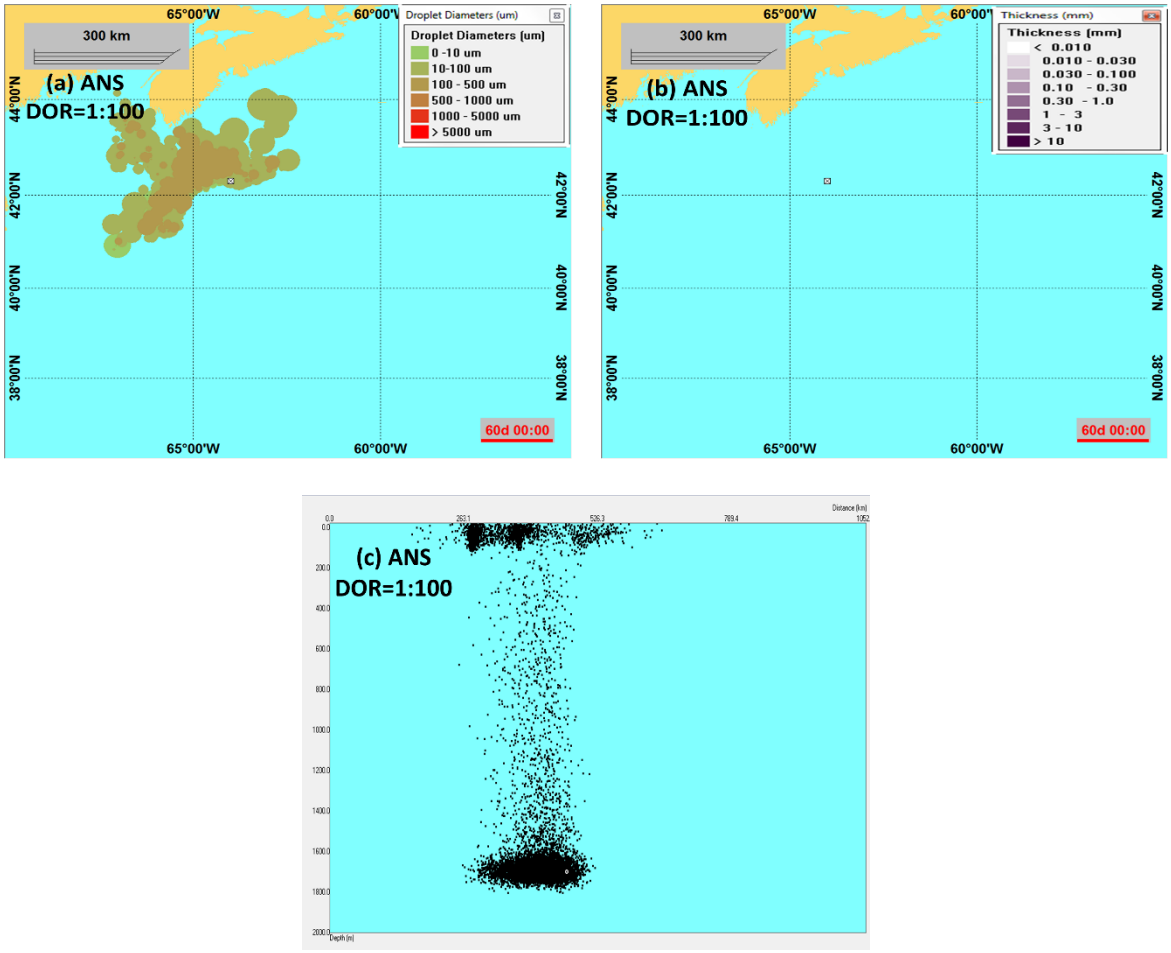

Figure 5-9: The distribution of droplet size over water column with and without chemical dispersant injection (a), oil slick on water surface (b) and vertical oil droplet size trajectory (c) for ANS with DOR=1:100 at the end of 60 days.

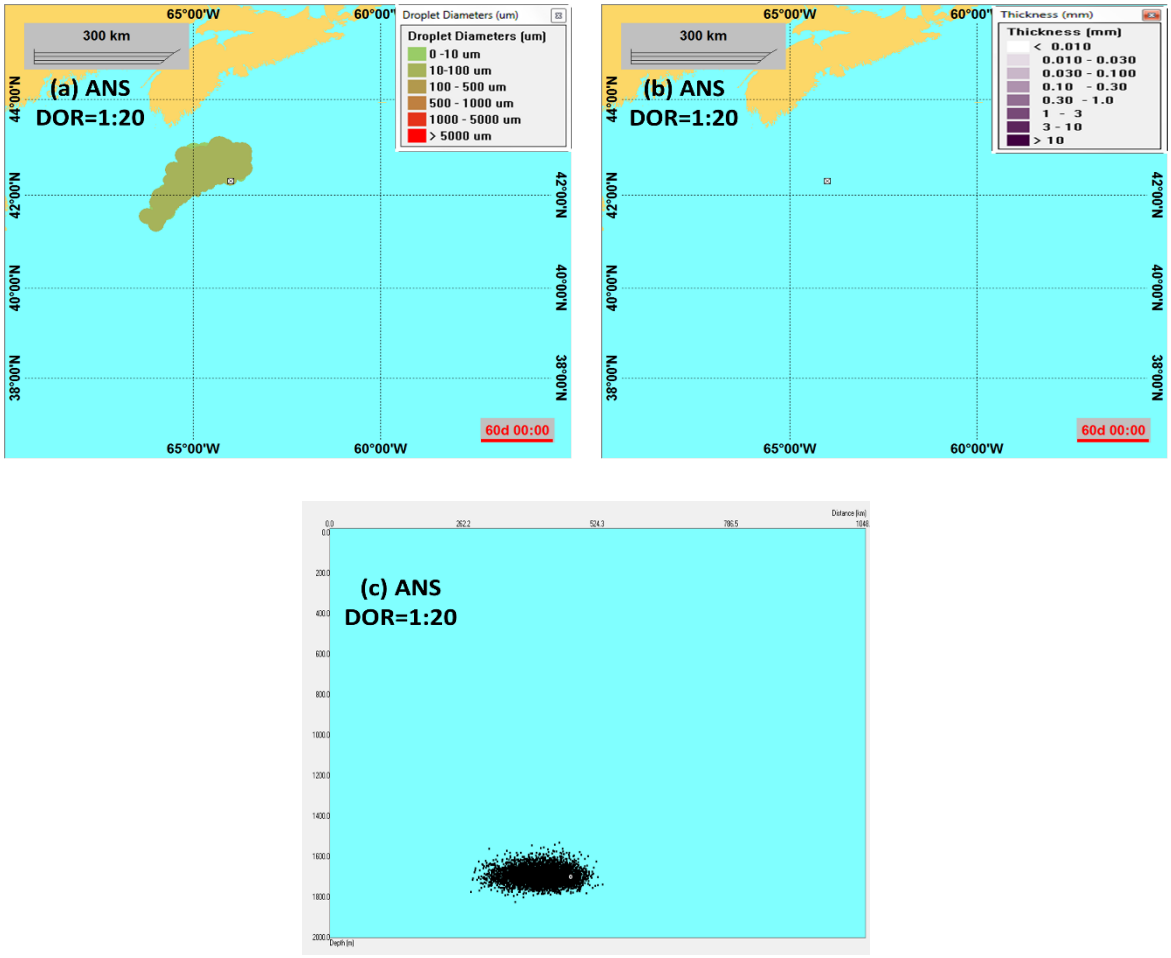

Figure 5-10: The distribution of droplet size over water column with and without chemical dispersant injection (a), oil slick on water surface (b) and vertical oil droplet size trajectory (c) for ANS with DOR=1:20 at the end of 60 days.

In terms of droplet trajectories of IFO-120 with DOR=0, DOR=1:100 and DOR=1:20, the horizontal trajectories were slightly different (a in Figure 5-11; a Figure 5-12; a in Figure 5-13). A noticeable amount of droplets moved closer to the shoreline in the case with DOR = 0, compared with DOR = 1:100 and DOR = 1:20. For the areas of trajectories (a in Figure 5-11, a Figure 5-12; a in Figure 5-13), more oil droplets were transported to a larger area in the cases with DOR=0 and DOR=1:100 than in the case with DOR=1:20. The significant difference between these three scenarios was found in the surface oil (b in Figure 5-11, b Figure 5-12; b in Figure 5-13), which was dramatically reduced with the

application of a high dosage of chemical dispersant (DOR=1:20). At the end of the simulation period, no oil slick was left on the water surface in the case with DOR=1:20. The effect of chemical dispersant on the trajectory was difficult to observe in these vertical cross sections of droplet size distribution among these three scenarios (c in Figure 5-11, c Figure 5-12; c in Figure 5-13); a large amount of droplets stayed and dispersed near the level of the release nozzle while a small amount of droplets dispersed at the upper water column and near the water surface. Even though there was no surface oil left at the end of 60 days in the case with DOR=1:20, the dissolved droplets trajectory in the vertical view showed that dispersed oil near the water surface may have resurfaced under the effect of strong surface current.

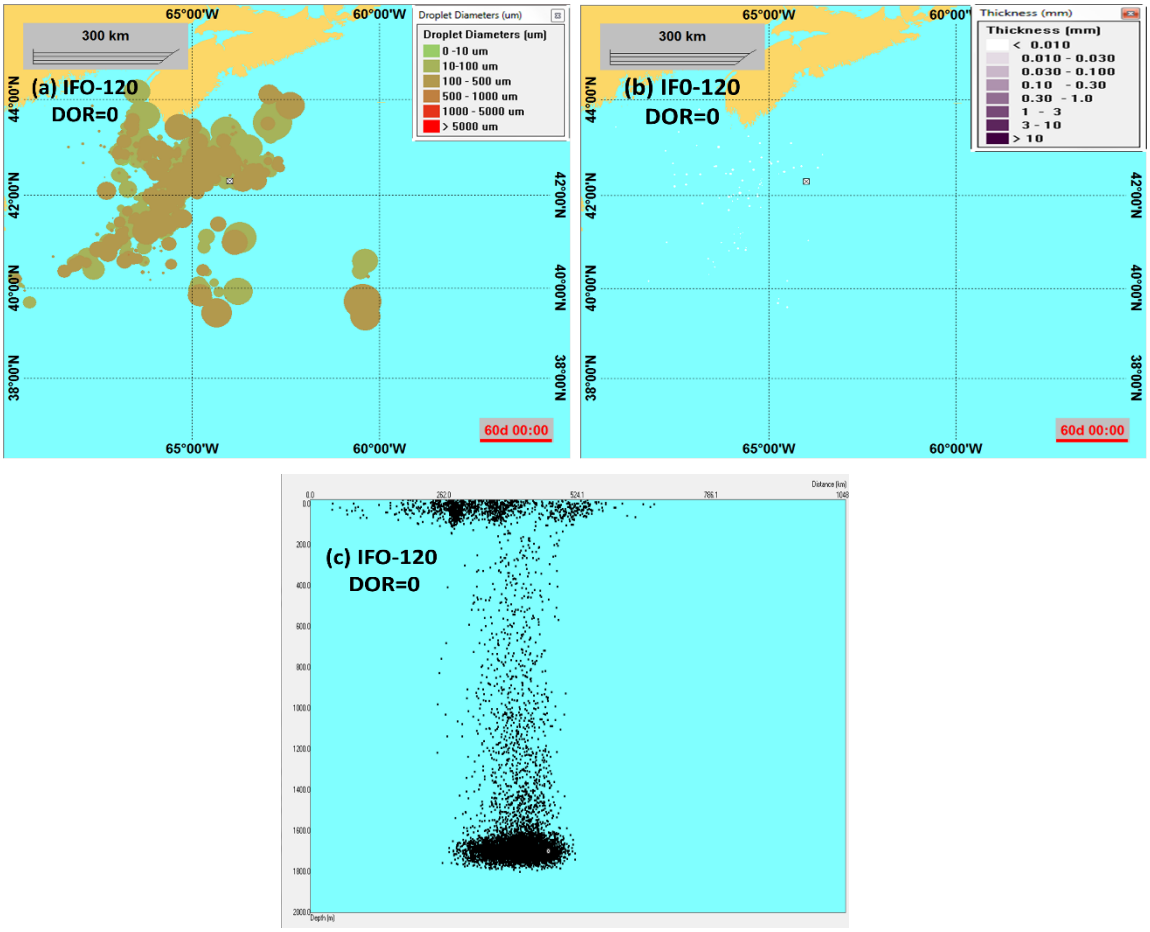

Figure 5-11: The distribution of droplet size over water column with and without chemical dispersant injection (a), oil slick on water surface (b) and vertical oil droplet size trajectory (c) for IFO-120 with DOR=0 at the end of 60 days.

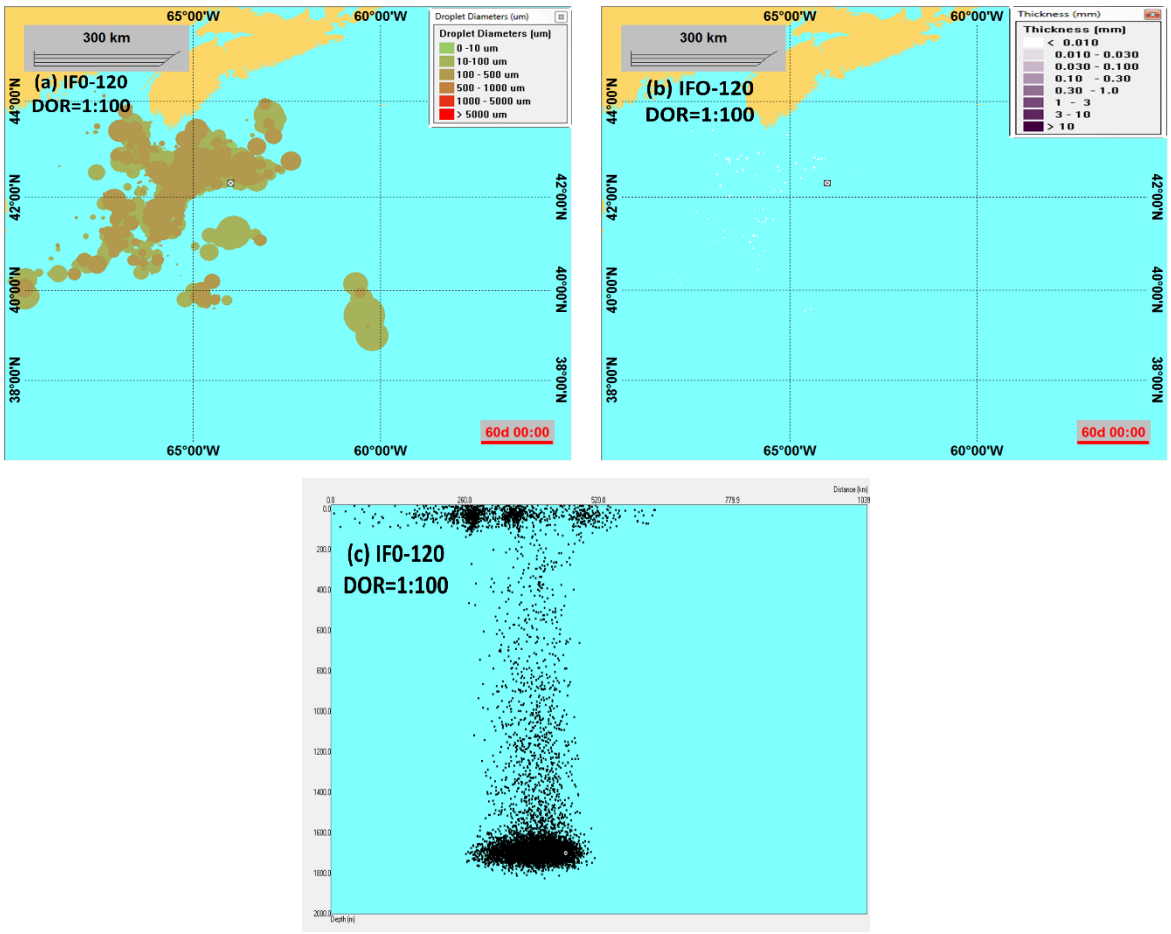

Figure 5-12: The distribution of droplet size over water column with and without chemical dispersant injection (a), oil slick on water surface (b) and vertical oil droplet size trajectory (c) for IFO-120 with DOR=1:100 at the end of 60 days.

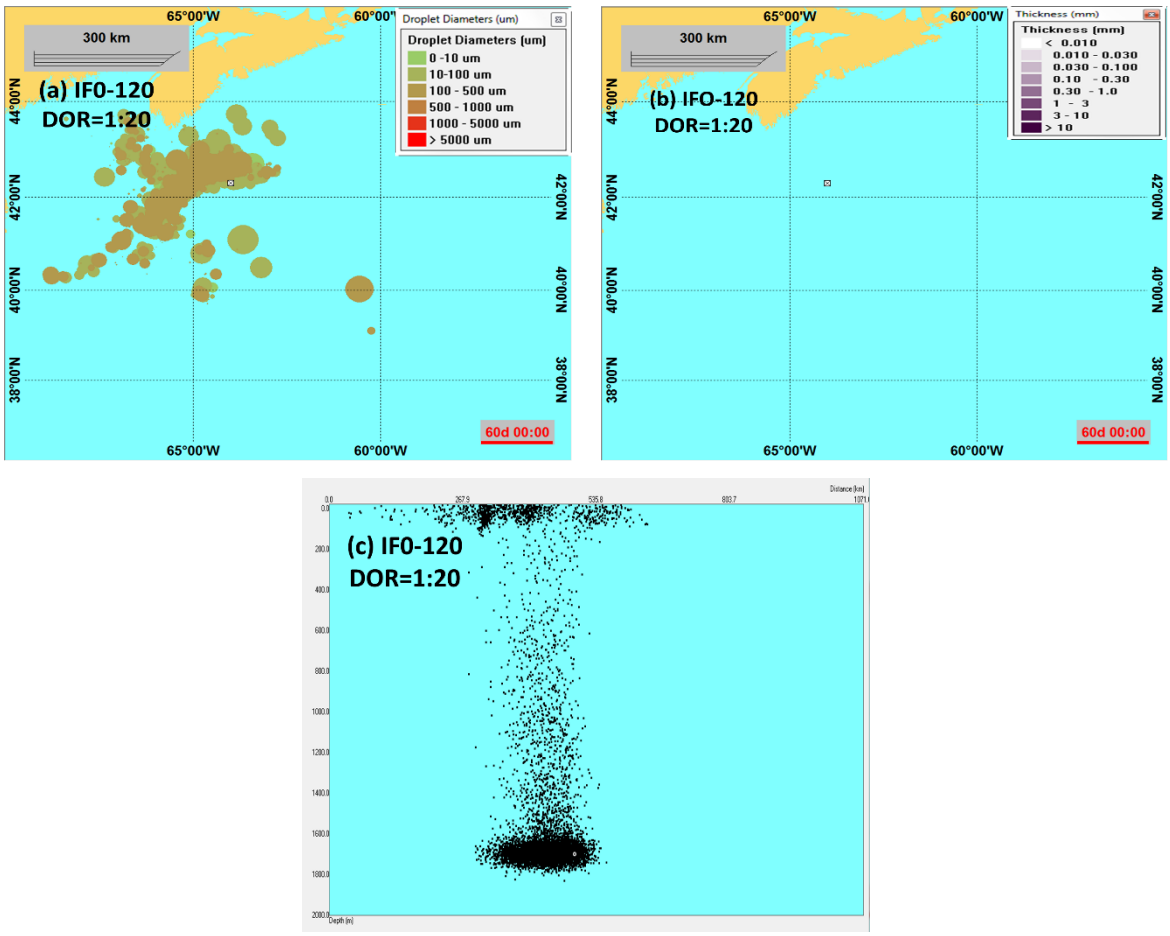

Figure 5-13: The distribution of droplet size over water column with and without chemical dispersant injection (a), oil slick on water surface (b) and vertical oil droplet size trajectory (c) for IFO-120 with DOR=1:20 at the end of 60 days.

5.5.3 Conclusion

Based on the modeling results, the effect of chemical dispersant on the fate and transport of oils were observed from the variation of mass balances and trajectories of oil droplets. The mass balances at the end of the simulation period showed that ANS (medium crude oil) can be dispersed well on the Scotian Shelf with application of chemical dispersant (60.0% of oil in water column, 39.5% of oil in biodegraded and 0.5% of oil in atmosphere in DOR=0). By adding high dosage of chemical dispersant (DOR=1:20), the oil was mostly dispersed into the water column or in biodegradation (60.3% of oil in water column and 39.7% of oil biodegraded). In the case of IFO-120 (heavy crude oil) without chemical dispersant application, a noticeable amount of the oil was observed on the water

surface at the end of the simulation period (1.6% of oil on water surface). The application of a high dosage of chemical dispersant (DOR=1:20), in the case of IFO-120, showed significant reduction in the fraction of surface oil and evaporated oil (surface oil: from 1.6% to 0%; evaporated oil: from 2.1% to 0%), the oil was dispersed into the water column and in biodegradation (60.3% of oil in water column and 39.7% of oil biodegraded). The effects of chemical dispersant on the mass balance for different oil states were more significant for dispersing heavy crude oil (IFO-120) than that for medium crude oil (ANS).

The effects of dispersant were greater on the trajectories of ANS than on IFO-120. For ANS, when the dosage of chemical dispersant increased from DOR=0 to DOR=1:20, the amount of small oil droplets rose, as well, because of the smaller velocities of these small droplets, they were mostly dispersed near the release wellhead. For IFO-120, the high dosage of chemical dispersant (DOR=1:20) reduced the surface and evaporated oil significantly. The noticeable amount of large droplets were predicted to disperse in the upper water column, and they may have resurfaced over time under the effects of the ocean current.

CHAPTER 6. CONCLUSIONS AND RECOMMENDATIONS

6.1 Conclusions

In this study, experiments were conducted to measure droplet size distribution of ANS (medium crude oil) and IFO-120 (heavy crude oil), with and without chemical dispersant, in the mesoscale wave tank facility. Based on the results of data analysis, without the effect of dispersant, the increased water temperatures had effects on the dispersed droplet sizes, resulting in increases of d_{50}, but this increase was not evident in the chemically dispersed droplet size distribution. For both oils, chemical dispersant played a significant role in generating a large amount of smaller droplets (reduced the VMDs). The efficiency of dispersant was higher on ANS (medium crude oil) than on IFO-120.

Data obtained from this study, together with data from Brandivik *et al.* (2013), was used to assess two oil droplet size distribution approaches (Modified Weber Number approach and Reynolds Number approach), which were discussed in Chapter 4. Although Modified Weber Number approach has the advantages of using IFT to make prediction, the challenges of impractical in situ sampling prompted the using of the Reynolds Number approach to fit experimental data from this study. The relationship of the empirical coefficients (*A* values), as functions of DORs for both oils, were investigated. The results showed that the value of *A* can be affected significantly by the higher dosage of chemical dispersant (DOR=1:50 and DOR=1:20), but insignificantly by the lower dosage (0≤DOR≤1:100). However, this differs from using only one empirical coefficient (A=15) for all DOR cases (Johansen *et al*, 2013). As well, the different types of oil also affected the selection of *A,* with higher *A* value for light crude oil (Oseberg crude oil) and lower *A* value for heavy crude oil (IFO-120). This study also established the relation between *A* and DORs by using the exponential function ($Y=a*exp\ (bX)$). The coefficient values (*a* and *b*) appeared to be affected by the types of oils.

The data analysis also indicated that the statistical distributions of $d/d_{50} > 1$ and $d/d_{50} \leq 1$ are different, and if only a single spreading parameter (α) is used, the estimation results may not be accurate. The distribution results, using two separated spreading parameters (α_1 and α_2), provide a better fit to experimental data for ANS and IFO-120 and the selection of

spreading parameters appeared to be affected by different oil types. However, there is not enough data to determine the relation between the spreading parameters (α_1 and α_2) and different oil types in this study. The calculated droplet size distribution of ANS and IFO-120, with DOR=1:200, using the improved Reynold number approach integrated with two-step Rosin-Rammler distribution, as well as Rosin-Rammler distribution, were compared with the experimental data. The results showed that the calculated volume fractions, using the two-step Rosin-Rammler distribution, fit the experimental data better and showed relatively good prediction on droplet size distributions, especially for the oil droplet sizes larger than d_{50}. Generally, the improved Reynolds Number and the two-step Rosin-Rammler distribution approaches can provide a reliable prediction on droplet size distribution. A limitation of this approach is that Reynolds number approach is used for the oil with viscosity number larger than one. To develop a general prediction approach, the effect of different oil types on the selection of droplet size distribution parameters should be studied in the future.

To study the effect of chemical dispersant application on fate/transport of oil from subsurface release on Scotian Shelf and to evaluate the new approach for droplet size distribution prediction, a case study was conducted using the Oil Spill Contingency and Response (OSCAR) model. Three dispersant to oil ratios, DOR=0, DOR=1:100 and DOR=1:20, were used. The results showed that chemical dispersant had effects on both mass balance and trajectories of droplet sizes. The effect of chemical dispersant on mass balance was relative higher on IFO-120 than ANS, while the effect on trajectories of droplet sizes of ANS was more significant than that of IFO-120. These simulation results can be used to help on understanding of effects of chemical dispersant on subsurface release on the Scotian Shelf. The threshold of chemical dispersant to IFO-120 requires further study.

6.2 Research contributions

These experimental studies complement the limited oil droplet size distribution data which can be used for oil droplet size distribution approach validation. Study developed new equations, such as the quantified relationship between A and DORs and Two-step Rosin Rammler distribution function, helping to improve prediction approach to a more

general application. Case studies on the ANS and IFO-120 released from the deepwater of the Scotian Shelf with and without chemical dispersant release were also conducted in this study, the results show that chemical dispersant have effects on the trajectory of oil released from the deepwater of the Scotian Shelf.

6.3 Recommendations for further research

The following two recommendations are suggested for future research to develop universal prediction equations for different type of oils:

1. Quantify the effects of water temperature on the droplet size distribution. The current experimental work was conducted in an outdoor environment and therefore lacks control of water and air temperature. The inconsistence of temperature among repeated experiment may cause uncertainties, which affect the distribution results of oil droplet size. To better understand the effects of water temperature on oil droplet size distribution, it is recommended to have experiments conducted in a more controllable environment.
2. Further study of the effects of oil type on droplet size distribution. Oil properties have significant effects on the determination of empirical coefficients, such as A value for the Reynolds Number scaling, α values for the two-step Rosin-Rammler distribution, and coefficients (a and b) for the quantification relation between A and DORs. Future studies are recommended to quantify these correlations.

REFERENCES

1. Aman, Zachary M., Paris, C. B., May, E. F., Johns, M., L., & Lindo-Atichati, D. (2015). High-pressure visual experimental studies of oil-in-water dispersion droplet size. Chemical Engineering Science, 127, 392-400. doi: 10.1016/j.ces.2015.01.058
2. Applied Science Associates (ASA). (2011). Deep Water Oil Spill Model and Analysis System. Retrieved March, 2015 from: http://www.asascience.com/software/oilmap/oilmapdeep.shtml
3. ASCE Task Committee. (1996). State-of-the-art review of modeling transport and fate of oil spills. Journal of Hydraulic Engineering 122(11), 594-609.
4. Anderson, J.W., McQuerry, P.L., & Kiesser, S.L. (1985). Laboratory Evaluation of Chemical Dispersants for Use on Oil Spills at Sea." Env. Sei. Tech.. 19(5), pp. 454-457.
5. Brandivik, P.J., Johansen, Ø., Farooq, U., Davies, E., Krause, D., & Leirvik, F.(2015). Subsurface oil Releases-Experimental study of droplet size distributions Phase-II. A scaled experimental approach using the SINTEF Tower basin. SINTEF Materials and Chemistry. Environmental Technology.
6. Bureau of Safety and Environmental Enforcement (BSEE). (2015). Deepwater Production Summary by Year. Retrieved June 12, 2016, from: https://www.data.bsee.gov/homepg/data_center/production/production/summary.asp
7. Brandivik, P.J., Johansen, Ø., Farooq, U., Glen, A., & Leirvik, F. (2014). Subsurface oil releases-Experimental study of droplet distribution and different dispersant injection techniques Version 2 (Technical report No. SINTEF A26122).-SINTEF.
8. Brandvik, P. J., Johansen, Ø., Leirvik, F., Farooq, U., &Daling, P. S. (2013). Droplet breakup in subsurface oil releases - Part 1: Experimental study of droplet breakup and effectiveness of dispersant injection. Marine Pollution Bulletin, 73(1), 319-326. doi: DOI 10.1016/j.marpolbul.2013.05.020

9. British Petroleum (BP). (2013). BP Exploration Review. Retrieved June 12, 2015, from:http://www.bp.com/content/dam/bp/pdf/investors/bp_exploration_review_2013_10_18_slides.pdf
10. Bandara, U. C., & Yapa P. D. (2011). Bubble sizes, breakup, and coalescence in deepwater gas/oil plumes, J. Hydraul. Eng., 137(7), 729–738
11. Boyd, J. N., Kucklick, J. H., Scholz, D. K., Walker, A. H., Pond R. G., & Bostrom, A. (2001). Effects of Oil and Chemically Dispersed Oil in the Environment. Health and Environmental Sciences Department Cape Charles, Virginia.
12. Bishnoi, P., Gupta, A., Englezos, P., & Kalogerakis, N. (1989). Multiphase Equilibrium Flash Calculations for Systems Containing Gas Hydrates, Fluid Phase Equilibria 53: 97–104.
13. Canadian Environmental Assessment Agency (CEAA). (2015). Shelburne Basin Venture Exploration Drilling Project. Retrieved October 12, 2016, from: http://www.ceaa.gc.ca/050/documents/p80058/101799E.pdf
14. Crowley, D., Mendelsohn, D., Mulanaphy, N. W., Li, Z., & Spaulding, M. (2014, May). Modeling Subsurface Dispersant Applications for Response Planning and Preparation. In *International Oil Spill Conference Proceedings* (Vol. 2014, No. 1, pp. 933-948). American Petroleum Institute.
15. Conmy, R. N., Coble, P. G., Farr, J., Wood, A. M., Lee, K., Pegau, W. S., Walsh, I. D. *et al*. (2013). Submersible optical sensors exposed to chemically dispersed crude oil: wave tank simulations for improved oil spill monitoring," Environ. Sci. Technol. 48, 1803–1810.
16. Canada-Nova Scotia Offshore Petroleum Board (CNSOPB). (2013). Shell Shelburne Seismic Program. Retrieved June 12, 2016, from: http://www.cnsopb.ns.ca/offshore-activity/offshore-projects/shell-shelburne-seismic-program
17. Cleveland C.J. (2010). Energy in the Deepwater Gulf of Mexico. Source: he Bureau of Ocean Energy Management, Regulation and Enforcement (BOEMRE). Retrieved from HTTP://www.eoearth.org/view/article/158866

18. Chen, F. H. & Yapa, P. D. (2007). Estimating the oil droplet size distributions in deepwater oil spills. Journal of Hydraulic Engineering-Asce, 133(2), 197-207. doi: Doi 10.1061/(Asce)0733-9429(2007)133:2(197)
19. Chapman, H., Purnell, K., Law, R.J., & Kirby, M.F. (2007). The use of chemical dispersants to combat oil spills at sea: A review of practice and research needs in Europe. Marine Pollut. Bull. 54, 827.
20. Chandrasekar, S., Sorial, G. A., &Weaver, J. W. (2006). Dispersant effectiveness on oil spills — impact of salinity. ICES Journal of Marine Science, 63: 1418e1430.
21. Chandrasekar, S., Sorial, G.A., & Weaver, J.W. (2005). Dispersant effectiveness on three oils under various simulated environmental conditions. Environ. Eng. Sci. 22, 324.
22. Canada-Nova Scotia Offshore Petroleum Board (CNSOPB). (2004). Application to Amend the Cohasset Development Plant Decision Report. Retrieved May 12, 2016, from:http://www.cnsopb.ns.ca/pdfs/Cohasset%20Panuke%20Application%20to%20Amed%20Decision%20Report_2005.pdf
23. Canada-Nova Scotia Offshore Petroleum Board (CNSOPB). (2015). Canada-Nova Scotia Offshore Petroleum Board Issues Shell Canada Operations Authorization – Drilling. Retrieved June 12, 2016, from: http://www.cnsopb.ns.ca/offshore-activity/current-applications/incident-prevention-and-response
24. Chen, F. & Yapa, P. (2004a). Modeling gas separation from a bent deepwater oil and gas jet/plume, Journal of Marine Systems 45: 189–203.
25. Cooper, C., Forristall, G.Z. & Joyce, T.M. (1990). Velocity and Hydrographic Structure of Two Gulf of Mexico Warm-Core Rings. *J. Geophy. Res.*, 95(C2), 1663–1679.
26. Caneveri, G.P., Bock, J., & Robbins, M. (1989). “Improved Dispersant Based on Microemulsion Technology”. In: Proc. 1989 International Oil Spill Conf., American Petroleum Institute, Washington, DC. pp. 317-320
27. Canada-Nova Scotia Offshore Petroleum Board (CNSOPB). (n.d). Shell exploration activity. Retrieved June 12, 2016, from: http://www.cnsopb.ns.ca/offshore-activity/offshore-projects/shell-seabed-survey

28. Daling, P.S., Leirvik, F., & Reed, M. (2011) Weathering properties at of the Macondo MC252 crude oil. Presentation at Gulf Oil Spill Sectac Meeting, Pencacola Beach FL, April 26-28th. 2011
29. Daling, P.S., (1996). Recent Improvements in Optimizing Use of Dispersants as a Cost-effective Oil Spill Countermeasure Technique. Society of Petroleum Engineers, Inc.
30. Dasanayaka, L.K., & Yapa, P.D. (2009). Role of plume dynamics on the fate of oil and gas released underwater. Journal of Hydro-Environment Research, IAHR/Elsevier, 243e253.
31. Environmental Protection Agency (EPA). (2016). U.S. Environmental Protection Agency National Contingency Plan Product Schedule. Retrieved April 12, 2016, from: https://www.epa.gov/sites/production/files/2013-08/documents/schedule.pdf
32. Environmental Protection Agency (EPA). (2014). Retrieved April 15, 2016, from: http://www.epa.gov/oem/content/learning/oilfate.htm
33. ExxonMobil. (2009). Deepwater Drilling: Safeguarding a Valuable Resource. In The Outlook for Energy: A View to 2030, Retrieved from April 5, 2011 from http://www.exxonmobil.com/Corporate/Imports/eo/pdf/energy_o_deepwaterdrilling.pdf
34. ExxonMobil Research & Engineering Co. (2008). ExxonMobil Oil Spill Dispersant Guidelines, pp46-49
35. Exxon Corporation. Public Affairs Dept. (1978). Fate and Effects of oil in the sea. Exxon Background Series.
36. Fusco, L. (2007). Offshore Oil: An overview of Development in Newfoundland and Labrador. Occasional Paper #2 of the Project, Oil, Power and Dependency: Global and Local Realities of the Offshore Oil Industry in Newfoundland and Labrador.
37. Foreman, M. G. G., Beauchemin, L., Cherniawsky, J. Y., Peña, M. A., Cummins, P. F., & Sutherland, G. (2005). A Review of Models in Support of Oil and Gas Exploration off the North Coast of British Columbia. Canadian Technical Report of Fisheries and Aquatic Sciences 2612, 1–58.
38. Fanneløp, T., & Sjøen, K. (1980). Hydrodynamics of underwater blowouts, Technical report, The Ship Research Institute of Norway.

39. Fay, J. A. (1971). Physical processes in the spread of oil on a water surface. Proceedings of the Joint Conf. on the Prevention and Control of Oil Spills, 15-17 June, 1971, Publ. by API, pp. 463-7.
40. Grammeltvedt, E. B. (2014). Size Distribution for oil Droplets Dispersed in Water: An experimental Study by Image Analysis. Norwegian University of Science and Technology, Department of Petroleum Engineering and Applied Geophysics.
41. Grisolia-Santos, D., & Spaulding, M. L. (2000). The influence of oil particle size distribution as an initial condition in oil spill random walk models", in Oil and Hydrocarbon Spills II, Modelling, Analysis and Control, G.R. Rodriguez and C.A. Brebbia (eds), WIT Press, 19-27, 2000.
42. Huang, J. C. (2005). A review of the state-of-the-art of oil spill fate/behavior models, Miami Beach, FL, United states.
43. The International Tanker Owners Pollution Federation Limited (ITOPF). (2016). Oil tanker spill statistics 2015. Retrieved April 12, 2016, from: http://www.itopf.com/fileadmin/data/Documents/Company_Lit/Oil_Spill_Stats_2016.pdf
44. The International Tanker Owners Pollution Federation Limited (ITOPF). (2014). Fate of Marine oil spills. Retrieved June 12, 2016, from: http://www.itopf.com/knowledge-resources/documents-guides/document/tip-2-fate-of-marine-oil-spills/
45. The International Tanker Owners Pollution Federation Limited (ITOPF). (2005). The use of Chemical dispersants to treat oil spills. Technical Information paper. Retrieved June 12, 2016, from: http://www.cleancaribbean.org/download_pdf.cfm?cF=ITOPF%20Technical%20Information%20Papers%20(TIPS)&fN=The-Use-of-Chemical-Dispersants-to-Treat-Oil-Spills.pdf.
46. Johansen, Ø., Brandvik, P. J., & Farooq, U. (2013). Droplet breakup in subsea oil releases - Part 2: Predictions of droplet size distributions with and without injection of chemical dispersants. Marine Pollution Bulletin, 73(1), 327-335. doi: DOI 10.1016/j.marpolbul.2013.04.012

47. Johansen, Ø., & Durgut, I. (2006). Implementation of the near-field module in the ERMS model, Technical report, SINTEF.
48. Johnsen E. E., & Ronningsen H.P. (2003). Viscosity of 'live' water-in-crude oil emulsions: experimental work and validation of correlations. Journal of Petroleum Science & Engineering
49. Johansen Ø, Rye, H., & Cooper, C. (2003). DeepSpill—Field Study of a Simulated Oil and Gas Blowout in Deep Water, Spill Science & Technology Bulletin, Volume 8, Issues 5–6, 2003, Pages 433-443.
50. Johansen, Ø. (2003). Development and verification of deep-water blowout models. Marine Pollution Bulletin, 47(9-12), 360-368. doi: Doi 10.1016/S0025-326x(03)00202-9
51. Johansen, Ø. (2000). DeepBlow –a Lagrangian plume model for deep water blowouts. Spill Science &Technology Bulletin 6, 103-111.
52. Johansen, Ø. (1999). Field Experiment to Study the Behavior of a Deepwater Blowout. Technical Proposal No. STF66-99043, SINTEF, Trondheim, Norway, 1999.
53. Johnson, W. (1998). Data for Gulf of Mexico, US Minerals Management service (MMS), Herndon, VA, Personal Communications.
54. Kujawinski, E. B., Kido Soule, M. C., Valentine, D. L., Boysen, A. K., Longnecker, K., & Redmond, M. C. (2011). Fate of dispersants associated with the deepwater horizon oil spill. Environmental Science & Technology, 45(4), 1298-1306. doi: 10.1021/es103838p
55. Khelifa, A., & So, L.L.C. (2009). Effects of chemical dispersants on oil-brine interfacial tension and droplet formation. Proceedings of the 32 AMOP technical seminar on environmental contamination and response Volume 1, (p. 940). Canada: Environment Canada.
56. Lee, k. (2012). Degradation of dispersants and dispersed oil. Centre for Offshore Oil, Gas, and Energy Research, Fisheries and Oceans Canada.
57. LGL Limited. (2011). Environmental assessment of Statoil's Geophysical Program for Jeanne d'Arc and Central Ridge/Flemish Pass Basins, 2011-2019. LGL Rep. SA1121. Rep. by LGL Limited, in association with Canning & Pitt Associates Inc.,

and Oceans Ltd., St. John's, NL, for Statoil Canada Ltd., St. John's, NL. 227 p. + appendices.

58. Louis J. & Thibodeaux, *et al*. (2011). "Marine Oil Fate: Knowledge Gaps, Basic Research, and Development Needs; A Perspective Based on the Deepwater Horizon Spill." Environmental Engineering Science 28(2): 87-93.
59. Lehr, W., Bristol, S., & Possolo, A. (2010). Oil Budget calculator, Deepwater Horizon, Technical Documentation, A report by the Federal Interagency Solutions Group. Oil Budget Calculator Science and Engineering Team.
60. Li, Z. K., Lee, K., King, T., Boufadel, M. C., & Venosa, A. D. (2009b). Evaluating Chemical Dispersant Efficacy in an Experimental Wave Tank: 2-Significant Factors Determining In Situ Oil Droplet Size Distribution. Environmental Engineering Science, 26(9), 1407-1418. doi: DOI 10.1089/ees.2008.0408
61. Li, Z. K., Lee, K., King, T., Kepkay, P., Boufadel, M. C., & Venosa, A. D. (2009a). Evaluating Chemical Dispersant Efficacy in an Experimental Wave Tank: 1, Dispersant Effectiveness as a Function of Energy Dissipation Rate. Environmental Engineering Science, 26(6), 1139-1148. doi: DOI 10.1089/ees.2008.0377
62. Li, Z. K., Kepkay, P., Lee, K., King, T., Boufadel, M. C., & Venosa, A. D. (2007). Effects of chemical dispersants and mineral fines on crude oil dispersion in a wave tank under breaking waves. Marine Pollution Bulletin, 54(7), 983-993. doi: DOI 10.1016/j.marpolbul.2007.02.012
63. Lane, J.S., & LaBelle, R. P. (2000) Meeting the challenge of potential deepwater spills: cooperative research effort between industry and government. *Proceedings of the society of Petroleum Engineers Conference,* Slavenger, Norway, June 26-28, 2000
64. Lehr, W.J. (2001). Review of modeling procedures for oil spill weathering behavior. Advances in Ecological Sciences 9, 51-90.
65. Li, M. & Garrett, C. (1998). The Relationship between Oil Droplet Size and Upper Ocean Turbulence. Marine Pollution Bulletin, 36:961-970, 1998.
66. Lunel, T. (1995). Dispersant effectiveness at sea. In Proceedings of the International Oil Spill Conference, Long Beach, California, 27 February – 2 March

1995. Edited by J.O. Ludwigson. American Petroleum Institute, Washington, D.C. pp. 147–155.

67. Lefebvre, A. H. (1989). Atomization and Sprays, Taylor& Francies, P.421
68. Ma, X., Cogswell, A., Li, Z., & Lee, K. (2008). Particle size analysis of dispersed oil and oil–mineral aggregates with an automated ultraviolet epi-fluorescence microscopy system Environ. Technol. 29, 739.
69. Masutani S. M., & Adams E.E. (2001). Experimental Study of Multi-Phase Plumes with Application to Deep Ocean Oil Spills Deep Spill JIP (pp. 147): University of Hawaii (UH) and Massachusetts Institute of Technology (MIT).
70. Mackay, D., & Hossain, K. (1982). Interfacial tensions of oil, water, chemical dispersant systems. *The Canadian Journal of Chemical Engineering*, *60*(4), 546–550. doi:10.1002/cjce.5450600417
71. Niu. H. & Li, S.(2016). Stochastic Modeling of Oil Spill in the Salish Sea. Proceedings of the Twenty-sixth (2016). International Ocean and Polar Engineering Conference. Rhodes, Greece, June 26-July 1, 2016.
72. Nissanka, I. D., & Yapa P. D. (2015). Oil droplet size calculation with and without dispersants in an underwater well blowout, paper presented at E-proceedings of the 36th IAHR World Congress, The Hague, Netherlands.
73. National Oceanic and Atmospheric Administration (NOAA). (2015). Oil types. Retrieved June 12, 2016, from: http://response.restoration.noaa.gov/oil-and-chemical-spills/oil-spills/oil-types.html
74. National Research Council (NRC). (1988). Using Oil Spill Dispersants on the Sea. National Academy Press, Washington, D.C.
75. National Research Council (NRC). (2005). Oil Spill Dispersants: Efficacy and Effects. Washington, DC: National Academies Press.
76. Ocean Portal Team (OPT). (2015). Gulf Oil Spill. Smithsonian National Museum of Natural History. Retrieved June 12, 2016, from: http://ocean.si.edu/gulf-oil-spill
77. Ortmann, A. C., Anders J., Naomi S., Gong, L., Anthony G. M., & Condon, R.H. (2012). Dispersed Oil Disrupts Microbial Pathways in Pelagic Food Webs. PLOS ONE 7 (7): e42548. Doi 10.137/ journal. pone.0042548

78. Overstreet, R., Lewandowski, a, Lehr, W., Jones, R., Simeck-Beatty, D., & Calhoun, D. (1995). Sensitivity analyss in oil spill models: case study using adios - Poster session T4. *1995 Oil Spill Conference*. Retrieved from ASR 00250
79. Paris, C.B., Le Hénaff, M., Aman, Z.M., Subramaniam, A., Helgers, J., Wang, D.-P., Kourafalou, V.H., & Srinivasan, A. (2012). Evolution of the Macondo well blowout: simulating the effects of the circulation and synthetic dispersants on the subsea oil transport. Environ. Sci. Technol.
80. Price, J. M., Johnson, W. R., Marshall, C. F., Ji, Z.-G., & Rainey, G. B. (2003). Overview of the Oil Spill Risk Analysis (OSRA) Model for Environmental Impact Assessment. *Spill Science & Technology Bulletin*, *8*(5-6), 529–533. doi:10.1016/S1353-2561(03)00003-3
81. RPS ASA. (2017). OILMAP DEEP DeepWater Oil Spill Model and Analysis System. Retrieved from http://www.asascience.com/software/oilmap/oilmapdeep.shtml
82. Ryerson, T.B., Camilli, R., & Kessler, J.D., et al. (2012). Chemical data quantify Deepwater Horizon hydrocarbon flow rate and environmental distribution.
83. Reed, M., Johansen, Ø., Rye, H., Narve E., Ivar S., Per D., & Brandvic, P.J. (1999). Deepwater Blowouts: Modeling for Oil Spill Contigency Planning, Monitoring, and Response. Paper presented at the 1999 International Oil Spill Conference, Seattle, US.
84. Reed, M., Hetland, B., & Emilsen, M. H. (2003). Numerical Model for Estimation of Pipeline Oil Spill Volumes. Paper presented at the 2003 International Oil Spill Conference, Vancouver, BC, Canada.
85. Reed, M., Daling, P. S., Brakstad, O.G., Singsaas, I., Faksnes, L.G., Hetland, B. A., & Efrol, N. (2000). OSCAR 2000: A multi-component 3-dimensional oil spill contingency and response model 2000. Paper presented at the Proceedings of the 23rd Arctic Marine Oilspill Program (AMOP) Technical Seminar.
86. Reed, M., Johansen, Ø., Brandvik, P., Daling, P., Lewis, A., Fiocco, R., Mackay, D., & Prentk, R. (1999). Oil Spill Modeling towards the Close of the 20th Century: Overview of the State of the Art, Spill Science & Technology Bulletin 5: 3–16.

87. Rygg, O.B., & Emilsen, M. H. (1998). A Parameter Study of Blowout Rates for Deep Water and their Effect on Oil Droplet and Gas Bubble Generation", Technical Report, Well Flow Dynamics, Billingstad, Norway, 1998.
88. Rye, H., Brandvik, P. J., & Strøm, T. (1997). Subsurface blowouts: Results from field experiments. Spill Science & Technology Bulletin, 4(4), 239-256.
89. Rye, H., Brandvik, P. J., & Reed, M. (1996). Subsurface oil release field experiment-observations and modelling of subsurface plume behavior. Proc., 19th Arctic and Marine Oil Spill Program (AMOP) Technical Seminar, Vol. 2, Ottawa, Canada, 1417–1435.
90. Reed, M., Aamo, O. M., & Daling, P. S. (1995a). Quantitative analysis of alternate oil spill response strategies using OSCAR. *Spill Science & Technology Bulletin*, *2*(1), 67–74. http://doi.org/10.1016/1353-2561(95)00020-5
91. Reed, M., French, D., Rines, H., & Rye, H., (1995b). A three-dimensional oil and chemical spill model for environmental impact assessment. In proceedings of the 1995 International Oil Spill Conference, pp.61-66
92. Socolofsky, S., Dissanayake, A. L., Jun, I., Gros, J., Arey, J. S., & Reddy, C.M. (2015). Texas A&M Oilspill Calculator (TAMOC): Modeling Suite for Subsea Spills, Proceedings of the thirty-Eighth AMOP Technical Seminar, Enviornment Canada, Ottawa, ON, pp153-168.
93. SINTEF Marine Modeling Group. (2015). Userguide MEMW, SINTEF Materials and Chemistry.
94. Sequoia Scientific, Inc. (2012). LISST-100X Particle Size Analyzer, User's Manual, Version 5.0.
95. Spaulding, M.L., Bishnoi, P.R., Anderson, E., & Isaji, T. (2000). An integrated model for prediction of oil transport from a deep water blowout. *Proceedings of the 23 Arctic and Marine Oilspill Program (AMOP) Technical Seminar,* (p. 1077). Canada: Environment Canada.
96. Strøm-Kristiansen, T., Lewis, A., Daling, P.S., Hokstad, J.N., & Singaas, I. (1997). Weathering and dispersion of naphthenic, asphaltenic and waxy crude oils. In: Proceedings of the 1997 International Oil Spill Conference, Florida US, pp. 631–636.

97. Sebastiao, P., & Soares, C.G. (1995). Modeling the fate of oil spills at sea. Spill Science & Technology Bulletin 2(2), 121-131
98. Thibodeaux, L. J., Valsaraj, K. T., John, V. T., Papadopoulos, K. D., Pratt, L. R., & Pesika, N. S. (2011). Marine Oil Fate: Knowledge Gaps, Basic Research, and Development Needs; A Perspective Based on the Deepwater Horizon Spill. *Environmental Engineering Science*. doi:10.1089/ees.2010.0276
99. The Federal Interagency Solutions Group, Oil Budget Calculator Science and Engineering Team (TFISG-OBCSET). (2010), Oil Budget Calculator: Deepwater Horizon, Technical Documentation. Retrieved from http://www.noaanews.noaa.gov/stories2010/PDFs/OilBudgetCalc_Full_HQ-Print_111110.pdf
100. Topham, D.R. (1975). Hydrodynamics of an Oilwell Blowout, Beaufort Sea Technical Report #33, Department of the Environment, Victoria, BC.
101. Venosa, A. D. & Zhu, X. (2003). Biodegradation of Crude Oil Contaminating Marine Shorelines and Freshwater Wetlands. Spill Sci. Tech.
102. Wells, P. G. & Harris, G. W. (1980). The acute toxicity of dispersantsand chemically dispersed oil. Proceedings of the 3rd Arctic Marine Oil Spill Program Technical Seminar, Edmonton, Alberta, ppl44-152
103. Wells, P. G. (1984). The toxicity of oil spill dispersants to marine organisms: a current perspective, in Oil Spill Chemical Dispersants: Research, Experience and Recommendations, T. E. Allen, ed. STP 840. American Society for Testing and Materials, Philadelphia, Pennsylvania, ppl77-202. A detailed discussion is presented in NRC.14.
104. Yapa, P. D. (2013). CDOG (Comprehensive Deepwater Oil and Gas) Model. Retrieved June 12, 2016, from: http://people.clarkson.edu/~pyapa/comp_model/cdog.html
105. Yapa, P. D., Wimalaratne, M. R., Dissanayake, A. L., & DeGraff, J. A. (2012). How does oil and gas behave when released in deepwater? Journal of Hydro-environment Research, 6(4), 275-285

106. Yapa, P. D., & Chen, F. H. (2004). Behavior of oil and gas from deepwater blowouts. Journal of Hydraulic Engineering-Asce, 130(6), 540-553. doi: Doi 10.1061/(Asce)0733-9429(2004)130:6(540)
107. Yapa, P. D., Zheng, L. and Chen, F. H. (2001). A model for deepwater oil/gas blowouts. Marine Pollution Bulletin, 43(7-12), 234-241.
108. Yapa, P. D., & Zheng, L. (1997). Simulation of oil spills from underwater accidents .1. Model development. Journal of Hydraulic Research, 35(5), 673-687.
109. Zhao, L., Shaffer, F., Robinson, B., King, T., Ambrose, C. D., Pan, Z., & Gao, F., et al. (2016). Underwater oil jet: Hydrodynamics and droplet size distribution, Chemical Engineering Journal, Volume 299: 292-303
110. Zhao, L., Torlapati, J., Boufadel, M. C., King, T., Robinson, B., & Lee, K. (2014a). VDROP: A comprehensive model for droplet formation of oils and gases in liquids - Incorporation of the interfacial tension and droplet viscosity. *Chemical Engineering Journal*, *253*(August), 93–106.
111. Zhao, L., Boufadel, M.C., Socolofsky, S., Adams, E.E., King,T., & Lee,K. (2014b). "Evolution of droplets in subsea oil and gas blowouts: Development and validation of the numerical model VDROP-J." Marine Pollution Bulletin 83(1): 58-69.
112. Zheng, L., Yapa, P.D., & Chen, F. (2002). A Model for Simulating Deepwater Oil and Gas Blowou Part I: Theory and Model Formulation. Journal of Hydraulic